PROTON CONDUCTION IN ORGANIC SOLIDS

by

Robert Yatshein Chan-Henry

A thesis submitted to Rhodes University, in the Department of Chemistry, in fulfilment of the requirements for the Degree

of

MASTER OF SCIENCE

February 1971

INDEX

ABSTRACT

Dielectric, d. c. conductivity and electrolysis measurements have been made principally on solid imidazole and urea. Electrode effects, especially the development of a suitable protode, and techniques for detecting mobile protons in solids were pursued. The dielectric data have been correlated with the d. c. results. A mechanism for extrinsic proton conduction in urea has been proposed.

ACKNOWLEDGEMENTS

The author wishes to express his deep appreciation to Professor L. Glasser for his instruction and guidance throughout all phases of this investigation.

Thanks are also due to:

Mr C. A. R. Phillpotts and Mr H. I. Philip for advice and many invaluable discussions.

Dr S. K-M. Tim and Mr G. A. Eagle for assisting in the preparation of this thesis.

The technical staff of the Chemistry Department, Rhodes University.

A special word of thanks is also extended to Mr J. B. Murray, whose skill as a glass blower has made much of this work possible.

Finally, I would like to express my gratitude to Mrs I. Inggs, who so patiently undertook the typing of this thesis.

FUTURE WORK

The techniques for detection of mobile protons in intrinsic and extrinsic protonic conductors has been evolved to a stage where detection is systematic and direct.

The development of imidazole as a protode has opened up a wide field of study, including the possibility of "protonics" as an extension of electronics (Glasser 1971).

Under the direction of Professor L. Glasser, F. M. Saba has already established extrinsic protonic conduction in benziimidazole, thiourea and succinimide, a material which is not an intrinsic proton conductor, even in the melt.

It will now be valuable to seek other materials than imidazole as protodes so that, if a material of high enough conductivity can be found, the properties of extrinsic proton conductors under injecting conditions can be examined in more detail, to develop the mechanistic explanations of the conductivity and, perhaps, to aid understanding of certain bioelectric phenomena.

CHAPTER I

THEORETICAL ASPECTS

SECTION I : INTRODUCTION

Many electrical phenomena of biochemical interest occur in nature. For instance, dynamic electrical potentials as high as 0.1 volt per cell exist in living tissue; enzymatic processes occur via a very rapid mechanism of charge exchange and charge transfer between molecules; the processes of sorting and retrieving the vast amount of information stored in the brain take place extremely rapidly. The suggestion (Riehl 1940, Szent-Györgyi 1941) that radiationless energy- and charge-transfer processes observed in non-living systems might shed some light on the elucidation of bioelectric phenomena, stimulated considerable interest in the possible biological implications of organic semiconductors. The discovery of photo-conduction in certain dyed proteins (Szent-Györgyi 1946) was claimed by the author as further proof of this suggestion.

Investigations into biological mechanisms showed that the process of diffusion of large molecules was too slow to account for the rapid charge exchange and charge transfer found in nature, so attention was focussed on more elementary particles, namely protons and electrons. Although the static mass of the proton is 2000 times that of the electron, the effective mass of the proton is only about 20 times that of the electron under tunnelling conditions (Kemeny and Rosenberg 1970), and although polarization of the immediate surroundings by a charge carrier increases its "effective size", the charge and bare size of the proton and electron are approximately equal, so that their

effective sizes should be about the same. Thus, when formulating mechanisms for energy transfer, it is necessary to consider (Terenin et al. 1959) the feasibility of proton as well as electron transport, since most of the biologically important macromolecules (proteins and polynucleic acids) are hydrogen bonded.

The electrical free energy change of biological systems cannot be converted into work by an oxidation-reduction process, since the presence of a metal electrode is required to supply electrons at the reaction sites. Thus, in the absence of metallic conductors, Shedlovsky (1952) proposed acid-base reactions with proton transfer through the biological medium, to be the immediate energy precursor in nature. To substantiate this hypothesis, Shedlovsky devised a workable protochemical cell which derived electrical energy from a proton-transfer reaction through solid lauric acid.

Today, there would seem to be little doubt that many of the fundamental biological processes in living systems are directly connected with the transfer of electrons and protons. The significance of the high mobility of electrons in conjugated biological systems has been extensively investigated (Szent-Györgyi 1959, Pullman and Pullman 1962). The profound influence of proton mobility in biological systems is forcefully illustrated in the following three examples:

A. Deoxyribonucleic acid (DNA), is a giant molecule which is believed to be the essential hereditary substance carrying the genetic information in the cell. According to the Watson-Crick model of DNA, the structure consists of a double helix of sugar-phosphate chains which are joined by pairs of nucleotide bases, and are held together

by hydrogen bonds (Watson and Crick 1953). In this model, the genetic code is essentially contained in the arrangement of the hydrogen bonds. Löwdin (1963) showed that proton tunnelling between the base pairs in DNA may be responsible for the occurrence of spontaneous mutations during replication, causing tumours and cancer. Löwdin also attributed the phenomenon of aging to a loss of useful genetic information due to tunelling of the proton across the hydrogen bonds.

B. Using model systems, which reveal that proton mobility in ice is comparable with the mobility of electrons in technically useful semiconductors, Riehl (1965) has suggested that proton migration across hydrogen bonds may even be used in such processes as the storage and distribution of information in the brain. Riehl has indicated that molecules, such as the hydroxy acridines (Campbell and Cairns-Smith 1961), which exhibit prototropy, may be of interest as model substances in the biophysical studies of memory devices.

C. In a recent experiment, Thomas et al. (1969) demonstrated that for a carefully selected pyrimidine base, isocytosine (2-amino-4-oxopyrimidine), it is possible, by using an appropriate electrode (a proton-injecting electrode), to draw currents enormously greater (by factors of about 10^{10}) than those usually associated with so-called organic semiconductors (Eley 1968, Terenin 1961). The significance of this work is that, provided similar electrodes can exist in living systems, much larger currents and very much more effective pathways of energy transfer may be available than was previously suspected.

Since there are many hydrogen bonded inorganic and organic compounds which are much simpler than the complex biological macromolecules, it is not surprising that the study of proton conduction has rapidly branched out into these spheres. Today, proton conduction has been discovered in a wide variety of solids, ranging from ice to sulphates and phosphates, minerals, acids, alcohols, amines, sugars, cellulose, haemoglobin and protein.

SECTION 2 : THE SEMICONDUCTION EQUATION

Solids may be classified, in terms of their electrical properties, as follows:

A. Conductors.

Metals are typical of this group and have room temperature conductivities of the order of 10^4 to 10^6 ohm^{-1} cm^{-1}. The electrical conductivity decreases with temperature.

B. Insulators.

Because of the large energy gap (i. e., the difference in energy between the top of the valence band and the bottom of the conduction band), the electrical conductivities are very small, ranging from 10^{-22} to 10^{-10} ohm^{-1} cm^{-1}. Diamond is an example of a nearly perfect insulator at room temperature, with an energy gap of about 120 kcal mol^{-1}.

C. Semiconductors.

The conductivity of semiconductors increases with temperature, since thermal activation can promote charge carriers across the small energy gap (20 kcal mol^{-1}), from the valence band into the conduction band.

Semiconducting organic solids are grouped into molecular crystals, charge-transfer complexes and polymers. Their conductivity dependence on temperature is usually described by the two-constant semiconductor equation

$$\sigma = \sigma_o \exp(-E/kT) \quad \ldots\ldots\ldots\ldots \quad (1:2.1)$$

where σ is the electrical conductivity, σ_o is the pre-exponential

factor, E is the activation energy associated with the conduction process and k and T have the usual meaning (Mott and Gurney 1940).

A plot of log σ vs 1/T generates a straight line whose slope yields the value of -E/k and whose intercept yields the value of σ_o. Thus, the temperature dependence of the conductivity is characterised experimentally by the two constants, E and σ_o.

An early survey of the literature by Many, Harnik and Gerlich (1955) showed that for a variety of polynuclear hydrocarbons and phthalocyanines, the values of σ_o varied over a range of 10^{23}. They noted, however, that a rough correlation existed between the activation energies and the pre-exponential factors. A plot of $\log\sigma_o$ vs E for these data was presented by Gutmann and Lyons (1967); a roughly straight line with a large amount of scatter among the data points was obtained, which suggests the general relationship,

$$\log\sigma_o \sim \alpha E + \beta \quad \ldots\ldots\ldots\ldots\ldots \quad (1:2.2)$$

where α and β are constant for the entire class of compounds listed. Cardew and Eley (1957) found a similar type of correlation to hold for a series of amino acids and proteins, with values of α and β different from the case above. The existence of this correlation suggests that the 2-constant equation is inadequate to describe this conduction behaviour.

Eley (1967) recently discussed these plots in detail and pointed out that a somewhat similar situation obtains in inorganic semiconductors and is known, in that field, as the Meyer-Neldel rule (Meyer and Neldel 1937). This rule is discussed by Mooser and Pearson (1960) in relation to compound semiconductors, where a single compound is capable of exhibiting a number of different activation energies depending on the method of preparation. For

these single compounds, the Meyer-Neldel rule holds. This is quite different from the data described by Many et al. or Eley for the organic semiconductors where each point on the $\log\sigma_o$ vs E plot refers to a different compound.

Rosenberg et al. (1968) proved that the Meyer-Neldel rule also holds for single organic compounds by varying the activation energy of semiconduction of single compounds and obtaining linear plots of activation energy versus $\log\sigma_o$ for each compound.

The activation energies of semiconduction were varied as follows:

1. hydration of the crystals - crystalline haemoglobin (Rosenberg 1962)
2. formation of weak donor-acceptor complexes - oxidized cholesterol (Rosenberg and Bhowmik 1969)
3. use of different cis-trans isomers of the substance when possible - cis-trans isomers of retinal crystals and glasses (Rosenberg and Harder 1967).

These results clearly demonstrated that the two-constant equation for semiconduction was also inadequate in the case of a single organic compound, so Rosenberg et al. (1968) proposed a three-constant equation of the form

$$\sigma = \sigma_o' \exp(E/kT_0) \exp(-E/kT) \cdot \ldots\ldots \quad (1:2.3)$$

(This equation is often referred to as the "Compensation Rule")
The constant, σ_o', is independent of the activation energy, and the characteristic temperature T_o, is a molecular property, as it is independent of the crystalline state of the sample or the nature of the electrodes used.

Comparison of equation (1:2. 1) with equation (1:2. 3) gives

$$\sigma_o = \sigma'_o \exp(E/kT_o) \quad \ldots\ldots\ldots \quad (1:2.4)$$

and on taking the log on both sides of this equation, there is obtained:

$$\log\sigma_o = \log\sigma'_o + (kT_o)^{-1}E \quad \ldots\ldots \quad (1:2.5)$$

which has the same form as that of equation (1:2.2), obtained empirically from the data. The two constants σ'_o and T_o can be obtained in the usual way from a linear plot of $\log\sigma_o$ vs E. From the limited number of results available at the time, it was found that there is an inverse relationship between $(kT_o)^{-1}$ and σ'_o. T_o was always found to be greater than or equal to zero, which implies that there are several constraints on the Meyer-Neldel rule as applied to organic compounds.

In order to explain the newly established pre-exponential factor, Eley (1967) considered various conduction mechanisms, including tunnelling through intermolecular potential barriers.

Kemeny and Rosenberg (1969) considered a similar tunnelling mechanism, where there was tunnelling through intermolecular barriers from activated energy levels. They took into account the characteristic temperature and the barrier shape, height, and width, and the effective mass of the electrons. The triangular barrier assumption was found to give a qualitative, but not quantitative, agreement with experiment.

Since the mass of the proton is only about 20 times the effective mass of the electron (Kemeny and Rosenberg 1970), and since the total barrier height for proton tunnelling should be of the same order as that for electrons, it was suggested that proton tunnelling should play a role in phenomena such as electrical conduction.

SECTION 3 : THE EFFECT OF HYDROGEN BONDING ON CONDUCTIVITY

A number of investigations have dealt with the relationships between molecular structure and the conductivity parameters, σ_o and E, for a variety of types of compounds (Inokuchi and Akamatu 1961, Okamoto and Brenner 1964, and Guttmann and Lyons 1967, and the references therein), but systematic studies are lacking which deal with the relationship between electrical properties and hydrogen bonding in solids for structurally related compounds.

Pollock and Ubbelohde (1956) have studied the effect of different types of hydrogen bond linkages on the energy of activation of a series of anhydrous polycrystalline organic acids and their hydrates. (See table 1:3. 1)

They found that acid dimers held merely by van der Waals' forces to their neighbours, as in benzoic or furoic acid, have relatively large values of activation energy, comparable with those in ionic crystals. On the other hand, the presence of spirals of hydrogen bonds, especially where these involved amphoteric

$$\left.\begin{matrix} OH_3^+ \ldots {}^-OOC.R. \\ OH_2 \ldots HOOC.R. \end{matrix}\right)$$

systems in the acid hydrates, led to comparatively low migration energies, notably for acetylene dicarboxylic acid.

Assuming protons to be the charge carriers, the differences in energies of activation were accounted for as follows:

Since acid dimers form isolated molecules, the transfer of a proton from an acid dimer to an interstitial position in the crystal must

TABLE 1 : 3. 1

Acid	Hydrogen Bond Type	Activation Energy (E) kcal mol^{-1}	Conductivity (σ) at 50° C $ohm^{-1} cm^{-1}$
Acetylenedicarboxylic acid dihydrate	Spiral of bonds linked by ...O-C=O...	6.5	3.5×10^{-6}
Acetylenedicarboxylic acid dehydrated	--	12.3	7.1×10^{-7}
Oxalic acid dihydrate	Spiral of bonds linked by ...O-C=O...	23.5	2.2×10^{-8}
Oxalic acid dehydrated	Probably chain of bonds linked by oxalate residues	40.5	1.1×10^{-9}
Benzoic acid	Closed circuit - dimer	48.9	1.8×10^{-9}
Furoic acid	Closed circuit - dimer	68.4	1.8×10^{-8}

(After Glasser 1960)

take place

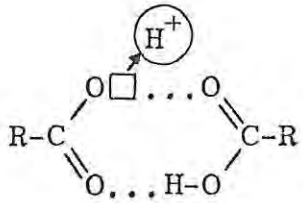

The formation of a vacant proton site, □ , on the dimer, together with an interstitial proton H^+, is analogous to the formation of Frenkel defects in ionic crystals. The activation energy for this process was found to be much lower when spirals of hydrogen bonds were present, since there were numerous alternative sites within the spiral for the interstitial proton. The approximate two-fold increase in energy of activation on dehydration was attributed to the loss of some of the low energy sites.

Direct current conductivity measurements on single crystals of oxalic acid dihydrate (OAD) revealed a marked anisotropy along the b axis (Glasser 1960a). Since conduction by interstitial protons could not account for the high mobility of the charge carriers, Glasser proposed a mechanism for proton conduction along the spirals of hydrogen bonds in the b axis. Nevertheless, he considered the evidence for proton conduction inconclusive. After further investigation (Giesekke 1965a), in which dielectric- and electrolysis- measurements were pursued, and in the light of X-ray- (Robertson 1959) and nuclear magnetic resonance- (Richards and Smith 1951, Itoli et al. 1953) studies of OAD, Giesekke concluded that the hydrogen bonds between the water and the oxalic acid molecules are so strong that proton transfer between these molecules is unlikely to occur.

Charge transfer in a bulk sample (single crystal) must actually move from molecule to molecule - not just around a closed ring or down a long molecular chain, so that the reason why some materials

show semiconducting properties in the crystalline state cannot be sought within the molecule itself; benzene, for example, is not a semiconductor, but a superconductor on a molecular scale (Garrett 1959). Thus, the size of a conjugated system, and the variation of substituents on a molecule, which affect the degree of intermolecular interaction, can produce considerable changes in conductivity.

Gravatt and Gross (1967) chose two types of structural variation to study these effects. The effect of molecular length and intermolecular hydrogen bonding on the conductivity parameters was studied by selecting a series of para-substituted mono- and di-carboxylic acids and derivatives containing one to three benzene rings, which can be represented by:

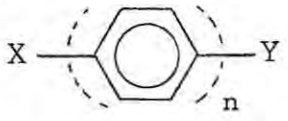

where

X, Y = COOH, H, $COOCH_3$, COCl, CN,
$COO^- M^+$

n = 1, 2, 3.

A second series of benzene carboxylic acids, having from one to six carboxyl groups per ring, was chosen to study the relationship between conductivity and the number and position of acid groups on the aromatic nucleus (See table 1:3. 2). A definite relationship was found between the activation energy for conduction and the position and number of carboxyl group substituents on an aromatic system. This relationship was interpreted as a combination of the hydrogen-bonding and electron-withdrawing properties of the carboxyl groups on the assumption that the aromatic pi electrons were involved in the generation of charge carriers, since substituents which reduced the electron density of the aromatic system produced a substantial increase in the energy of activation.

(After Gravatt and Gross 1967)

TABLE 1 : 3. 2

Compound	Activation Energy (E) kcal mol^{-1}	$ohm^{-1}\ cm^{-1}$	(100^{o}) $ohm^{-1}\ cm^{-1}$	(150^{o}) $ohm^{-1}\ cm^{-1}$	Melting point (^{o}C)	Purification method
Benzoic Acid	42.2	$6X10^{12}$	$2X10^{-14}(75^{o}C)$	...	123.5	Zone refined
Terephthalic acid	38.8	$4X10^{1}$	$1X10^{-17}$	$1X10^{-15}$	...	Sublimed
-Phenylbenzoic acid	46.1	10^{8}	$6X10^{-18}$	$7X10^{-16}$	225	Recrystallized from benzene
4,4′-Biphenyldicarboxylic acid	37.1	$6X10^{2}$	$1X10^{-17}$	$3X10^{-16}$	...	Hydrolysis of purified salt
Phthalic acid	62.3	10^{21}	$1X10^{-15}$	$3X10^{-11}$	212	Hydrolysis of purified salt
Isophthalic acid	36.9	10^{3}	$7X10^{-18}$	$8X10^{-17}$	344	None, reagent grade material
Trimesic acid	37.4	$1X10^{8}$	$1X10^{-14}$	$5X10^{-12}$	367	Recrystallized from water
Mellitic acid	34.6	$4X10^{5}$	$2X10^{-15}$	$6X10^{-13}$	...	Recrystallized from ethanol
Dimethyl terephthalate	39.9	$1X10^{9}$	$4X10^{-15}$	...	140.9	Zone refined
Terphenyl-4,4″-dicarbonyl-dichloride	71.5	10^{24}	$1X10^{-16}$	$2X10^{-13}$	221	Recrystallized from benzene
Terephthalonitrile	66.9	10^{24}	$4X10^{-15}$	$2X10^{-10}$	223	Zone refined
Sodium terephthalate	28.6	$1X10^{2}$	$3X10^{-15}$	$3X10^{-13}$	...	Extraction with ethanol
Potassium terephthalate	27.2	$1X10^{1}$	$1X10^{-15}$	$1X10^{-13}$	...	Extraction with ethanol
Tetramethylammonium terephthalate	23.0	10^{4}	$5X10^{-14}$	$1X10^{-11}$		Recrystallization from acetone-water mixtures

The possibility of proton conduction in these compounds should not be precluded, as crude thermoelectric measurements performed by Gravatt and Gross indicate that the charge carriers in some of the compounds studied are positive.

SECTION 4 : OTHER FACTORS WHICH INFLUENCE CONDUCTIVITY

In interpreting the experimental observation on protonic semiconductors, investigators have had to take into consideration factors which influence the measured conductivity. These factors are usually of two types: those which influence solely the resistivity, without affecting the energy of activation, and those which may influence both of these. Some of the variables involved include the presence of impurities, electrode effects, voltage effects, polarization effects and crystal defects.

1 : 4 : 1 Impurity Effects

Since the electrical conductivity of organic compounds is extremely sensitive to the presence of impurities (Brown and Aftergut 1962), the following general methods of purification will be discussed:

1. Recrystallisation from a solvent
2. Sublimation
3. Chromatography (either from solution or from the vapour)
4. Zone-refining.

Recrystallisation from a solvent is generally not efficient enough to yield measurements of the intrinsic conductivity of organic solids, and there is also the problem of occlusion of protic solvents when recrystallising a prospective proton conductor. Preparative chromatography on a large scale is laborious. Sublimation is a convenient technique, but the relatively high operational temperature may generate decomposition or oxidation products. Zone-refining is

a method for multiple recrystallization from the melt and is therefore an extremely efficient purification procedure for those compounds which are stable at the melting point, but will only work for impurities that have a favourable distribution coefficient between the solid and the liquid. The temperature for zone-refining is even higher than that required for rapid sublimation.

The necessity to undertake a critical comparison of the different purification methods was recognised by Brown and Aftergut (1963), who took two samples of recrystallised imidazole and subjected the one to repeated zone-refining and the other to repeated sublimation, hoping that the conductivities of both samples would converge to an identical, constant, and therefore intrinsic, conductivity.

However, the conductivity measurements showed no correlation with the number of sublimations, varying by as much as two decades and sometimes the $\log\sigma$ vs $\frac{1}{T}$ curve exhibited two slopes (this erratic behaviour could have been due to moisture picked up during preparation and handling of the discs, as the conductivity of imidazole is known to be extremely sensitive to moisture (Kawada et al. 1969, Chan-Henry and Glasser 1970.)

On the other hand, zone-refining proved to be more successful; the recrystallised material, before zone-refining, had a relatively low resistance and the $\log\rho$ vs $\frac{1}{T}$ curve exhibited two slopes (see fig. 1 : 4. 1 and table 1 : 4. 1). The resistance increased appreciably on zone-refining, but the curves were still characterised by two slopes up to 33 passes. After 39 passes, a single slope (50. 7 kcal mol^{-1}) was obtained; Ohm's law was obeyed at applied potentials of 500 and 2500 V cm^{-1}. Thus, Brown and Aftergut (1963) concluded that for imidazole, the presence of two slopes in the ($\log\sigma$, 1/T)

TABLE 1 : 4. 1

Electrical properties of zone-refined imidazole

No. of passes	Resistance* at 27° ohm cm	Activation Energy (E) kcal mol^{-1}	Temp. range (° C)
0	6×10^{8}	20. 7 24. 2	26-44 44-69
16	2×10^{11}	24. 0 29. 8	25-43 43-69
25	2×10^{11}	20. 6 36. 2	26-59 59-69
33	8×10^{10}	29. 7 27. 0	26-43 43-69
39	4×10^{10}	25. 6	27-68
49	6×10^{10}	25. 3	27-68
56	1×10^{11}	25. 5	27-68
80	2×10^{11}	25. 6	27-68

* At 100 V applied potential

(After Brown and Aftergut 1963)

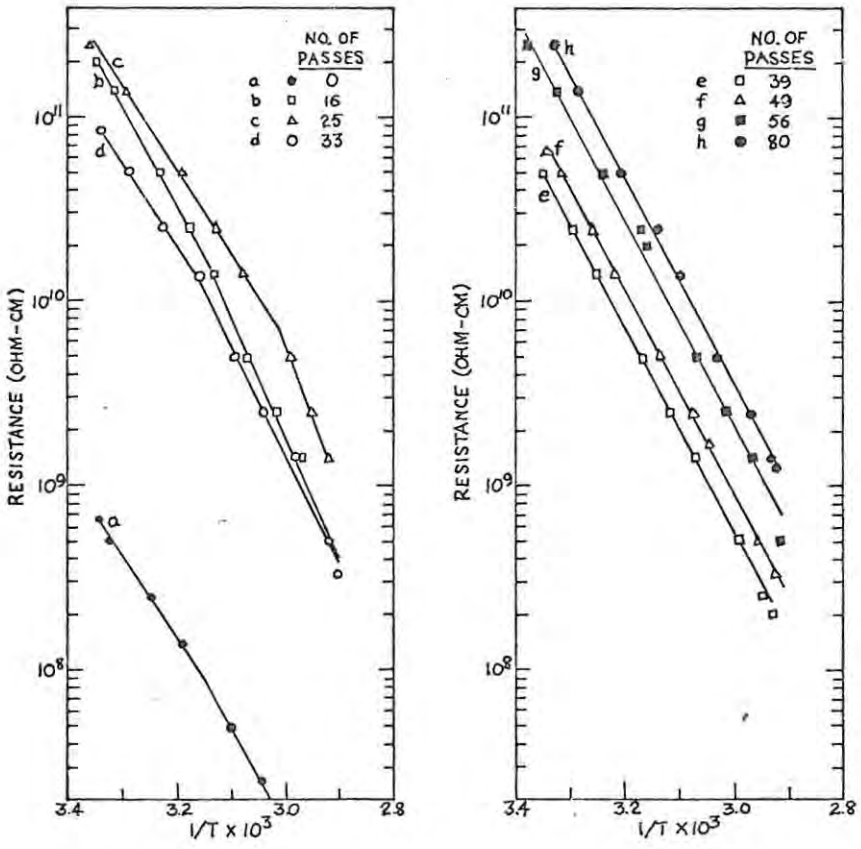

Fig. 1 : 4. 1. Temperature dependence of the resistance of imidazole as a function of the number of zone-refining passes, using blocking electrodes.

(After Brown and Aftergut 1963)

curves was indicative of an impure specimen, since further purification gave rise to a single slope and that,as purification proceeded, both the activation energy and the conductivity changed, and E only became constant after the curve became characterised by one slope.

Gravatt and Gross (1967) observed similar changes in conductivity on purification of terephthalic acid and several other compounds in which various purification methods were employed, but the upper-temperature activation energy was found to be relatively insensitive to change, which indicated that the high-temperature activation energy was a characteristic property of the material and was not a function of the sample purity. Northrop and Simpson (1956) reported similar effects for a series of doped polyacenes.

Adsorbed water, as an impurity, affects both the magnitude (Rosenberg 1962) and the nature (Riehl 1957, Maricic and Pifat 1966) of the conductivity of organic solids. Thus, Gravatt and Gross (1967) observed that traces of moisture, undetectable by ordinary weight-loss measurements, had a marked effect on the conductivity of the organic acids studied.

The effect seemed to be of two distinct types. In the first type, surface adsorption of moisture on a dry pellet caused a large (reversible and reproducible) increase in conductivity. The second type of effect was a slow decrease in conductivity with temperature cycling of a pellet, which generally became insignificant after several cycles. This change in conductivity was thought to be due to a slow loss or redistribution of traces of water within the interior of the pellet, somewhat analogous to the situation in borax (Giesekke and Glasser 1967). This interior moisture was probably adsorbed on the material and was trapped during the pressing process; a similar situation

obtained where freshly ground, compressed powders exhibited large transient dielectric constants (Dryden and Meakins 1953). In the case of surface adsorption of moisture, it was assumed that the water diffused into the pellet and reduced the interparticle resistances by forming conductive bridges at the particle interfaces; any loss or redistribution of this water would have caused an increase in the resistance. Water was not, however, considered to be involved in the charge generation processes, since no change in activation energy was noted as the conductivity decreased during repeated temperature cycling.

In some work on moist proteins, Rosenberg (1962) found that the decrease in activation energy with hydration was due to the effective increase in the polarizability of the lattice. A simple theory relates these two effects (Rosenberg 1962, Rosenberg and Postow 1969) and yields the following equation:

$$\sigma(T,\varepsilon') = \sigma_o \exp(-E_D/2kT)\exp[(e^2/2kTR)(\varepsilon^{-1}-\varepsilon'^{-1})]$$

where E_D is the dry-state activation energy, ε is the dry-state dielectric constant (low frequency), and ε' is the effective dielectric constant in the hydrated state. Since the theory is quite general, it predicts that any method of decreasing the dielectric constant will decrease the activation energy and increase $\sigma(T)$.

1 : 4 : 2 Crystal Defects

Electrical measurements obtained from compressed powders are subject to the following disadvantages:

1. Adsorbed water affects the magnitude and nature of the conductivity (see section 1 : 4 : 1)
2. Anisotropic conduction cannot be studied

3. Surface conduction cannot be eliminated because of the large internal surface area.

In view of these disadvantages, the need to study single-crystal rather than polycrystalline samples has been sharply emphasised (O'Keefe and Perrino 1967, Pollock and Sharan 1967, and Thomas et al. 1969). However, one must be critically selective in choosing single crystals for measurement, as there is a pronounced tendency for solvents to be occluded (Thomas and Williams 1967, Dunning 1963) along dislocations which are inevitably present in single crystals (Engelhardt and Riehl 1966, Thomas and Williams 1968, Thomas et al. 1968, 1969), providing ionic conduction paths of magnitudes comparable with surface conduction in polycrystalline material - this is especially true of single crystals of biochemical importance, since most of these crystals have to be grown from protic solvents. Further evidence of solvent occlusion along crystal defects is provided by Clifford (1962) and Barr et al. (1963), who have attributed the presence of "fine structure" in the broad-line NMR spectra of solid organic compounds (i. e., the existence of a narrow line as part of the broad-line spectrum) to mobile "liquid-like" molecules at crystal boundaries or dislocations.

Clifford (1967) has produced NMR data which suggests that some form of interstitial liquid - possibly trapped water in ice capillaries - is present in an ice lattice at $-12^{\circ}C$, which seems to confirm an earlier claim (Faraday 1850) that liquid water probably exists on ice surfaces well below $0^{\circ}C$.

1 : 4 : 3 Voltage Effects

Faraday's laws of electrolysis imply that the molar yield of products formed at the electrodes should be a function only of the

number of coulombs crossing the electrode interface. It should therefore be independent of the voltage gradient for a given current and always proportional to the first power of the current, yet, in the electrolysis of cellulose, Murphy (1963) found that, at voltages greater than that bringing about decomposition, the molar yield of gas per Faraday is proportional to $i^{1.25}$, where i is the current. Since the applied voltage was much larger than the decomposition potential, there was no basis in the theory of electrolysis to account for the excessive yield; an explanation was attempted, based on the quantum mechanical theory of electrolysis proposed by R. W. Gurney (1931), where neutralization of the ion occurs by wave-mechanical tunnelling between states of equal energy in the metal on the one hand and in the ion on the other. Murphy (1963) proposed that the liberation of gas at the electrodes created narrow gaps between the electrodes and the dielectric, giving rise to large field strengths (of the order of 10^6 V cm^{-1}, which led to field emission on the Fowler-Nordheim theory (see Murphy 1963). The field emission electrons were accelerated in the gap by the field and, on collision with the ions in the solid dielectric, created a small number of unstable, excited molecules which decomposed or reacted to produce some gaseous products, resulting in an excessive molar yield. This effect increased as the applied voltage increased because more kinetic energy would have to be disposed of by creating excited states.

Evidence in support of this is provided by investigations of chemical reactions occurring in electric discharges in gases at low pressures, where a large molar yield per Faraday was attributed to reactions between excited molecules generated in the discharge (Linder 1931).

1 : 4 : 4 Polarization Effect

Since most electrode systems are blocking with respect to ionic (protonic) conduction (i. e., energy is required to discharge the charge-carriers when they reach the electrodes), it is always difficult to obtain reproducible and meaningful conductivity results because of rapid polarization. The value of the conductivity therefore depends on which current is used, the initial, the equilibrium or any arbitrarily chosen value in between, so that it is desirable to specify a "true" current, one which is independent of polarization effects.

Significant in this respect is the work of Gross and Gravatt (publication pending - see Gravatt and Gross 1967), who found that for the compounds they investigated, a combination of polarization mechanisms were present and it was impossible to choose a "true" current. In some further work on organic solids (Gravatt and Gross 1967), the authors defined the conductivity by the equilibrium current. Although the magnitude of the conductivity was dependent on whether the initial or equilibrium value of the current was used, the value of the activation energy was independent of the current. The ratio of the initial and equilibrium conductivities was found to be temperature independent and the scaling method of Sutter and Nowick (1963) showed that the entire polarization process for each compound was characterised by one activation energy only, that for conduction. Thus, in order to compare the conductivity parameters among a series of compounds, it was not necessary to know the "true" conductivity if the comparisons were made primarily on the basis of the differences in activation energy.

1 : 4 : 5 Electrode Effects - Protodes - Space-Charge-Limited Currents

Experiments with a variety of metallic electrodes have indicated (Glasser 1960b) that the conductivity of oxalic acid dihydrate is unaltered by the electrode material. A similar observation has been reported in connection with some work done on haemoglobin (Rosenberg 1962), in which brass, aluminium, stainless steel and monel metal electrodes were tried, so it would seem that, in general, the conductivity of organic semiconductors is unaffected by the type of material used for blocking electrodes. However, considerable enhancement of conductivity has been reported (Thomas et al. 1969, observed a 10^{10} fold increase) with the use of "protodes", electrodes which are reversible to protons rather than to electrons (Shedlovsky 1952). Such electrodes will both supply protons to the conducting medium to prevent exhaustion of the current carriers, and will discharge protons without polarization occurring as the consequence of a progressive increase in the concentration of undischarged protons near the cathode.

An ion-exchange membrane was first tried as a protode (Eigen and De Maeyer 1958) to study the bulk conduction of ice, and later Williams et al. (1967) used saturated, acidified solutions of copper sulphate as protodes to investigate proton-conduction in single crystals of copper sulphate pentahydrate, but the protode generally used (Bradley 1957, Engelhardt and Riehl 1965, Riehl 1965, Thomas and Williams 1968, Thomas and Clarke 1969, Thomas et al. 1969) consists of finely divided palladium powder electrolytically deposited on a platinum or palladium plate from a bath of palladous chloride,and saturated with hydrogen by electrodecomposition of acidified water.

Space-Charge-Limited Currents

The use of proton-injecting electrodes gives rise to space-charge-limiting currents (see fig. 1 : 4.2), the significance of which will be best assessed after first summarising the relevant features of such effects.

According to the theory of space-charge-limiting (SCL) current (Shockley and Prim 1953, Rose 1955, Lampert 1956, 1964), the voltage dependence of the steady-state current for proton injection into a crystal containing traps, is given by

$$j = \theta\mu\varepsilon\,(V^2/d^3) \quad \ldots\ldots\ldots\ldots\ldots\ldots \quad (1:4.1)$$

Where j is the current density, V the applied voltage, d the crystal thickness, ε the dielectric constant and μ the drift mobility of free carriers. The coefficient, θ is the ratio of the density of free carriers to the total density of injected carriers in the crystal. Thus, for a perfect (trap-free) crystal, θ assumes the value 1. In the case of a discrete level of shallow traps of energy E_t,

$$\theta = \frac{N_c}{N_t} \exp\,(E_t - E_c)\,/kT \quad \ldots\ldots\ldots \quad (1:4.2)$$

where N_c is the effective density of states in the conduction band, N_t is the density of traps and E_c is the energy at the bottom of the conduction band. The Fermi-level, F, rises with injection level, but as long as E_t lies above F (as is the case for shallow traps), equation (2) holds, so that

$$j \propto V^2/d^3 \quad \ldots\ldots\ldots\ldots\ldots\ldots \quad (1:4.3)$$

The traps are said to be "deep" if the Fermi-level lies in or above an energy distribution of traps, and θ will be voltage-dependent. In the case of a uniform distribution of traps, the SCL current increases exponentially with voltage. For a distribution of traps which decreases with distance from the conduction band,

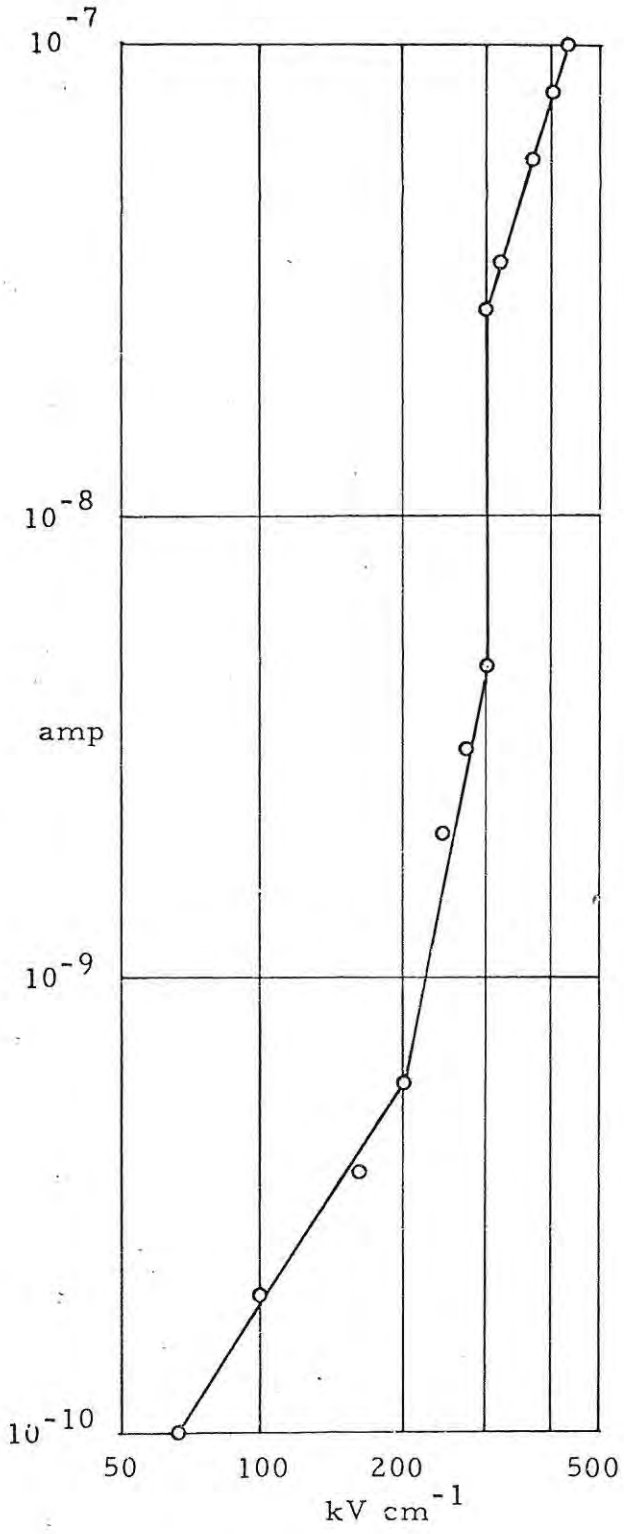

Fig. 1 : 4. 2. Typical current - voltage characteristic for a pure ice single crystal with proton injecting electrodes at 77 K.

(After Engelhardt and Riehl 1966)

$$j \propto v^{(T_c/T) + 1} \quad \ldots\ldots\ldots\ldots \quad (1:4.4)$$

where T_c $(\geq T)$ is a temperature which characterises the steepness of the trap distribution, such that

$$n_t \propto e^{-\Delta E/kT_c}$$

Thus, by measuring the voltage dependence of the current, the energy distribution of the trap density may be deduced.

Although at any voltage V, however small, there will be excess charge injected into the insulator, given by

$$Q = CV \sim \frac{\varepsilon}{d} V$$

(since $C \sim \frac{\varepsilon}{d}$; Lampert 1956)

there cannot be significant departures from Ohm's law until the average injected excess free proton density n_i becomes comparable with the thermally generated, hence neutralized, density n_o. The crossover voltage, V_t, from Ohm's law to SCL current injection is characterised by

$$V_t \sim \frac{qn_o d^2}{2\varepsilon\varepsilon_o} \quad \ldots\ldots\ldots\ldots\ldots \quad (1:4.5)$$

where q is the carrier charge and $\varepsilon, \varepsilon_o$ are the dielectric permittivities of the sample and of free space, respectively.

As the voltage is raised, and more charge is injected, there is a progressive filling of the traps. At the voltage, V_{TFL} at which all the traps are filled,

$$V_{TFL} \sim \frac{qn_t d^2}{2\varepsilon\varepsilon_o} \quad (1:4.6)$$

(where n_t is the trap density)

a very steep rise (see fig. 1 : 4. 2) in the current occurs, since $\theta = 1$ for $V \geq V_{TFL}$.

The family of (j, V) characteristics (fig. 1: 4. 3) form a closed triangle bounded by Ohm's law, the trap-free square law and the TFL law and consists essentially of two sub-families, one for which

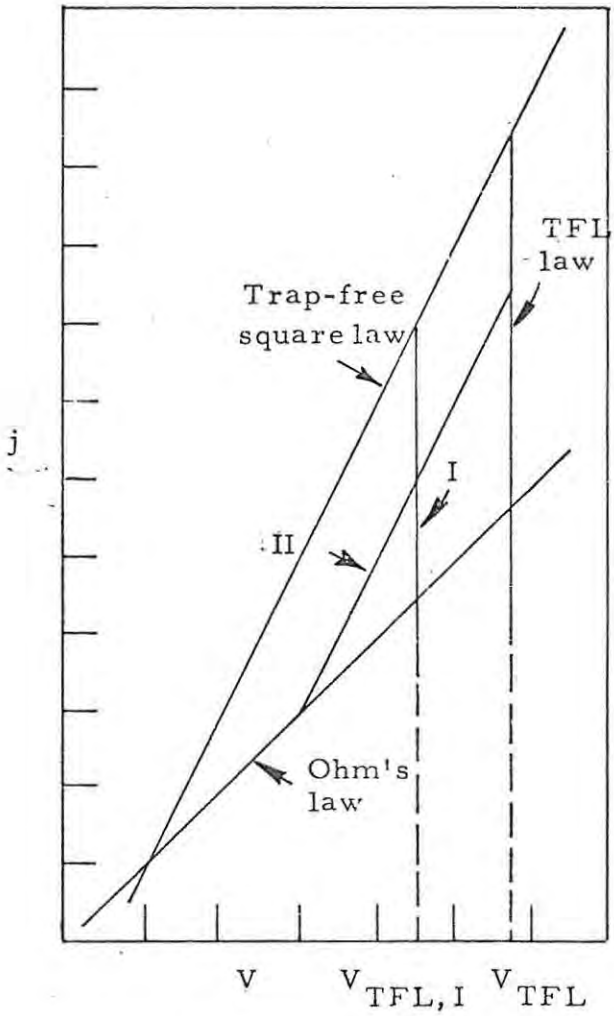

Fig. 1 : 4. 3. Schematic current-voltage (j,V) characteristics for one-carrier space-charge-limited current injection controlled by a single set of traps; log-log plot, each unit corresponding to a decade. I corresponds to F_o lying above E_t, II to F_o lying below E_t.

(After Lampert 1964)

E_t lies below F_o (curve I - deep traps) and the other for which E_t lies above F_o (curve II - shallow traps). Shallow traps have a cross-over voltage as well as a trap-filled limit voltage, whereas for deep traps, these two voltages are equal.

The condition applicable to an electrode in order for it to be injecting (Weisz et al. 1966) is

$$n_e > n_c \quad \ldots\ldots\ldots\ldots \quad (1:4.7)$$

where n_e and n_c are the densities of free protons in the electrode region and in the conduction band respectively. Since n_c depends on the applied voltage, the current will no longer be space-charge-limited for voltages at which condition (1 : 4. 7) is no longer satisfied. The current after this departure can either be ohmic or saturated (as in isocytosine - Thomas et al. 1969) depending on the nature of the electrode.

Although the origin of the traps in copper sulphate pentahydrate is not certain, the fact that the derived trap density (10^{13} cm^{-3}) compares quite favourably with that of ice, $6x10^{12}$ cm^{-13} (Engelhardt and Riehl 1965) and $Li_2 SO_4 . H_2O$, 10^{13} cm^{-3} (Thomas and Clarke 1969) led Williams et al. (1967) to consider that the chains of water molecules in the copper sulphate are involved. Furthermore, the effective proton mobility of copper sulphate, $1x10^{-5}$ cm^2 V^{-1} s^{-1} is comparable in magnitude with that of lithium sulphate, $6x10^{-5}$ cm^2 V^{-1} s^{-1}, evaluated from dielectric loss measurements (van Beek 1963). However, the much lower mobility for protons in lithium sulphate, determined by electrical measurement, $1x10^{-8}$ cm^2 V^{-1} s^{-1} (Thomas and Clarke 1969), serves to emphasise the fact that effective mobility values deduced from Child's law constitute lower limits, since the effect of traps is ignored. Only when the true mobility,

can be determined, will it be possible to formulate some general mechanisms for proton mobilities which would account for values ranging from 6×10^{-10} cm^2 V^{-1} s^{-1} (for potassium dihydrogen sulphate - O'Keefe and Perrino 1967) to 2 cm^2 V^{-1} s^{-1} (for isocytosine - Thomas et al. 1969).

The concentration of thermally produced charge carriers in lithium sulphate, 10^{11} cm^{-3} (Thomas and Clarke 1969) is in very good agreement with that calculated from the data of Gurevich and Zheludev (1960), for the same compound which means that since there are roughly 10^{22} protons per cm^3, only about 1 in 10^{11} of the total number of protons functions as carriers at room temperature.

SECTION 5 : ICE AS A MODEL FOR PROTON CONDUCTION

By virtue of its simple structure, ice is the most suitable "protonic semiconductor" on which to base a model for proton conduction in solids.

The oxygen atoms in the structure of ice Ih, the stable form of ice at 1 atmosphere pressure and at temperatures near $0^{\circ}C$, are arranged in a nearly perfect tetrahedral configuration, as suggested by Bragg (1921), but the protons are disordered (Pauling, 1935;1960) while obeying the Bernal-Fowler rules (Bernal and Fowler 1933), namely that:

1. There are two protons near each oxygen atom (thus the H_2O molecule is preserved in the ice structure).
2. There is only one proton on or near the line joining two oxygen atoms.

Breaches of these rules constitute point defects in the ice structure. For example: an ion-pair defect is created when thermal agitation causes a proton to jump to a free site near a neighbouring O atom (Fig. 1 : 5. 1a); a D, L pair of defects, known as 'Bjerrum defects' (after Bjerrum 1951) are created, when thermal agitation forces an H_2O molecule to rotate through 120° round one of its O-H. . . O axes. A D defect is a doubly occupied hydrogen bond (O-H. . . H-O) and an L defect is a vacant bond (O. . . . . O).

Glen (1969) has pointed out that repulsion of the two protons on an O-O linkage would make a D defect energetically unstable;

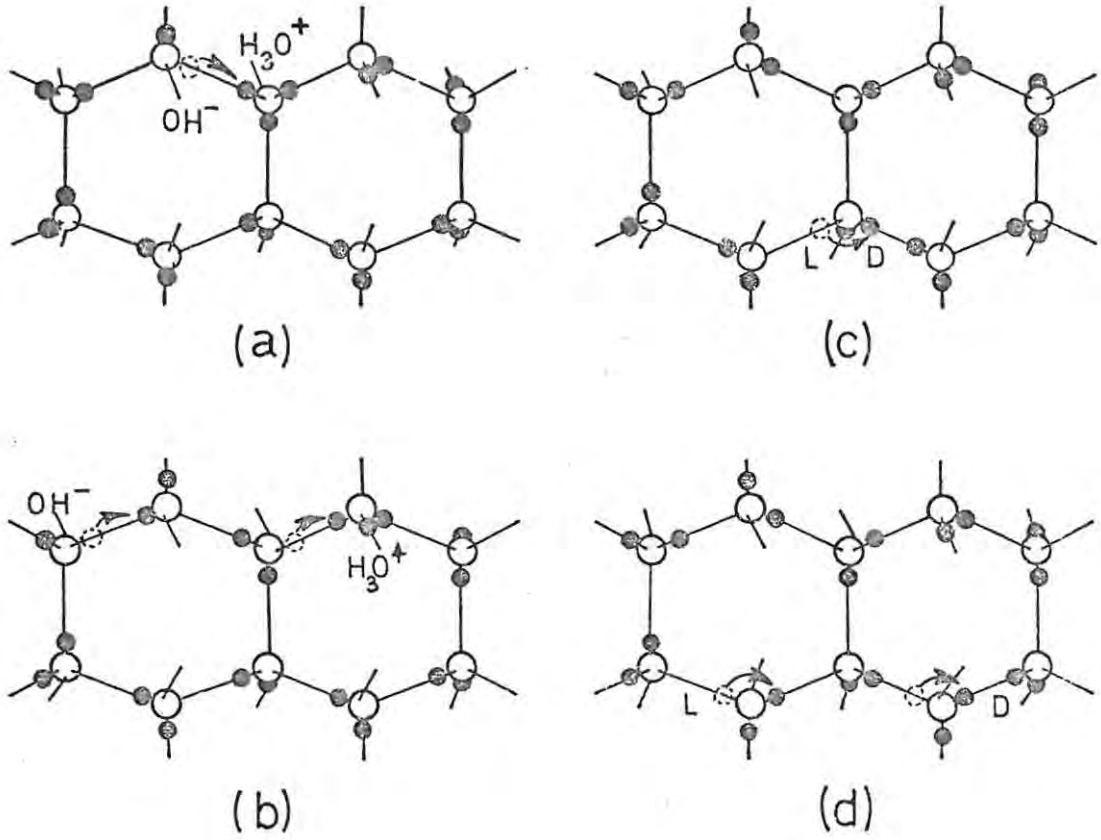

Fig. 1 : 5. 1 Diagram to indicate the creation and movement of electrical point defects in ice. (a) translation of a proton, creating an excess- and defect- proton pair (ionization) (b) migration of the excess- and defect- proton (c) rotation of a water molecule creating a pair of L- and D- defects (d) migration of the L- and D- defects.

(After Glen 1969)

calculations by Eisenberg and Coulson (1963) have shown that equilibrium will be attained if two protons expand the O-O distance of the D defect by 0.5 A^{o}, but it must be borne in mind that such an expansion will raise the energy of the immediate surroundings. Other investigators have considered the possibility that one (Dunitz 1963) or both (Cohan et al. 1962) of the O-H bonds associated with a D defect are rotated with respect to the O-O linkage.

There is no direct evidence for the existence of D- and L- defects, but the interpretation of the observed dielectric properties and conductivity of ice in terms of these defects (Gränicher et al. 1957, Jaccard 1959, Onsager and Dupuis 1962, Onsager 1969, Onsager and Runnels 1969), shows good agreement. Most of these results are summarised by Gränicher (1963) and by Jaccard (1965).

Bjerrum (1951) and Gränicher (1958) have considered and rejected many alternative mechanisms for re-orientation of ice molecules, from which it would seem that conduction in ice almost certainly involves ionic defects (Bjerrum 1951, Eigen and De Maeyer 1958, Eigen, De Maeyer and Spatz 1964). However, some of these ionic defects may be trapped by orientational defects forming associations with ionic defects (Eigen and De Maeyer 1958, Onsager and Dupuis 1962), or with interstitial molecules (Haas 1962), and may thus make no contribution to the conductivity.

The conduction process in ice is probably initiated by ion-pair defect formation (Fig. 1 : 5. 1a), after which the proton quickly migrates through the crystal, along the chain of hydrogen bonds, by a mechanism of co-operative tunnelling (Fig. 1: 5. 1b). The movement of this proton turns the molecules in the chain into a reversed orientation so that no other proton can pass. However, the chain can be re-oriented to

permit further conduction, by the migration of a D defect from the anode to the cathode, or in the opposite direction for an L defect (Fig. 1 : 5. 1d). Eisenberg and Kauzmann (1969) have pointed out that, although the rate of proton jumps is very rapid, the concentration of jumping protons is so small that the frequency of jumps per molecule is small. Thus re-orientations at a given molecule are much more frequent than are proton jumps, and the observed energy of activation for conduction is

$$E = \tfrac{1}{2}E_d + E_m \qquad \text{(Riehl 1965)}$$

where E_m is the activation energy for proton migration

E_d is the dissociation enthalpy $\sim$ 22.5 kcal mol^{-1}

(Eigen, De Maeyer and Spatz 1964)

$E \sim$ 11.5 kcal mol^{-1} (Murphy 1950).

Therefore E_m is approximately zero and the migration of excess and defect protons must take place via a tunnelling process.

If the usual metal (blocking) electrodes are applied, the charge carriers in the stationary current have to be supplied by thermal dissociation within the crystal only. The activation energy for defect proton transfer is higher than that for excess proton transfer since the potential function is steeper in the former (Eigen and De Maeyer 1958). Thus - apart from electrode effects - for $\mu^+ \sim 50\ \mu^-$ (Bullemer et al. 1969), a steady polarization occurs due to the different concentration gradients of the positive and negative charge carriers in the bulk of the crystal.

The mechanisam for conduction in ice Ih may be summarised as follows:

1. Ion-pair defect formation by thermal activation (ionization).
2. Migration of these ionic defects by tunnelling, which reverses the array of protons, preventing further conduction along the same chain.
3. Re-orientation of the chain by thermal orientational defects, which are usually present in sufficient concentration to ensure prompt re-orientation; at very low temperatures, the concentration of Bjerrum defects will be low, but the chain can be re-oriented by L defect injection at the cathode, and subsequent migration of the L defect to the anode. (Engelhardt et al. 1969).

SECTION 6 : A SURVEY OF PROTON CONDUCTION MECHANISMS FOR SOLIDS

Although the primary interest here is in organic protonic semiconductors, a considerable amount of work has been done on the inorganic analogues; the mechanisms elucidated in these solids are of great relevance to the study of organic protonic semiconductors.

In general, two modes of charge transport by protons are possible in a hydrogen bonded solid. The first is by a Grotthuss-type hopping mechanism in which there is a co-operative movement of the protons along a hydrogen-bonded chain (e. g. , ice) and the second is by an interstitial Frenkel- or Schottky-type mechanism. Since intersitial protons have to overcome electrostatic interaction with structure through which they pass, whereas co-operative movement of the protons along hydrogen bonds only involves proton shifts between energy minima within hydrogen bonds, Grotthuss-type conduction should predominate. Thus, Wise (1967) favoured a Grotthuss-type mechanism rather than an interstitial mechanism to account for the relatively high conductivity of ammonium perchlorate, as compared to the alkali halides, as well as to explain the marked influence gaseous ammonia has on the conductivity. The mechanism proposed involved movement of a proton from an ammonium ion in the structure to an ammonia molecule located at a lattice vacancy or at an interstitial position. The neutral ammonia molecule thus formed at a lattice site may then become the recipient of a proton from an adjacent cation in the lattice. By this means, charge transport is greatly facilitated over that associated with excess proton migration via Schottky or Frenkel defects.

However, in a system of isolated hydrogen-bonded units such as in KHF_2, Pollock and Sharan (1967) have proposed proton conduction by an interstitial mechanism, initiated by Frenkel defect formation. They considered the lattice structure (Rogers and Ubbelohde 1950) to be sufficiently open for the observed activation energy for conduction (21.7 kcal mol^{-1}) to be due to ionic defect formation only. This energy is less than that calculated to break an F-H-F hydrogen bond (27kcal) since the presence of neighbouring F ions facilitates the removal of the proton.

1 : 6 : 1 Hydrogen Bonds to Oxygen - Hydrates

The proton conduction mechanisms proposed for crystal hydrates such as borax (Maricic et al. 1962), Giesekke and Glasser 1967), lithium sulphate monohydrate (Maricic et al. 1961, Thomas and Clarke 1969) and copper sulphate pentahydrate (Williams et al. 1967) all involve the waters of hydration. A typical mechanism of conduction in this group is that proposed for $Li_2SO_4.H_2O$ (Thomas and Clarke 1969), where bulk protonic conductivity is favoured only along the b axis. Since the waters of crystallization form a continuous hydrogen-bonded chain along this axis, it was proposed that conduction was aided by transmission of the thermally generated oxonium ions along the chain, as in ice. However, the large amplitude thermal oscillations of the water molecules are insufficient to re-orient the chain for further conduction, a process which would require a 60° rotation of the water molecules, so it would seem that, in the absence of free rotation, it is necessary to invoke L defect injection at the cathode to re-orient the chain (see Engelhardt et al. 1969).

1 : 6 : 2 Hydrogen Bonds to Oxygen - Non-Hydrates

Cellulose molecules consist of long chains of cellobiose units with the group HCOH repeated at regular intervals. Because of similarities in the infra-red spectra and dielectric constants of water and cellulose, Murphy (1963) made two assumptions to explain proton conduction in cellulose, namely that:

1. The HCOH groups can ionize according to the equation
   $2(HCOH) \rightleftarrows (HCOH_2)^+ + (HCO)^-$
2. The time involved in the penetration of the potential barrier by the proton is much smaller than the relaxation time for changes of orientation of molecules and ions (Wannier 1935).

The latter assumption implies that the mobility of the proton is determined by the lability or local mobility of the molecule or of sections of the crystal structure, and the main influence of the introduction of tunnelling into the model is to select the proton as the charge carrier, rather than a larger ion.

The energy of dissociation, E_d and the energy of activation for mobility, E_m, were obtained from the theoretical, two-term ionic conduction expression.

$$\sigma = \sigma_1 \exp[-(\tfrac{1}{2}E_d + E_m)/RT] + \sigma_2 \exp(-E_m/RT)$$

where the second term is ascribed to impurities which have a negligible energy of dissociation into ion pairs in the solid (Koch and Wagner 1937). Using experimental results previously obtained (Murphy 1960) and the above equation, Murphy calculated that

E_m = 10.6 kcal mol^{-1}

E_d = 40.6 kcal mol^{-1}

Since for ice (see section 5) $E = \frac{1}{2} E_d = 11.5$ kcal mol^{-1} (Murphy 1950), the value of 10.6 kcal mol^{-1} for the charge-carrier mobility of cellulose was interpreted as an activation energy derived from the need to break two hydrogen bonds simultaneously in order for the HCOH groups to assume an orientation favourable to tunnelling (the strength of a hydrogen bond being about 5 kcal mol^{-1}).

For ammonium dihydrogen phosphate (ADP), as for cellulose, consideration of the roles of tunnelling and relaxation in the mobility of the protons in ice led Murphy (1964) to propose a similar mechanism of self-ionization and subsequent tunnelling between states of equal energy. By doping the crystal with Ba^{2+} and SO_4^{2-} ions, Murphy obtained an average energy of activation for the mobility of 10.5 kcal mol^{-1}, again in good agreement with that for water, and an activation energy for ion pair formation of 19.8 kcal mol^{-1}.

Pollock and Sharan (1969) have since confirmed Murphy's finding that the protons in ADP are mobile, but they warn that the impurities can interrupt the H-bond chains and thus provide greater numbers of "short" defective chains. A comparison of the conductance and diffusion results obtained by Pollock and Sharan also shows that the Einstein relation is not obeyed; the deviations have been interpreted in terms of correlated proton jumps in the crystal.

From structural considerations, Mata Arjona and Fripiat (1967) consider that the mode of formation and diffusion of defects in boehmite is similar to that in ice, but that thermally created Bjerrum defects, as contrasted to injected defects, are less probable since the small

separation of the D defect protons (0.70 A^{o}, as compared to 0.80 A^{o} in ice and 0.74 A^{o} in H_2), would necessitate the twisting of the O-H bond with respect to the Al-O bond to an unrealistic extent. Conduction is by an excess or defect proton mechanism. Ion-pair defects facilitate proton transfer along the O-H . . . O zig-zag chain which characterises the hydrogenic structure of boehmite. No mechanism of re-orientation of the chain was proposed, but L defect injection at the cathode, as in ice (Engelhardt et al. 1969) certainly seems possible.

The proton conduction mechanism for KH_2PO_4 (KDP) proposed by O'Keefe and Perrino (1967) is one of the few complete mechanisms discussed by investigators in this field. Since this mechanism differs from that of water in that there is no need to invoke molecular rotation, it will be dealt with more fully.

The structure of KDP (Slater 1941) is equivalent to the generally accepted model for the disposition of the protons in ice (Pauling 1960), the stable, low-temperature form having both the protons which are associated with each PO_4 group either on upper or lower oxygens (Fig. 1 : 6. 1a). Part (b) of the Figure shows a crystal with a chain of M defects (one proton on an upper and one on a lower oxygen so that the associations within the crystal are unchanged) terminating in an L- and a D- defect (a vacant and a doubly occupied band, respectively). The numbered arrows in part (c) show the possible sequence of proton jumps, resulting in excess- and defect- proton migration. The steps are:

1. intrabond motion, creating an ion pair:

$$2H_2PO_4^- \rightarrow HPO_4^{2-} + H_3PO_4$$

2. ion migration by intraband motion involving

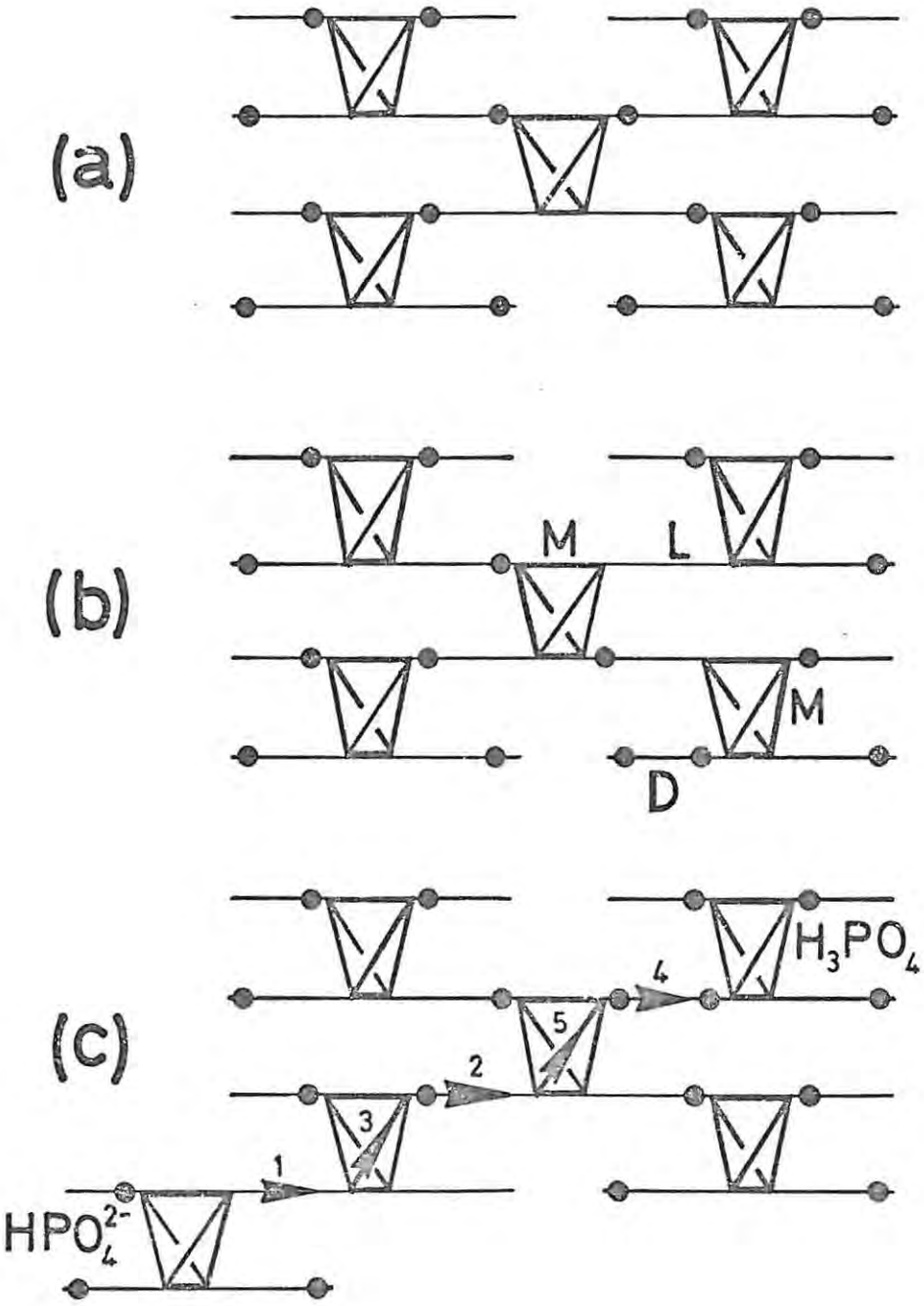

Fig. 1 : 6. 1 Proton configurations in KH_2PO_4. The horizontal lines represent hydrogen bonds between PO_4 tetrahedra; the small filled circles represent hydrogen atoms. (a) "perfect" ferroelectric KH_2PO_4 (b) a crystal with a chain of M defects terminating in an L and D defect (c) formation of an ion pair followed by migration of H_3PO_4. The numbered arrows represent a possible sequence of jumps in going from the perfect crystal (a) to the final situation shown.

(After O'Keefe and Perrino 1967)

formation of an M defect:

$$H_3PO_4 + H_2PO_4^- \rightarrow (H_2PO_4^-, M) + H_3PO_4$$

3. interbond jump creating an L and D pair, and removing M:

$$(H_2PO_4^-, M) \rightarrow H_2PO_4^- + L + D$$

4. intrabond jump creating an M defect, as in step 2:

$$H_3PO_4 + H_2PO_4^- \rightarrow (H_2PO_4^-, M) + H_3PO_4$$

5. removal of the M defect by intrabond jump:

$$D + (H_2PO_4^-, M) \rightarrow H_2PO_4^- + D$$

Steps 4 and 5 constitute the migration process.

As in ice (Kröger 1964, Jaccard 1959, and Gränicher 1963), proton migration in KDP must be followed by D- or L- defect migration to re-orientate the chain for subsequent conduction. There is an additional premium in KDP, however, on having both ions and D- and L- defects migrate simultaneously, as migration of one defect alone through the crystal would leave behind a chain of M defects, which would raise the energy of the crystal as a whole.

As has been discussed particularly by Jaccard and by Gränicher for ice, a mechanism such as steps (4) and (5) will proceed at a rate equal to that of the slower step. Since, in the case of KD_2PO_4, the low-temperature activation energy for conductivity is the same as that for interbond jumps of deuterons (Schmidt and Wehling 1962), the jump of an L defect (step 5) will be the slower step. Substitution of HSO_4^- for $H_2PO_4^-$ leaves a hydrogen bond without a hydrogen atom (an L defect) so that, for a doped sample, the conductivity is given by the standard relation:

$$\sigma = N_L q \mu_L$$

but where N_L is the concentration of L defects (which is equal to the sulphate concentration) of mobility μ_L and charge q.

Using this equation, and the measured conductivity of 25°C, O'Keefe and Perrino calculated a value for μ_L of 6×10^{-10} $cm^2 V^{-1} s^{-1}$.

1 : 6 : 3 Hydrogen Bonds to Nitrogen

Polyamides (long-chain polymers in which the chains are cross-linked by hydrogen bonds of the type $\geq C = O \ldots HN \leq$) are partly crystalline and partly amorphous. Eley and Spivey (1961) have suggested that the high conductivity of these polyamides is due to the generation of protonic charge carriers by a self-ionization process. Below the transition temperature (in the crystalline region), the rate determining process in the conduction is one of rotation of chain segments, which is a necessary preliminary to transfer of protons between amide groups on neighbouring chains. Since chain rotation is ruled out in proteins, proton conduction cannot occur in these structurally rather similar compounds.

The crystal structure of imidazole (Martinez-Carrera 1966) shows that the intermolecular N-H ... N separation of 2.81 A° is much less than an average value for hydrogen-bonded nitrogens of 3.07 A° (Wallwork 1962), so that facile proton tunnelling will be favoured, as suggested by Riehl (1965). There is now ample evidence of this, since, just as in ice, proton exchange between neutral imidazole and the imidazolium ion (or the imidazole anion) in the hydrogen bonded chain can occur rapidly (Joop and Zimmermann 1962, Ralph and Grunwald 1968).

Kawada et al. (1970) have utilized the postulate (Riehl 1965) that proton defects are necessary to maintain a steady current in solid imidazole. The mechanism they proposed is similar to that of Riehl's and parallels that in ice, namely, the thermal generation of an ion pair defect (Fig 1: 6 . 2b) in a properly oriented, hydrogen-bonded chain, (a), followed by migration of the imidazolium ion to the cathode under the action of the field, (c), which leaves the chain disoriented, (d), preventing further conduction along that chain. The injection of an L defect at the negative electrode by the discharge of the proton rotates each molecule successively as the L defect passes down the chain, (e),until the proper orientation is regained, (f).

Ice usually has a sufficient concentration of Bjerrum defects to effect prompt re-orientation, but the thermal concentration of these defects in imidazole is expected to be very low because of the extremely small inter-proton distance of 0. 59 A^{o} (Will 1969) calculated for a D defect, as compared to 0. 74 A^{o} for H_2. Therefore L defect injection and its movement was considered to be the limiting process, so that the effective mobility of the proton ($\sigma = N q \mu$) should be much less than that in ice (which is 1 $cm^2 V^{-1} s^{-1}$ at $-10^{o}C$). In view of the small intermolecular N-N distance (2. 81A^{o}), rotation of an imidazole molecule about an axis in the plane of the molecule and perpendicular to the chain would require a considerable amount of energy to expand the lattice about the rotating molecule, so Kawada et al. ascribed the observed energy of activation for conduction (40 kcal mol^{-1}) to molecular rotation.

On the other hand, Daycock et al. (1968), using NMR pulse techniques, calculated rotation rates of 1 Hz with an activation energy of 3. 7 kcal mol^{-1} for imidazole. However, it is not known whether

charge generation

(a)

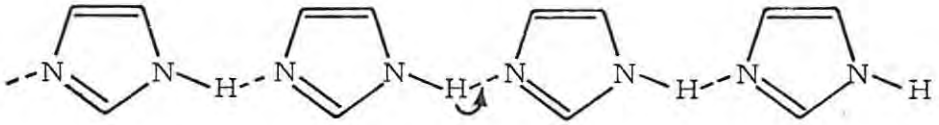

(b)

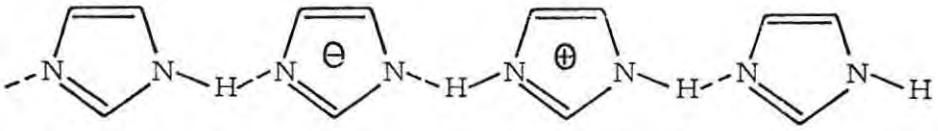

carrier transport and discharge at electrodes

(c)

anode

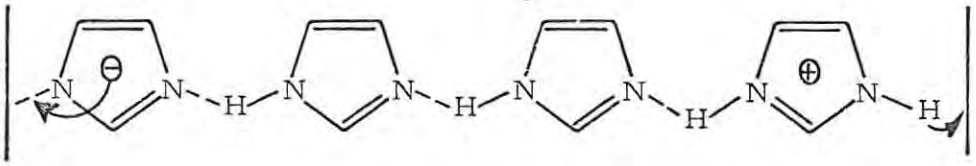

cathode

re-orientation

(d)

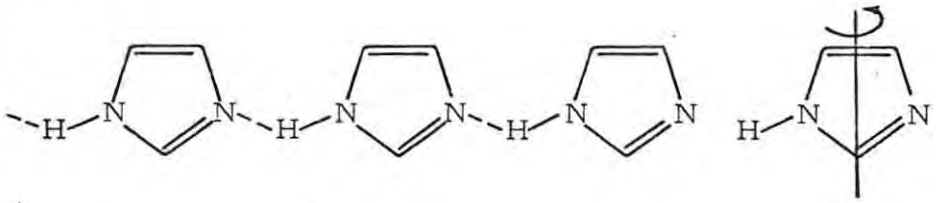

(e)

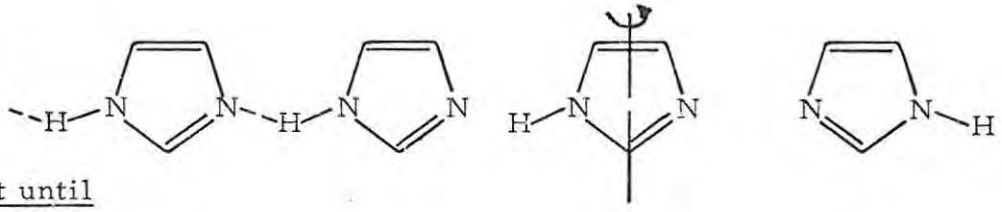

repeat until

(f)

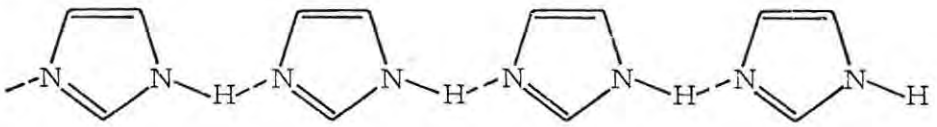

Fig. 1 : 6. 2. A series of steps showing the proton conduction mechanism in imidazole.

(After Kawada et al. 1970)

this rotation is the same as that involved in the conduction mechanism. Daycock et al. were, however, able to test the validity of the conduction mechanism for imidazole proposed by Riehl (1965), as follows. Using the rotation rate of 1 Hz, a lower limit for proton mobility can be estimated, by assuming rotation to be random (although all the molecules can rotate). Thus, for an average intermolecular separation of 5 A^{o}, the estimated mobility will be 10^{-8} cm^2 V^{-1} s^{-1}. If the observed mobility, calculated from the conductivity formula, $\sigma = Nq\mu$, is significantly greater than the estimated value, then rotation cannot be the rate-determining step in the conduction mechanism. Assuming that all the molecules can act as proton transmitters (so that $N = 10^{22}$ cm^{-3}) and taking a value of 10^{-11} ohm^{-1} cm^{-1} for the specific conductivity (Brown and Aftergut 1963), an observed value for mobility of 10^{-4} cm^2 V^{-1} s^{-1} is obtained on substitution into the conductivity formula. It is therefore apparent, from the ratio of the estimated and observed mobilities, that rotation will be rate-determining, even if only 1 in 10^6 of the protons participate in conduction, and Riehl's (and Kawada et al.'s) mechanism is acceptable.

Since rotation appears to be the rate determining step in the conduction mechanism for imidazole, the processes of dissociation, translation and rotation will all contribute to the activation energy for conduction (see section 1:9). Although the activation energy for translation within the hydrogen bond chain is probably negligible, the dissociation energy should be appreciable, so that the assumption made by Kawada et al., that the activation energy for conduction is attributable to rotation only, is incorrect.

Since the conductivity of a hydrogen-bonded solid is dependent on both the transfer and re-orientation of protons along the chains,

any perturbation of the molecules in the chain could affect the conductivity so that the experimentally determined activation energy for conduction is not always a direct measure of the potential barrier met by the proton. The point is illustrated in the case of lithium hydazinium sulphate, $L_i(N_2H_5)\,SO_4$, a solid in which conduction parallel to the c-axis is effected by proton transfer along the ...N-H... N-H ... chains via a vacancy mechanism (Vanderkooy et al. 1964). A large decrease in the second moment of the proton magnetic resonance signal of this compound was observed by Cuthbert and Petch (1963) between 25 and 160°C; this decrease they attributed to the onset of hindered rotation of the $-NH_2$ groups about the N-N axes, which introduced disorder in the N-H chains and resulted in a decrease in the conductivity. Since the degree of disorder also has an exponential dependence on temperature, these two contributions to the activation energy cannot be readily separated. Consequently, the measured value of 19.6 kcal mol^{-1} is a composite value and not a direct measure of the potential barrier encountered by the proton in jumping from one $-NH_2$ group to the next.

SECTION 7 : NATURE OF THE ELECTRODE PROCESSES

1 : 7 : 1 Cathode Reaction

The cathode reaction in proton conduction usually involves the discharge of a proton at the cathode solid interface, either by the injection of a hole, which then migrates to the anode via the movement of an L defect, or by the discharge of an excess or interstitial proton. There is usually no further chemical reaction, according to observation and discussion in numerous papers.

1 : 7 : 2 Anode Reaction

Murphy (1963) in his work on cellulose, is one of the few investigators who have endeavoured to formulate an anode reaction, comment usually being limited to the observation that "a black, scaly deposit" formed at the anode!

Proton conduction in cellulose leads to the appearance of $(CHO)^-$ groups (that is, proton holes) at the anode, which are neutralised by electron capture. Murphy (1963) assumed the neutral molecule so formed to be unstable, dissociating into CO and CO_2, along lines similar to the spontaneous thermal dissociation of cellulose, and that neutralization produced either a CO or a CO_2 molecule, with a definite probability(say, 0.5, for each) so that the total yield of $H_2+CO+CO_2$ is 1.5 moles per Faraday. This is in agreement with the experimentally determined yields of gas, at different voltage gradients, within a factor of 2.

In general, the gaseous products of the anode reaction cannot be stoichiometrically accounted for, which is not surprising, in view of

the large quantities of carbonaceous residue usually formed on the anode surface; which perhaps explains the reluctance of investigators to deal with this aspect of the conduction mechanism.

SECTION 8 : REQUIREMENTS FOR PROTON CONDUCTION

A survey of the literature on proton conduction has revealed that a Grotthuss-type mechanism of conduction prevails in almost every case, KHF_2 being the only exception. The following basic requirements are necessary for proton conduction to occur in (organic) solids by a non-interstitial mechanism:

1. The crystal structure must exhibit a linked hydrogen-bonded network in the form of chains, sheets or spirals.
2. The proton in the hydrogen bond must be sufficiently mobile to be able to surmount (or tunnel through) the energy barrier separating the two potential energy wells, under the action of the field.
3. The hydrogen-bonded chain must be capable of re-orientation, either by molecular rotation or by intrabond proton jump.

SECTION 9 : A GENERALISED MECHANISM FOR PROTON CONDUCTION IN ORGANIC SOLIDS

The conduction mechanism proposed by Kawada et al. (1970) for imidazole is really quite versatile and can be extended to suit most organic solids.

Thus, a general mechanism for intrinsic conduction by proton transfer in organic solids with chains of hydrogen bonds, which comply with the postulates already laid down for proton conduction, should proceed as follows:

1. Charge-carrier initiation by thermal dissociation of a molecule in a properly oriented hydrogen-bonded chain, forming an excess proton (i. e., a proton associated with a neutral molecule, e. g., H_3O^+) and a proton hole (i. e., a proton vacancy, e. g., OH^-)

2. Migration of the excess proton along the chain by sequential (Grotthuss-type) hopping of the excess proton between neutral molecules in the direction of the cathode

3. Migration of the proton hole to the anode by a similar process to that in step (2), but involving sequential transfer of protons in the direction of the cathode between proton holes

4. Steps (2-3) reverse the array of protons so that no further proton transfer along that chain can occur until the chain has been re-oriented by Bjerrum defect migration.

The following implications are inherent in this model:

1. Although the mobility of the proton hole is determined by movement of the proton, the activation energy for mobility of the proton in the case of the hole is greater than that of the excess proton because of the differences in the shapes of the potential well across which the transfer is occurring, so that the mobility of the proton hole is less than that of the excess proton. On the other hand, the mobility of the excess proton is just that of the proton moving between neutral molecules (Glasser 1960c, Eigen and De Maeyer 1958).

2. When charge-carrier initiation takes place in the bulk of the crystal, both excess and defect protons must be mobile for steady-state conduction to be secured. If only excess protons are mobile, then carrier initiation must occur at the anode/solid interface.

3. If the hydrogen bond length in the solid is small, the large energy of formation of D defects will reduce the thermal concentration of Bjerrum defects so that it might be necessary to invoke L defect injection at the anode, and subsequent migration, to facilitate re-orientation (Engelhardt et al. 1969, Kawada et al. 1970).

4. The mechanism for conduction involves a number of processes, each having its own rate constant (k) and activation energy (E). The order in which these processes are involved in the mechanism is

   a. dissociation k_d, E_d
   b. translation k_m, E_m
   c. re-orientation k_r, E_r

If dissociation leads to the formation of two charge carriers, then the observed activation energy for conduction has the components

$$E = \tfrac{1}{2}E_d + E_m + E_r$$

All the energy components up to, and including, the rate-determining step, will contribute to E. For example, in ice, mobility is the rate-determining step, so that

$$E = \tfrac{1}{2}E_d + E_m$$

5. When there is no carrier injection and current flow is governed solely by the charged species produced thermally within the crystal, the conductivity is, in general, described by the relation:

$$\sigma = (n_+\mu_+ + n_-\mu_-)\ q$$

where n_+ and n_- are, respectively, the concentration of the positively and negatively charged species: $\mu_\pm$ and q, are the mobilities and the electronic charge. In practice, owing to the dominance of protonic charge carriers, the equation may be written:

$$\sigma = n_+\mu_+ q$$

SECTION 10 : DETECTION OF MOBILE PROTONS

1 : 10 : 1 Nuclear Magnetic Resonance (NMR)

A necessary, but not sufficient, condition for a solid to be a proton conductor, is the existence of a linked hydrogen bonded network; in addition, the solid must also be characterised by a high degree of mobility of the protons in the hydrogen bridges, a point which is illustrated by the case of oxalic acid dihydrate (OAD), a compound which is not considered to be a proton conductor (see section 1:3), despite the presence of spirals of hydrogen bonds along the b axis. The NMR spectrum of OAD does not exhibit any motional narrowing of the absorption curve (Richards and Smith 1951, et al. 1953), indicating that the protons are firmly bound since, according to Gutowsky and Pake (1950) and Andrew (1950), any motion of the protons within a solid will reduce the line width (or the second moment, which is a measure of the line width) of the NMR signal.

A line-narrowing process in the NMR spectra of pentaerythritol, $C(CH_2OH)_4$, which takes place at temperatures just below the transition to the "plastic" phase (Smith 1969) suggests the possibility of this hydrogen-bonded compound being a proton conductor.

Information on the role of the water molecules and the proportion of "free" protons which participate in the conduction processes of borax (Maricic et al. 1962) and of $Li_2SO_4 \cdot H_2O$ (Maricic et al. 1961) was gleaned from studies of the temperature dependence of the intermolecular second moment of the PMR signal of these compounds.

1 : 10 : 2 Infrared Spectroscopy

Infrared spectroscopy has proved to be another useful tool in the examination of proton transfer in solids. Spectroscopic evidence for the formation of $^{+}$NH ... N hydrogen bonds led Fripiat et al. (1970) to postulate proton transfer along the $^{+}$N-N axis of a system consisting of layers of ammonia adsorbed on the hydroxylated surface of an Aerogel (amorphous silica partially covered by silanol groups - Fripiat et al. 1970).

The energy of activation for diffusion of the protons in boehmite, obtained from the infrared spectra of the progressively deuterated mineral (Mata Arjona and Fripiat 1967), has been correlated with that for defect ion pair formation, a process which is linked with the conduction mechanism.

1 : 10 : 3 Dielectric Measurements

According to postulates (1) and (2) (see section 1 : 8) a proton-conducting solid must have the attributes of an easy mobility of the protons in the hydrogen bridge and the molecule must be capable of rotation. These properties will be reflected in the dielectric dispersion curves.

When the dielectric loss and d. c. conductivity of polyamides were first studied by Baker and Yager (1942), they found two loss maxima, one at low frequencies, which they associated with a proton transfer between neighbouring amide groups, and one at higher frequencies, which they associated with conventional dipole orientation loss.

The relationship between proton conduction and dielectric loss due to mobile protons has been extensively studied in ice (Steinemann and Gränicher 1957, Steinemann 1957, Jaccard 1959 and Auty and Cole 1952).

Steinemann found that pure ice had a dielectric loss region with a tan δ maximum at about 12 kHz, which he ascribed to motion of protons over molecular distance due to molecular rotation (Bjerrum defects). Steinemann and Gränicher (1957) introduced lattice defects into the ice structure by HF doping, which caused a second loss region to appear at frequencies below 100 Hz. This low-frequency dispersion was interpreted as a space-charge polarization due to mobile protons in the ice being unable to be discharged at the electrodes, resulting in very high values of the dielectric constant and loss.

The available dielectric data on other known proton conductors, for example, lithium sulphate monohydrate (van Beek 1963a, 1963b), tincalconite (Giesekke 1965b) borax (Giesekke and Glasser 1967) and imidazole and urea (Chan-Henry and Glasser 1970b), all also display the high- and low-frequency loss regions exhibited by ice, so it would seem that this dispersion profile is characteristic of an ionic (protonic) conductor.

The mobility, μ, and the concentration, N (per m^3), of the mobile protons, can be calculated from the low-frequency dispersion region in terms of the theory of Macdonald (1953). For the special case where only charge carriers of one sign (e. g., protons) are mobile, (Van Beek 1963a) a dielectric dispersion effect will have the relaxation time

$$\tau_1 = \left(\frac{L}{\mu}\right)\left(\frac{\varepsilon_o \varepsilon_\infty}{2N_1 kT}\right)^{\frac{1}{2}}$$

where subscript 1 is used to denote space charge, L is the distance between the electrodes, ε_o the dielectric constant of vacuum (8.85×10^{-12} farad m^{-1}) and k, T have the usual meaning. This equation is in a form suitable for use with S. I. units. The concentration, N, may be determined by use of the equation:

$$N_1 = 2kT \frac{\varepsilon_c}{\varepsilon'_\infty} \left(\frac{\varepsilon'_s}{qL}\right)^2$$

where subscripts s, ∞ denote the static dielectric constant and the dielectric constant at infinite frequency, respectively.

It must be noted that although many investigators have proposed proton conduction in solids on the strength of their dielectric results only, proof of proton conduction is conclusive only when these measurements are accompanied by identification of the electrolysis gas as hydrogen, although electrode reactions can disturb even this conclusion (e. g. Na^+ is the cationic charge carrier in an aqueous NaCl solution, but H_2 gas is evolved at the cathode).

1 : 10 : 4 Direct Current Measurements and Electrolysis : Identification of the Cathode Gas

Direct current measurements on a solid proton conductor will show the following characteristics:

1. if blocking electrodes are used, a time-dependent current will be observed at constant applied voltage
2. if the blocking electrodes are replaced by non-blocking electrodes, a drop in the resistivity will be observed (see section 1 : 4 : 5)
3. conduction will be anisotropic in non-cubic systems, and will be favoured along the directions containing the hydrogen bonds. For example, the conductivity of imidazole in the hydrogen-bonded c-direction is 10^3 times that in the a-direction (Kawada et al. 1969)

Electrolysis of a solid affords the simplest and the most direct means to distinguish between electronic and ionic conduction, when

ionic conduction leads to the formation of gaseous products at the electrodes. King and Medley (1949) were the first to use this technique when they investigated the nature of the d. c. conduction in swollen polymers. Since then, many investigators engaged in the field of proton conduction have used this technique, and the apparatus has evolved along two lines:

a. Cells of the type used by Maricic et al. (1961) in which gas at each electrode is separately collected and monitored by the displacement of mercury. The cathode gas is introduced into $PdCl_2$ solution and the precipitation of elemental Pd is taken as proof of hydrogen evolution (Maricic, Pravdic and Veksli 1962). Mass spectroscopic identification of the gas, as in the present work, may also be undertaken. Variations of this design have since been reported by Schmidt (1965), Pollock and Sharan (1967) and Chan-Henry and Glasser (1970a, 1970b).

b. Cells of the type used by Kakiuchi et al. (1950) in which the pressure of the evolved electrolysis gas is monitored in a pre-evacuated system. The lines in the discharge spectrum of the electrolysis gas were identified as those belonging to the hydrogen spectrum. Murphy (1963, 1964) has used cells of a similar design and has employed condensation and analytical techniques to identify the various electrolysis gases.

As the hydrogen ion is univalent and the hydrogen molecule diatomic, the molar yield of hydrogen, according to Faraday's laws of electrolysis, should be 0. 5 moles per Faraday, assuming all the

charge to be transported by protons. Since the hydrogen is collected under known conditions of temperature and pressure, the number of moles per Faraday collected may be calculated. The "current efficiency" is then defined as the ratio of the experimental to the theoretical yield of hydrogen, multiplied by 100.

CHAPTER 2

EXPERIMENTAL

SECTION 1 : PLAN OF THE PRESENT WORK

Proton conduction has been established in a variety of materials, of which ice is a prime example. To date, a great deal of attention has been focussed on inorganic compounds and crystal hydrates, and some detailed mechanisms for conduction in these compounds have been proposed.

The study of proton conduction has now advanced to a stage where attempts can be made to relate the structure of a protonic semiconductor to its dynamic properties (IR, NMR, dielectric and d. c.) by examining the relations among a variety of similar organic compounds. Since endeavour nowadays is to relate macroscopic properties to microscopic structure, it is particularly interesting that very detailed mechanistic interpretations are possible in systems where the proton seems limited in its motion to the hydrogen-bond chain, which provides a ready path for motion. Thus, the objectives of the present study have been:

1. To characterise the d. c. behaviour of some organic proton conductors, namely those containing hydrogen bonds to nitrogen
2. To improve the techniques of conductivity measurement and hydrogen detection
3. To attempt to correlate the dielectric and d. c. properties of these compounds in that these show different aspects

of the dynamic electrical properties of the material

4. To consider mechanisms for proton conduction in the compounds investigated.

SECTION 2 : DESCRIPTION OF APPARATUS AND PROCEDURES

2 : 2 : 1 Direct Current Measurements

Direct current measurements were performed with the sample and ammeter (Keithley Electrometer, model 602) in series with the voltage source. As this source, a Farnell type L 30 power supply (0-30 V), a voltage-stabalized d. c. power supply (0-300 V) and a Brandenburg high-voltage type S 0530/10 generator (0-10 kV) were used to cover a broad range of measurement. Voltages were read directly from the calibrated, internal voltmeter on the Brandenburg power supply and a Taylor model 100A multi-meter (impedance 100 kohm V^{-1} d. c.) was used to measure the voltage across the output terminals of the other power supplies.

Figure 2 : 2. 1 provides an exploded view of the sample holder. The two Pt electrodes, cut from a sheet of foil, prevent reaction between the brass plates and the sample. When an imidazole protode is used, the Pt electrode is retained to prevent reaction of the imidazole with the brass plate. A heavy-gauge Pt disc, sealed into the perspex cap, makes electrical contact with the mercury in the bath. The sample holder is positioned in the mercury bath by the cork stopper and is sealed by the rubber "O" ring. The electrodes are firmly pressed against the sample by means of elastic bands looped over the four hooks and passed round the perspex cap.

2 : 2 : 2 D. C. Electrolysis Measurements

A block diagram of the electrical circuit used for transport measurements is shown in Fig. 2 : 2. 2. The EHT power supply is the same as that used in the conductivity measurements. The Keithley

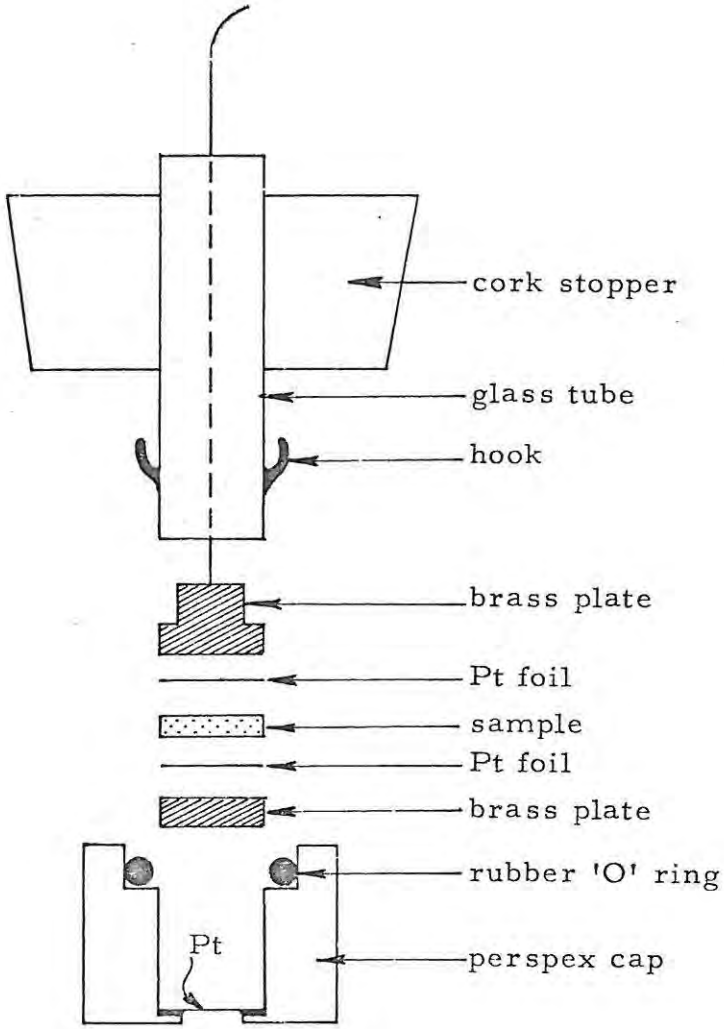

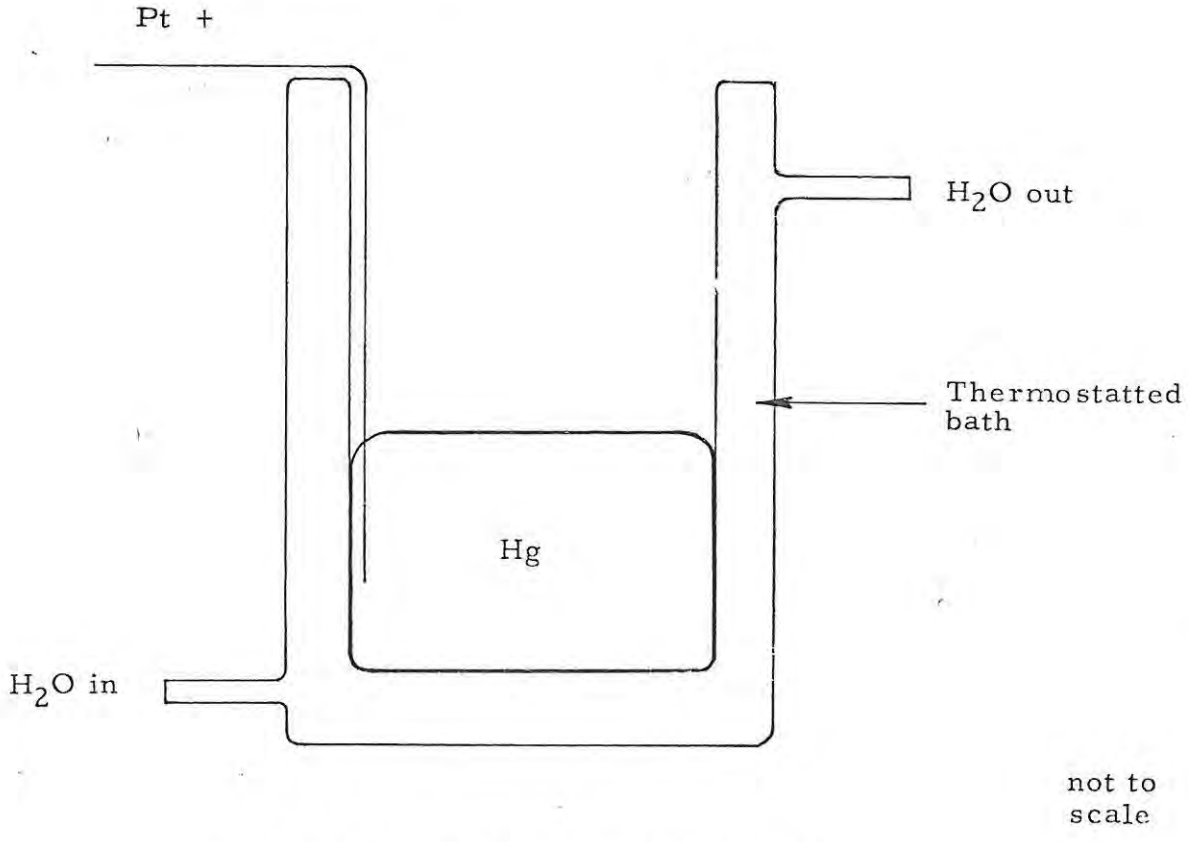

Fig. 2 : 2.1. CONDUCTIVITY CELL

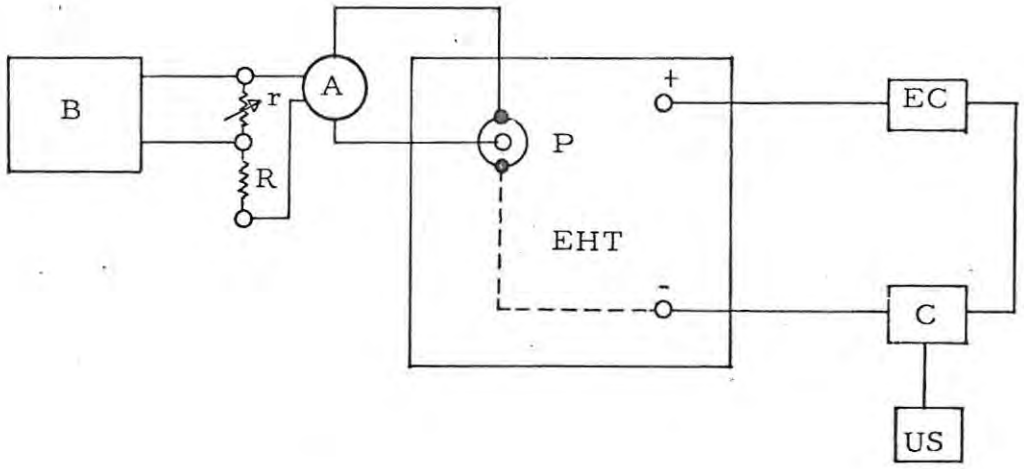

A = ammeter
B = recorder
C = digital coulometer
P = jack plug
r = 10 - 60 ohms
R = 5090 ohms

EC = electrolysis cell
EHT = power supply
US = universal scaler
--- = internal connection

Fig. 2 : 2.2. THE ELECTROLYSIS CIRCUIT

Electrometer, or a 'Lemouzy Multimeter' (offset current about 10^{-13}A, full scale deflection 10^{-6} A) was used as d. c. detector, to which a Bristol pen recorder was coupled by means of a potential divider. It was necessary to isolate the ammeter from the coulometer, because of interference from the digital switching of the latter. This was accomplished by means of a jack plug on the EHT power supply, which enabled the circuit current to be monitored through an internal connection. A Philips Universal Scaler (PW 4032) was coupled to a newly-designed digital coulometer to count the number of discharges of a capacitor in the coulometer circuit. The coulometer was calibrated by passing a known current for a given time and recording the number of counts, from which the charge passed per count was calculated. The coulometer was found to be accurate to within 3% in the count-range 2-20 counts per second. Since the current to the coulometer is passed through a calibrated internal potential divider network, to cover a wide range of currents, the count calibration was maintained independent of the applied current.

The electrolysis cell shown in Fig. 2:2. 3 was designed to monitor and collect the gaseous products of electrolysis. The sample is sealed to the base of the cell (which is angled to allow the evolved gas to escape from the sides of the sample) with "Pratley Paste", which is first evacuated in a vacuum desiccator to 0. 01 torr for about five minutes, to remove dissolved air. This paste-like epoxy-resin adhesive has a high specific resistivity, of about 10^{12} ohm cm at room temperature. The coulometer is filled with carefully cleaned and vacuum-dried mercury by passing down the capillary tube a fine flexible tube, attached to an hypodermic syringe filled with mercury.

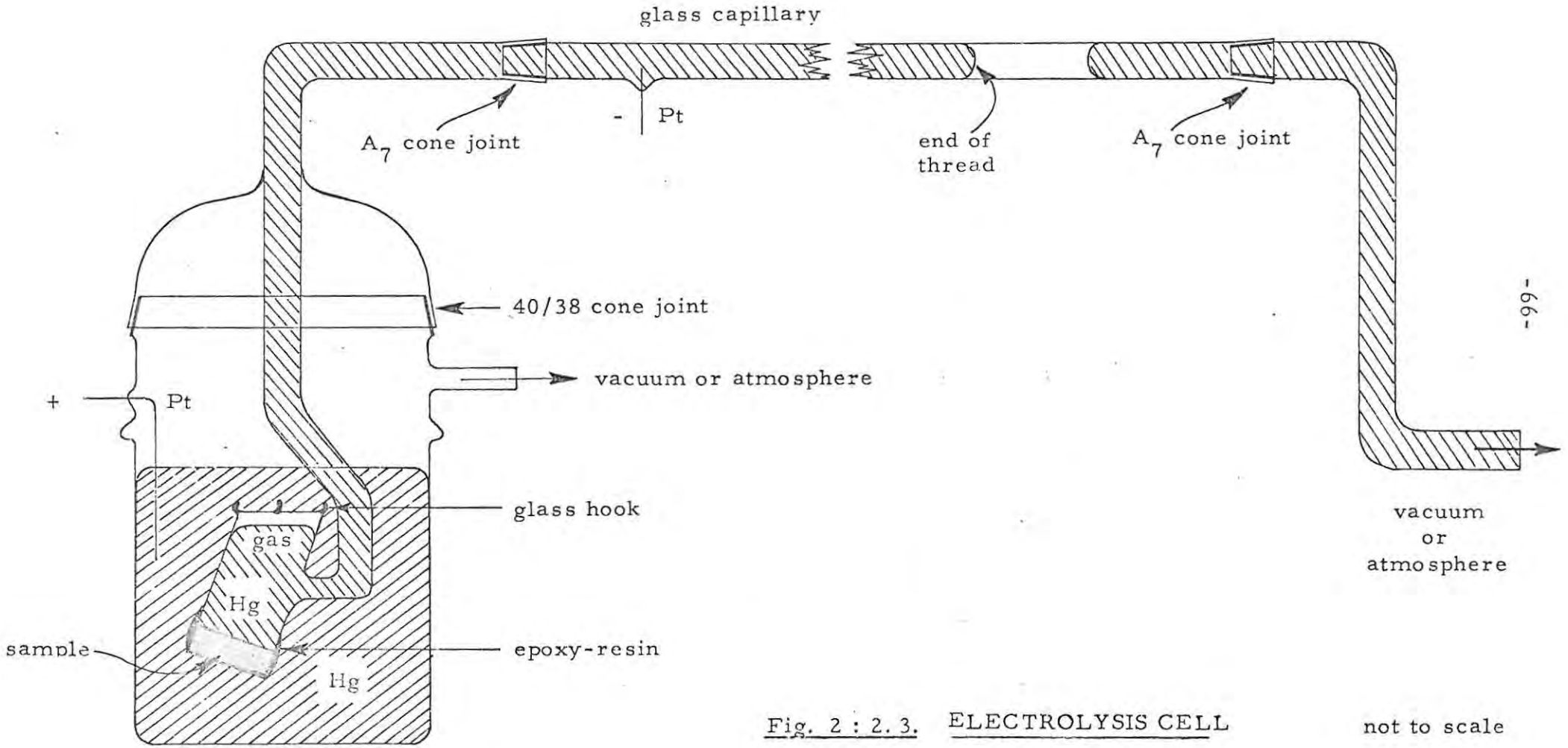

Fig. 2 : 2.3. ELECTROLYSIS CELL not to scale

The apparatus is then immersed in similarly cleaned mercury in a thermostatted bath. The sample is maintained in pressure equilibrium by an adjustable mercury leg, which is made out of polythene tubing. To increase the sensitivity of the gas detection, the whole system can be evacuated, pressure equilibrium across the sample being maintained by connecting both outlets to a common vacuum reservoir. The pressure of the system is monitored on a sealed "U" tube mercury manometer attached to the vacuum reservoir. The rate of evolution of gas is followed by observing with a travelling microscope the motion of the mercury thread in the horizontal capillary of uniform bore. Allowance has only to be made for changes in room temperature when working under evacuated conditions. When the system is open to the atmosphere, pressure fluctuations must also be taken into account. Unless care is taken to maintain pressure balance across the sample, there is a slow movement of the sample, leading to a "creep" of the mercury thread, hence the use of an adjustable mercury leg; the experiment is only commenced when the mercury thread has remained stationary for an hour.

The sample is desiccated while the epoxy-resin sets, by detaching the glass capillary tube and inserting the sample section in a desiccator. A variety of electrodes can be attached to the sample using components similar to those of the d. c. sample holder, but the components have to be made to 15 mm internal diameter, to allow additional clearance for the epoxy-resin.

If a sufficient current of protons can be drawn through the sample ($\sim$ 1μA) it is unnecessary to work under reduced pressure and a simplified version of this electrolysis cell can be used (see

fig. 2 : 2.4). A fine flexible tube, attached to a hypodermic syringe, can be used to remove mercury and so reduce the length of the mercury thread, if necessary.

The cathode gas was sampled for identification of hydrogen by replacing the capillary tube with a 6 cm length of polythene tubing. After half-filling the tube with carbon tetrachloride, a small volume of $PdCl_2$ solution was floated on top of this, and the filled portion of the tube sealed with a screw clamp. The cathode gas was then displaced up the tube as far as the clamp. The formation of a fine, black precipitate after a few minutes was taken as proof of the presence of free hydrogen gas. A control experiment, in which similar quantities of $PdCl_2$ solution floated on top of carbon tetrachloride was exposed to the atmosphere, showed no signs of precipitation.

2 : 2 : 3 Micro-Potentiometric Titrations

A micro-potentiometric titration was used to study the proton concentration in electrolysed imidazole. The content of base was analysed for by a potentiometric titration of the imidazole against perchloric acid in dry, glacial acetic acid as non-aqueous solvent. The Keithley electrometer was coupled to a Beckmann pH electrode and reference to monitor the voltage changes in the solution with volume of acid added. The potentiometric titration curves for the standardisation of $HClO_4$ in acetic acid using potassium hydrogen phthalate, and the titration of the standardised acid against an imidazole blank (fig. 2: 2.5) can be seen to display the necessary steep rise near the end point. Since water is a protic solvent, some

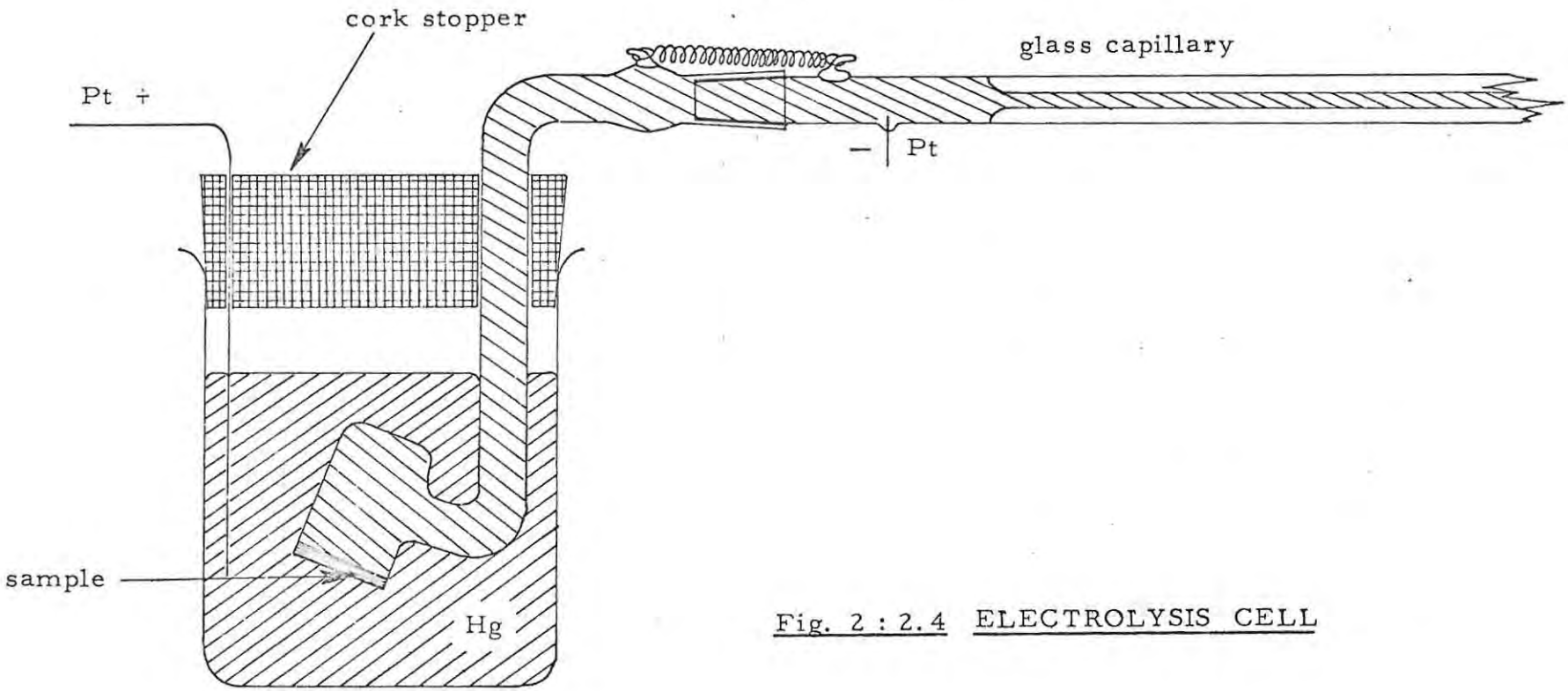

Fig. 2 : 2.4 ELECTROLYSIS CELL

acetic anhydride was added to the glacial acetic acid to remove any traces of water (Beckett and Tinley, third edition). The temperature of the standardised acetous perchloric acid in the micro-burette was noted before each titration, since the molarity of the standard acid changes rather rapidly with temperature (acetic acid has a large cubic coefficient of expansion). Thus, using this technique, the base content of imidazole in unelectrolyzed pellets could be determined to a precision of 0.4%.

Blocks of 5 to 10 pellets of imidazole in series were constructed by lightly pressing in a 13 mm die (0.75 kbar for 5 seconds) successive 150 mg quantities of singly sublimed imidazole dried over silica gel, and then pressing the complete stack of pellets at 7.5 kbar for 2 minutes. The block of imidazole pellets was then cemented to the base of the electrolysis cell in the usual way, and sufficient charge was passed through the cell (about 4 coulombs), so that a change in the concentration of base in the block should have been detectable, according to the amount of hydrogen discharged, if the concentration change were linear across the block.

2 : 2 : 4 Dielectric Measurements

Dielectric measurements were made in the frequency range 30-300 kHz, by the substitution method described in the revised edition (October 1965) of the General Radio Operating Manual for the type 716-C capacitance bridge. The bridge was driven by a Hewlett-Packard wide-range oscillator model 200CD/CDR and a Philips PM3200 oscilloscope connected as described by Czech (1957)

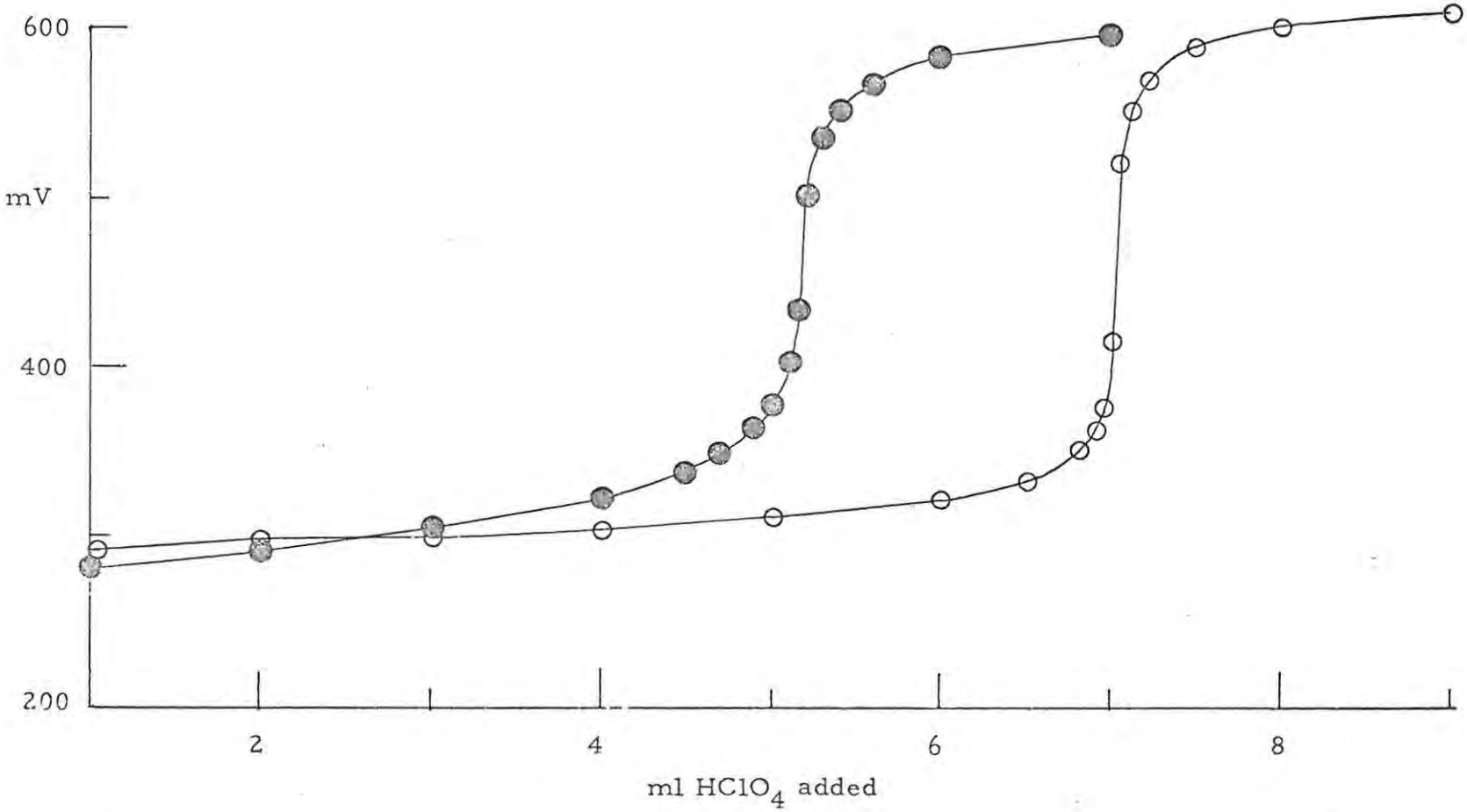

Fig. 2 : 2.5 Micro-potentiometric titration curves using Calomel/glass electrodes and a Keithley electrometer as a detector. Open circles indicate the standardisation of acetous perchloric acid against potassium hydrogen phthalate. Closed circles indicate the titration of an unelectrolysed imidazole pellet.

was used as a phase-sensitive detector. The dielectric sample holder described by Giesekke (1965c) was used, but the lower electrode was reduced to the same size as the upper electrode and the "paxolin" insulator, which isolated the high electrode from the casing, was replaced with teflon.

A computer programme was drawn up to calculate the results, using the standard dielectric relations (equations (46) - (49) in the manual), due allowance being made for fringe effects, residual capacitance and capacitance between the high electrode and ground, as described in the ASTM manual D150-59T (1959).

2 : 2 : 5 Sample Purification, Crystal Growing and Handling Procedures

Zone-refining of resorcinol in a vertical zone-refining apparatus proved unsuccessful mainly because of the appearance of gaps in the solidified material so, whenever possible, the material was purified by repeated vacuum sublimation. The sublimation apparatus shown in Fig. 2 : 2.6 was constructed by joining a shaped pyrex glass cylinder onto the opened bottom end of a flanged flask. Vacuum sublimation was brought about by submerging the apparatus in a heated liquid paraffin bath to a depth beyond the lightly-packed glass-wool plug. The middle fraction of the material, which condensed on the walls of the apparatus, was recovered. The recovery of the sublimate could have been facilitated by having cylindrical sections of glass (one on top of the other) in the sublimation chamber. These sections could then be removed to recover the middle fraction of the sublimate.

Benzimidazole (BDH, laboratory reagent grade) was found to decompose on sublimation, so the material was repeatedly decolourised with

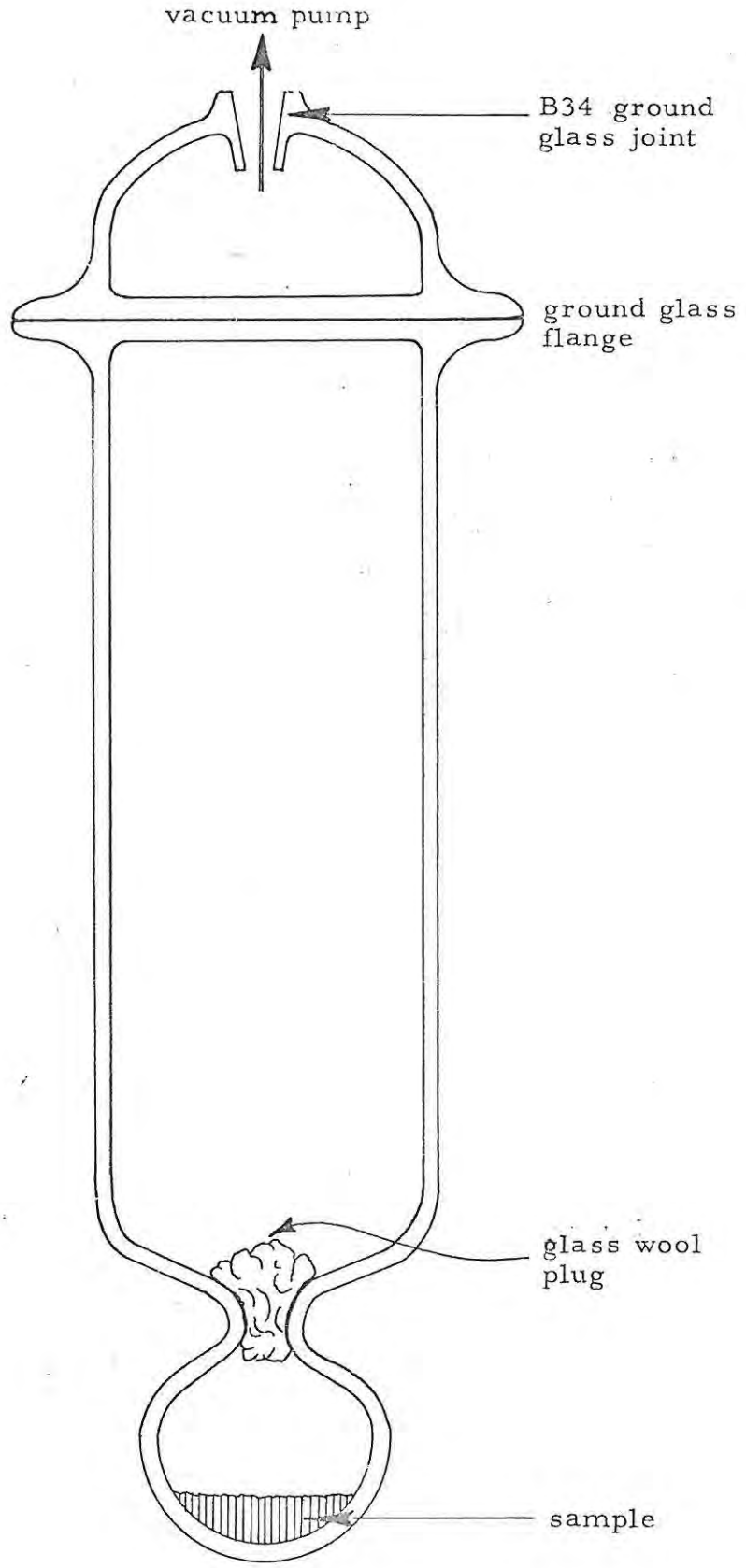

Fig. 2 : 2.6. SUBLIMATION APPARATUS

not to scale

animal charcoal and finally recrystallised from water (Fieser and Fieser 1967).

Although urea decomposes on melting to form cyanuric acid, it can be sublimed, unchanged, in a "cathode tube" vacuum (about 1 mm Hg) (Beilstein 1921). However, because of the distinct possibility of the sublimed urea being contaminated with biuret, the material was rather purified by repeated recrystallisation from methanol instead. Since methanol is a protic solvent, due care was exercised to try and remove all traces of the solvent by air-drying the crystals under reflected heat, periodically crushing and mixing the crystals. The recrystallised material was finally desiccated under vacuum over P_2O_5 for at least two days before use.

Single crystals of urea were grown from seeds by the method of lowering of temperature (Holden and Singer 1961), in a thermostatted vessel (fig. 2 : 2. 7) containing a solution of 90 g urea in 300 ml methanol, saturated at 37°C. Six seeds were suspended from a glass crystal tree by inserting the seed into a slit cut in a 6 mm length of polythene tubing (fig. 2 : 2. 8). The tree was suspended from a float (fig. 2 : 2. 9) which prevented spurious nucleation on the seeds and introduced a certain degree of random motion to the seeds, thereby preventing "veiling". The four radial arms prevented the float from sticking to the side of the container.

The crystal-growing vessel rested on a reciprocating cradle, suspended from an eccentric (Wig-L-Bug) bearing, which was driven at a rate of one cycle per minute by a synchronous motor.

The temperature of the vessel was kept constant by circulating water from an insulated bath, heated by a Braun stirrer pump. The

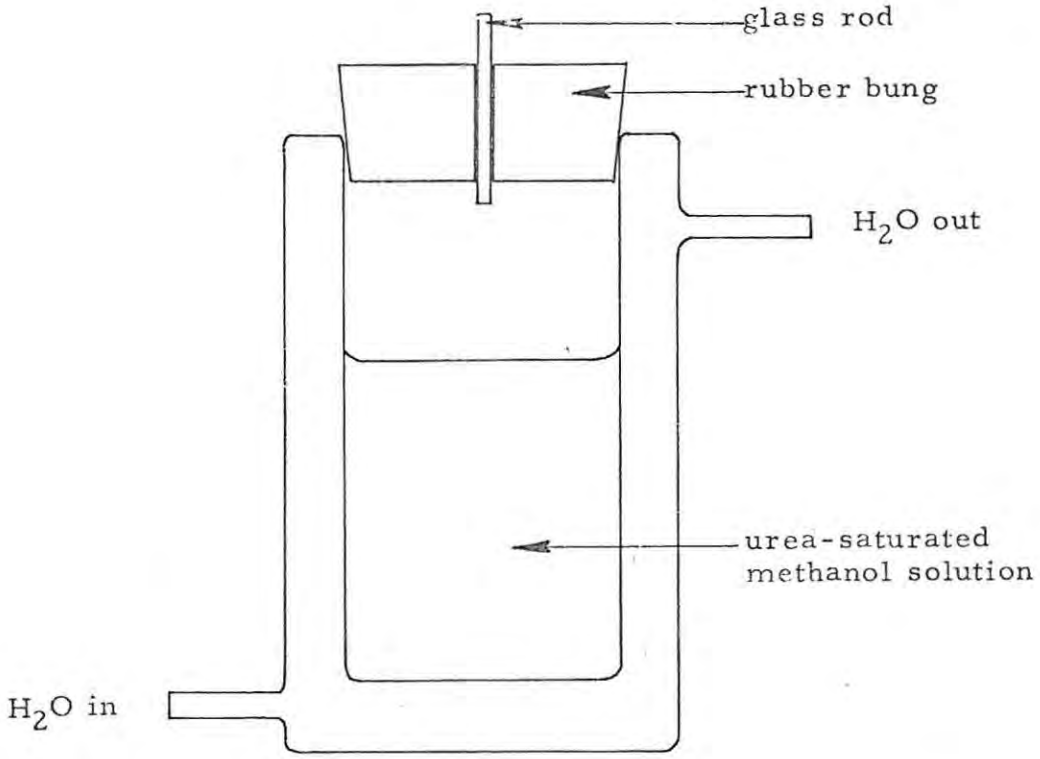

Fig. 2 : 2.7

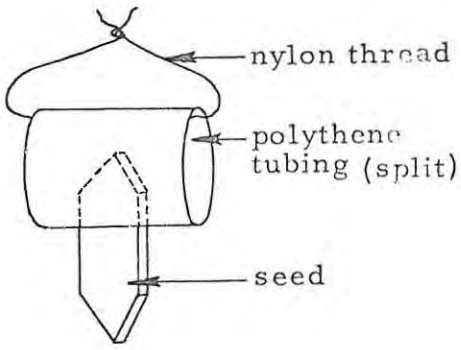

Fig. 2 : 2.8

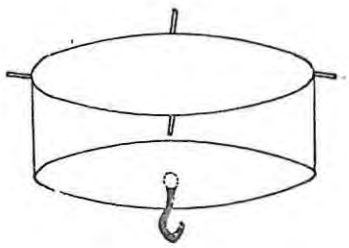

Fig. 2 : 2.9

not to scale

temperature was slowly lowered by the apparatus shown in fig. 2 : 2. 10. The nozzle, which was drawn out from a fine capillary tube and filed until a suitable flow-rate was obtained, was mounted on a spring paper clip which could slide along a vertical scale indicating the pressure head of water. A calibration graph of pressure head versus rate of decrease of temperature per day showed that the relationship was almost linear.

The temperature control of the Braun stirrer pump could be de-coupled from the pulley-system by removing the crocodile clip attached to the rubber tubing, which fitted loosely round the pulley shaft. This innovation was useful, as the crystal tree had to be inserted into the solution at a temperature of about $4^{o}C$ above the saturation temperature to prevent spurious nucleation in the solution, and to dissolve away any excess nuclei on the seed crystals. Once the tree was inserted, the temperature had to be lowered manually to saturation temperature to prevent complete dissolution of the seeds. A second crystal-growing apparatus was run off the same temperature-lowering system. A pulley with a number of different diameter tracks allowed the two sets of apparatus to operate at different cooling rates.

The temperature was initially lowered at less than $0.1^{o}C$ per day, increasing gradually to $1.2^{o}C$ per day when the growth conditions were fully established (Deprez and Fontaine 1965). Some crystals were grown with 2. 5g ammonium bromide added to the solution to inhibit growth along the c direction (Andrew and Hyndman 1955). Good crystals were also grown by "capping" the ends of the crystals (Fig. 2 : 2. 11) to inhibit growth along the c axis, otherwise the

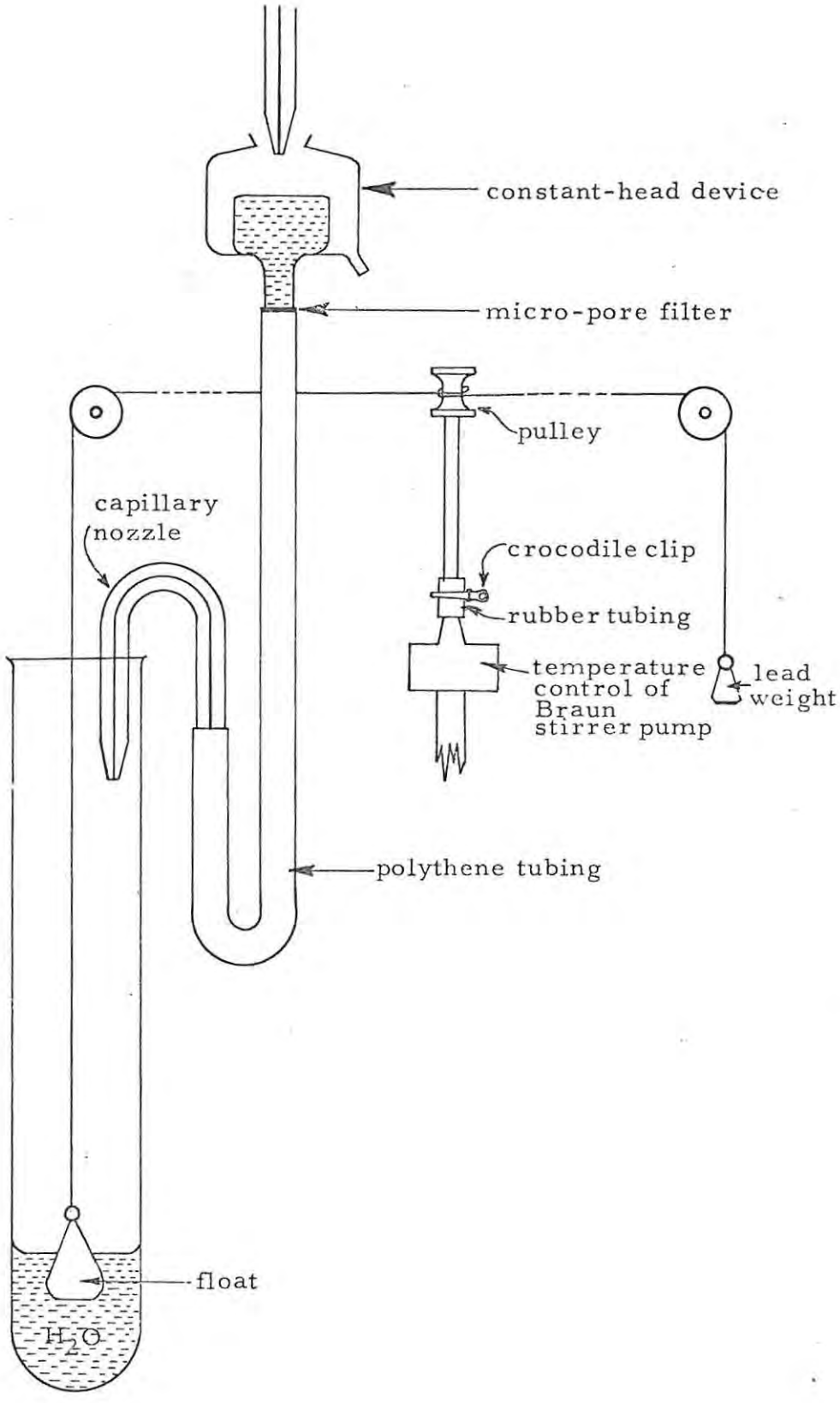

Fig. 2 : 2.10

not to scale

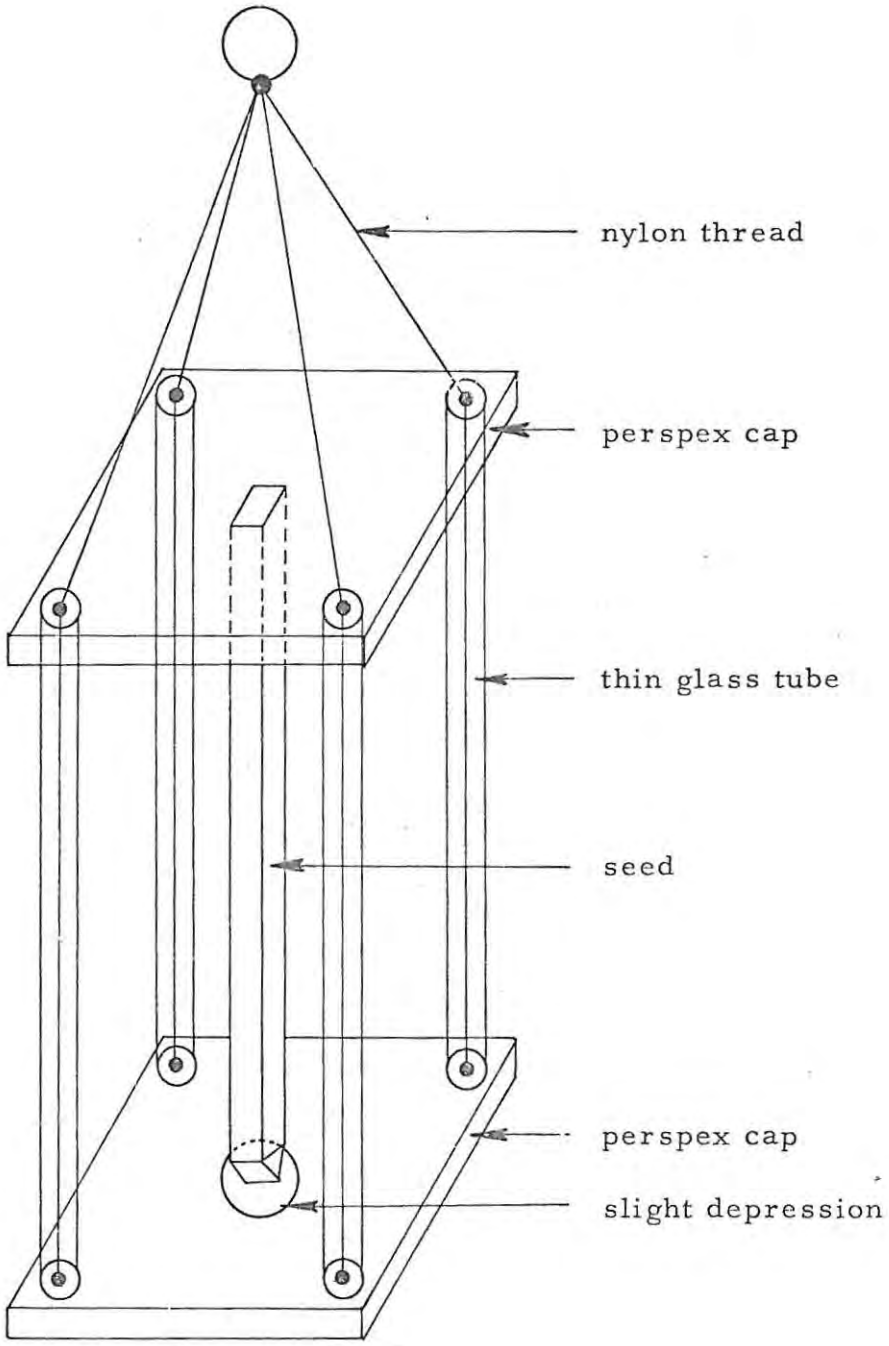
nylon thread
perspex cap
thin glass tube
seed
perspex cap
slight depression

Fig. 2. 2. 11

crystals had a needle habit.

The urea crystals have a well-defined cleavage along the ac- and bc- planes, but are extremely brittle parallel to the ab plane. A crystal-cutting apparatus was constructed whereby cuts along the ab plane were made with cotton wetted with methanol. The portions of crystals selected for measurement were mounted using "Pratley Paste" into perspex discs cut from 1.3 mm thick sheets with a hot cork borer. The excess epoxy-resin and crystal was ground away using various grades of dry emery powder, on a glass plate. The perspex disc was fixed to the base of the electrolysis cell as described for compressed pellets.

Imidazole, pressed at 7.5 kbar for two minutes in a 13 mm die, formed pellets 1 to 1.5 mm thick, with an average bulk density of 1.215 g cm^{-3} compared to the value of 1.297 g cm^{-3} for the single crystal density (Martinez-Carrera 1966, calculated at -150°C).

Pellets of urea were pressed as for imidazole, the bulk density of the pellets being 1.288 g cm^{-3} compared with 1.319 g cm^{-3} for single crystals (Beilstein 1954). The pellets were generally stored over fresh P_2O_5 in a vacuum desiccator for at least two days before commencement of electrical measurements.

2 : 2 : 6 Electrodes

Electrodes of Cu, Pt and Hg materials all proved to be blocking with respect to proton conduction, and results obtained with these were all similar.

Proton-injecting electrodes (protodes) were made by depositing

finely-divided palladium onto platinum from a palladous chloride bath. The palladium was saturated with hydrogen by using it as cathode while electrolysing a very dilute aqueous hydrochloric acid solution (see section 1 : 4 : 5). The electrode was washed in distilled water, blotted dry, and desiccated over P_2O_5.

Thin discs of imidazole, prepared in the usual way, were also used as protodes.

CHAPTER 3

RESULTS

SECTION 3 : 1 PRELIMINARY WORK

Preliminary electrical measurements on some hydrogen-bonded organic solids were performed to select materials which would produce proton currents.

Resorcinol (Riedel - de Haën A. G.) showed marked signs of d. c. polarization at constant applied voltage, but no evidence of hydrogen generation could be found, and the Cole-Cole plots of the dielectric dispersions evaluated at 73 and 80° C (but not reported here) did not exhibit the now familiar high-frequency dispersion of the dielectric constant and the low-frequency "tail" due to d. c. conductivity, associated with proton conductors (see section 1:10:3). On the other hand, electrolysis of imidazole (Koch-Light) was accompanied by copious evolution of gas at the cathode and the current decayed rapidly with time at constant applied voltage. In contrast to imidazole, electrolysis of urea (BDH) yielded very little gas at the cathode and the polarization process was rapid, but less pronounced. On the basis of these preliminary measurements, work was commenced on imidazole and urea.

As an extension of this work, benzimidazole (BDH), histamine diphosphate (Fluka A. G. - Buchs S. G.) and ethylenediaminetetra-acetic acid (EDTA) (Light and Co. Ltd.) were also examined. Polarization effects were found to be minimal and no evolution of gas at the cathode was noted for any of these compounds. The

conductivities of EDTA and benzimidazole were quite low (about 10^{-10} ohm^{-1} cm^{-1} at 60°C), while that of histamine diphosphate was a factor of 100 higher (10^{-8} ohm^{-1} cm^{-1} at 50°C). Although these compounds are not intrinsic proton conductors, their potential as extrinsic protonic semiconductors was not tested; some later work on these compounds confirmed that some of them are indeed extrinsic protonic semiconductors (see section on future work).

SECTION 3 : 2 IMIDAZOLE POWDERS

3 : 2 : 1 Effect of a Guard Ring

A guard-ring was painted with "Silver Print" around the edge of an imidazole disc which had previously been electrolysed for 5 hours under humid conditions. Conductivity measurements with and without the guard-ring in the circuit showed that the guard-ring had little effect on the resistivity (fig 3:2. 1). This result is not unreasonable, since a guard-ring can only eliminate currents along the surface of the pellets, but cannot eliminate the currents carried by the large internal surfaces of the powder compact. Thus the guard-ring was generally omitted, although there is indeed some likelihood of surface conduction if care is not taken, for it was observed that current-flow can be considerably increased, rapidly but temporarily, by breathing near the sample. This effect is clearly due to adsorption of moisture on the surfaces of the pellet.

3 : 2 : 2 D. C. Conductivity

The current passing through a singly sublimed imidazole sample at constant voltage (and temperature) is markedly time-dependent (see fig 3: 2. 2). The problems associated with conductivity measurements under such conditions have been discussed in section 1 : 4 : 4. It would not be practical to take conductivity measurements only after polarization has ceased, as some protracted electrolysis runs on singly sublimed imidazole have shown that polarization can persist for up to 200 hours, during which time the current decays to less than 5% of the initial value, in marked contrast to triply

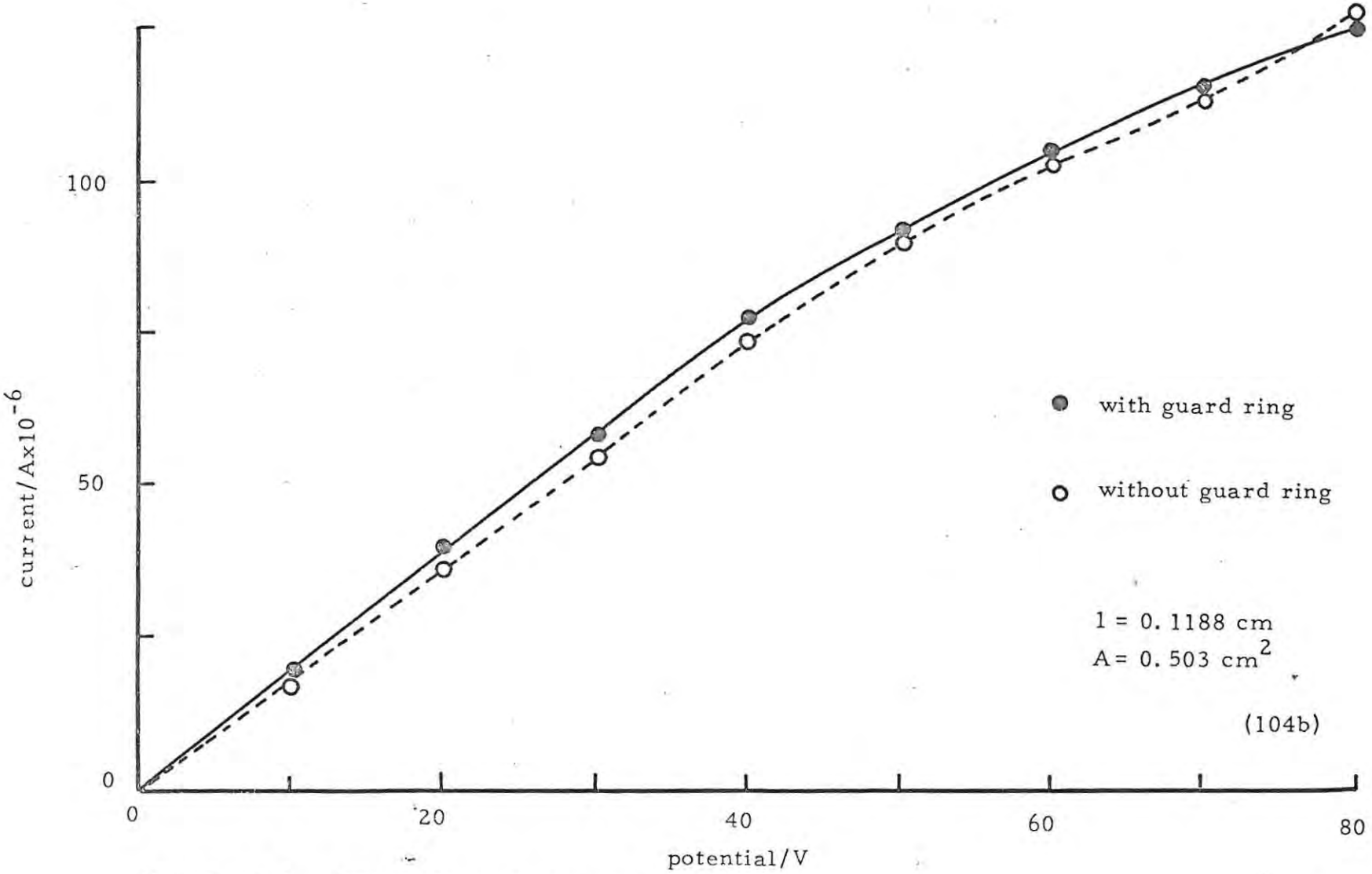

Fig. 3 : 2.1 Effect of guard ring - Hg electrodes

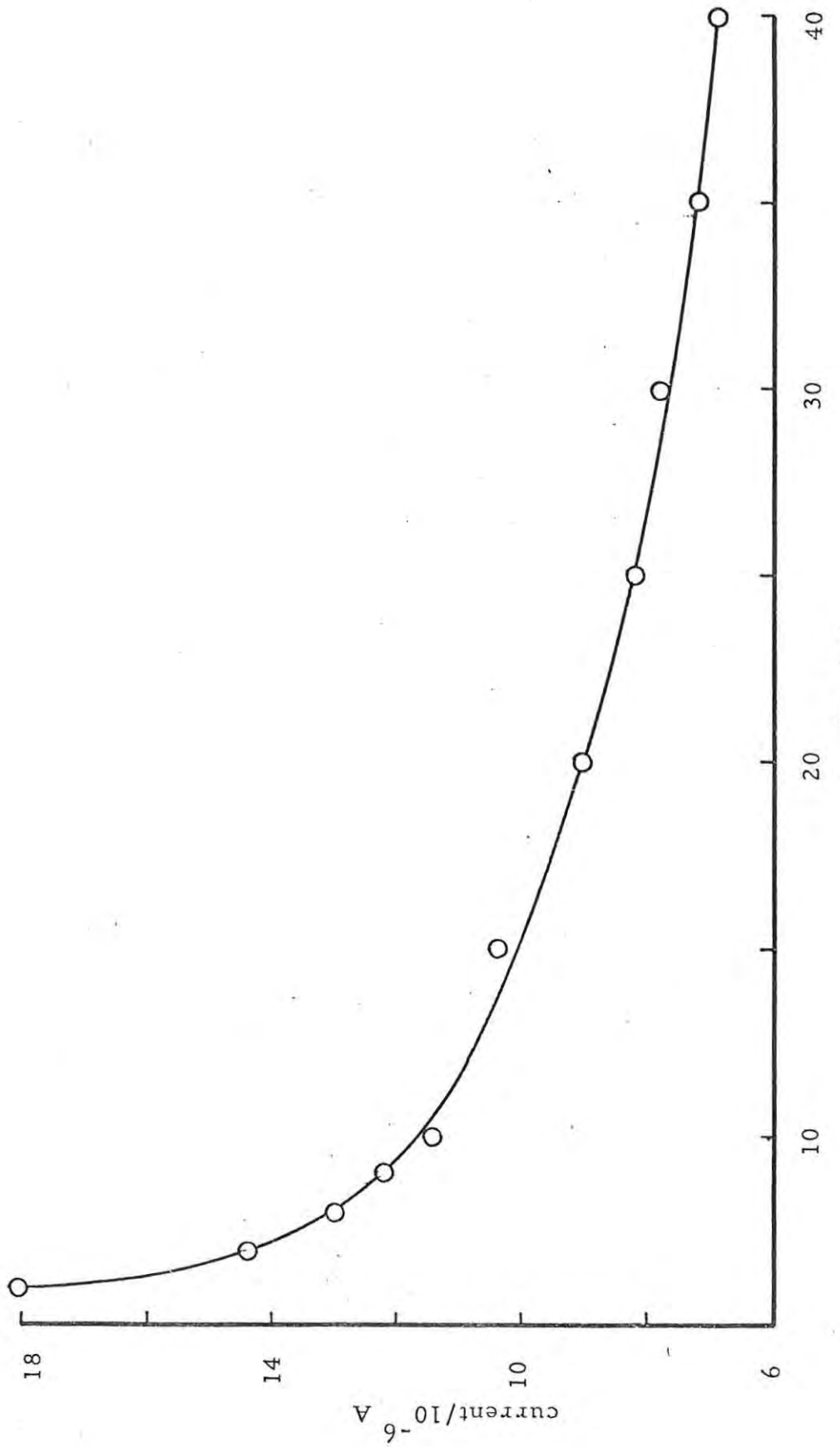

Fig. 3 : 2.2 Polarization of imidazole at 50°C

sublimed imidazole, where polarization ceased after about 30 minutes.

The effect of multiple sublimation on the electrical properties of imidazole is evident from the decrease in the room temperature conductivity from 2.9×10^{-10} ohm^{-1} cm^{-1} for singly sublimed imidazole to 1.0×10^{-10} ohm^{-1} cm^{-1} for the doubly sublimed material and 2.9×10^{-11} ohm^{-1} cm^{-1} for triply sublimed imidazole.

Because of polarization, it is very difficult to obtain consistent current-density vs field characteristics; in general, it was found that for triply sublimed imidazole Ohm's law was obeyed at field strengths up to about 1000 V cm^{-1}, but that thereafter the currents rose more steeply than linearly for Pd/H_2 protodes (see figure 3:2.3), confirming proton injection (Thomas and Clarke 1969), but less steeply for non-injecting electrodes, consonant with the lack of proton injection (Aftergut and Brown 1962). Although the singly and doubly sublimed material showed a 4- to 5-fold increase in conductivity with the Pd/H_2 protode, no steep rise, characteristic of space-charge-limited currents (see section 1:4:5) was observed. This may be due to the expected large trap density in powders, which would prevent super-linear conduction.

3 : 2 : 3 D.C. Electrolysis

Electrolysis measurements were performed at 50°C. Singly and triply sublimed material was electrolysed and the cathode gas was positively identified as hydrogen. Both types of sample gave a proton conduction efficiency of 98% with mercury (non-injecting)

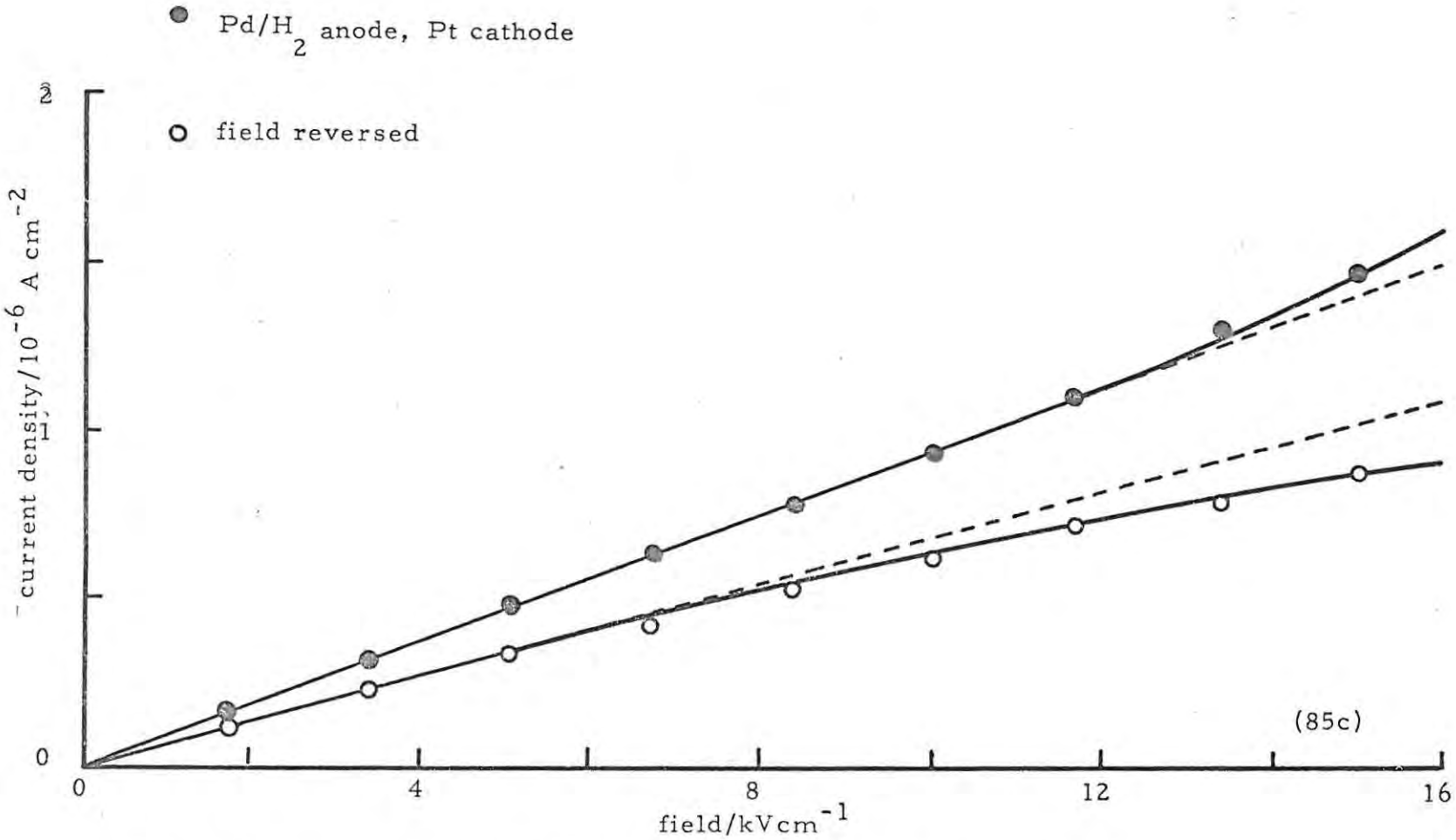

Fig. 3 : 2.3 Proton injection into triply sublimed imidazole at 25°C

electrodes; an efficiency of 101% for triply sublimed imidazole using a Pd/H_2 protode, is thought to have been due to a pressure differential across the sample, causing it to move slowly. The mode of attaching the protode has since been improved, but the run was not repeated.

Figure 3 : 2. 4 shows the constancy of the proton efficiency for a given pellet, in spite of the fact that the material was undergoing polarization and the applied voltage was continually being raised to maintain the current flow. The yield of hydrogen in studies of volume changes in electrolytic hydrogen evolution at mercury in aqueous hydrochloric acid (Smith and Heintze 1969) was found to be of the order of 50 - 80% of the theoretical yield expected from Faraday's laws of electrolysis. This discrepancy was tentatively ascribed by the authors to hydrogen absorption by the mercury. The high value and constancy of the proton efficiency in imidazole does not support this observation.

3 : 2 : 4 Reverse Electrolysis and Electrolysis of the Melt

It was observed, in common with reports of other workers (see section 1 : 7 : 2), that a black deposit occurred at the anode surface of the pellets, particularly with Hg electrodes. In order to study the process at the anode, the field direction on a pellet pressed from singly sublimed imidazole, was reversed, using Hg (blocking) electrodes. A colourless gas evolved at a slow, voltage-dependent, rate (see fig. 3 : 2. 5). Evolution of gas at the anode virtually ceased after the passage of 17 coulombs in

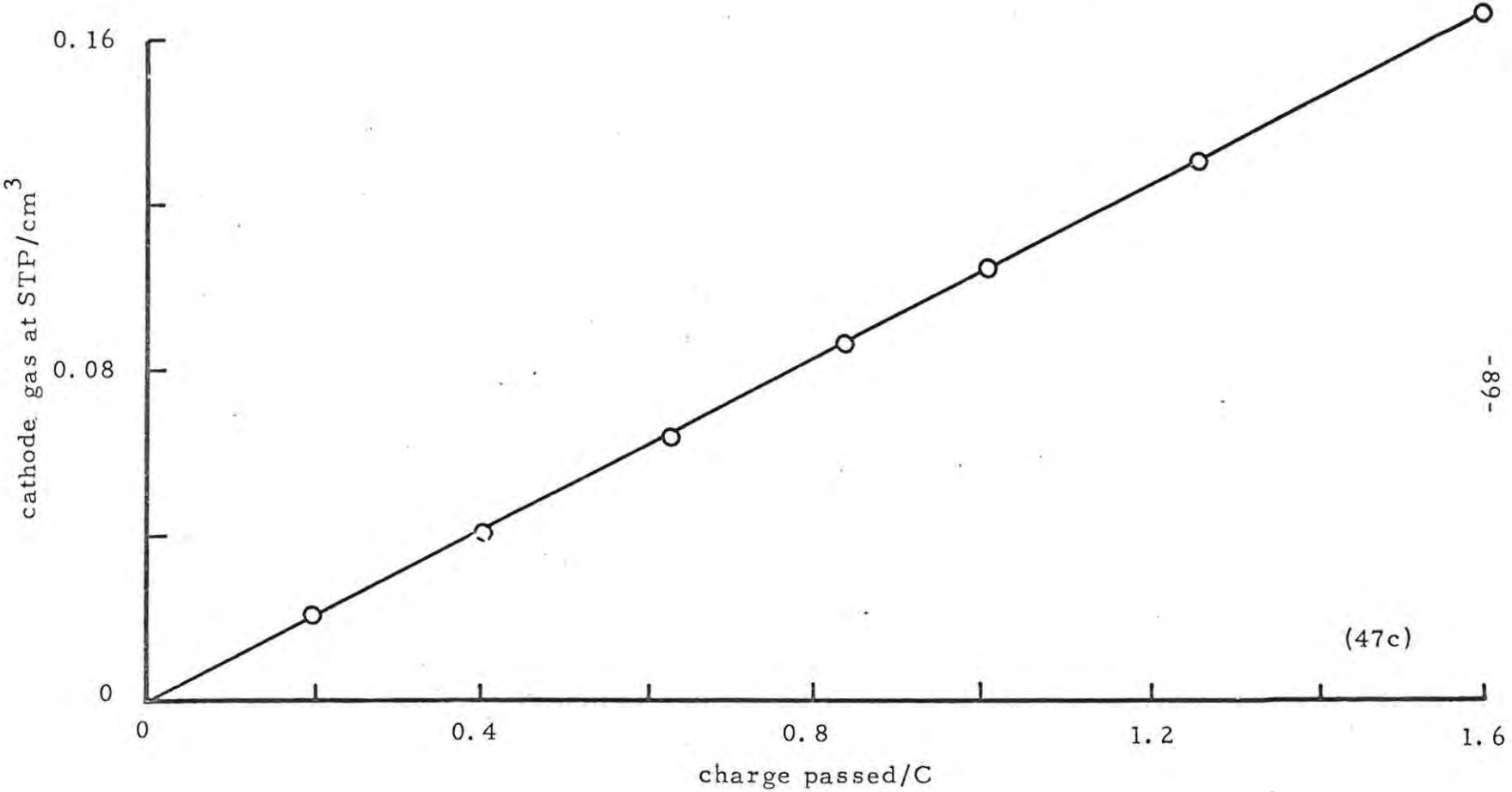

Fig. 3 : 2.4 Protolysis of imidazole block

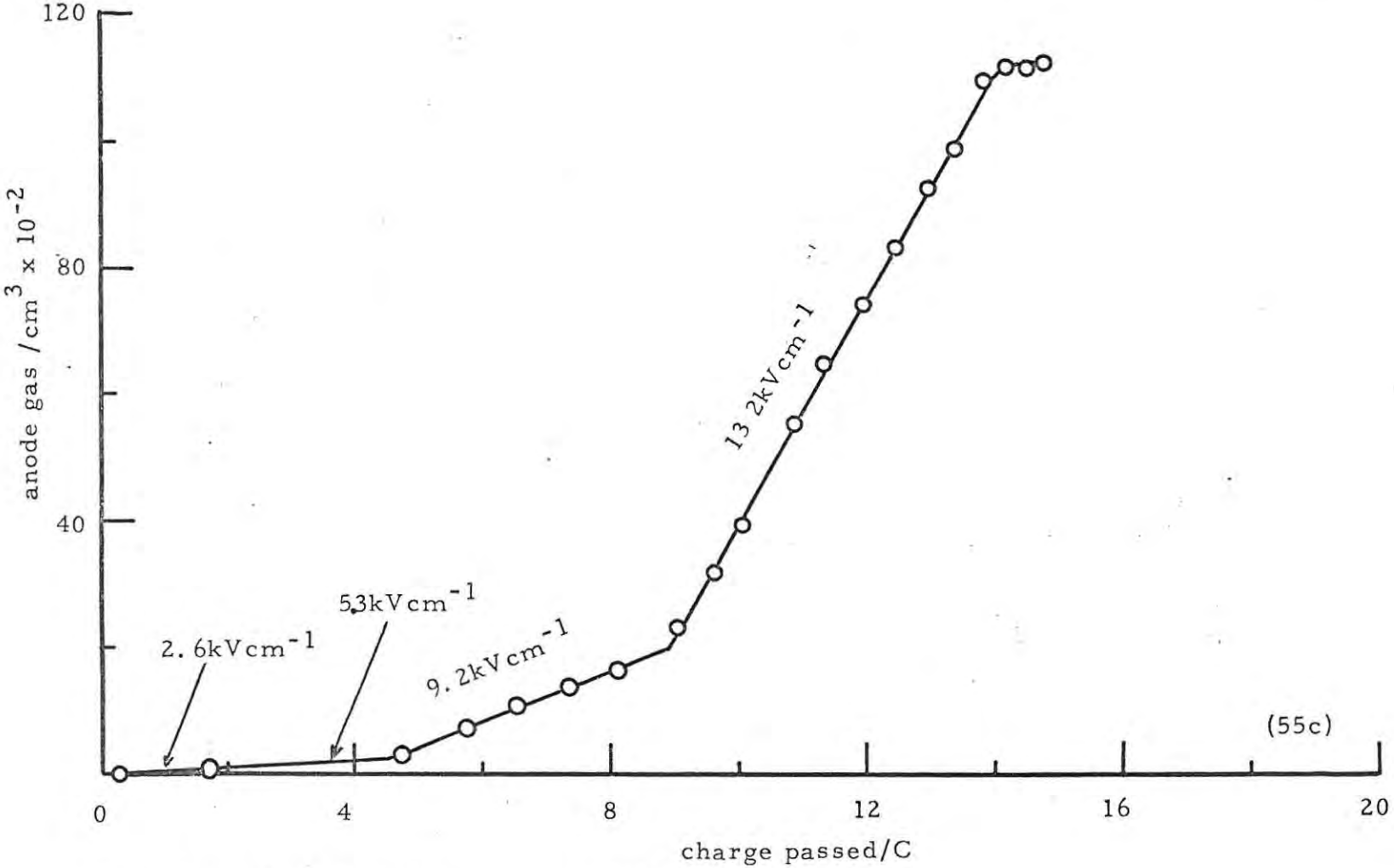

Fig. 3 : 2.5 Imidazole - reverse electrolysis

24 days through the singly sublimed pellet, when the volume of anode gas totalled 7% of the volume of hydrogen evolved over the same period (assuming 98% proton efficiency). In contrast to this, evolution of gas at the anode of a triply sublimed pellet ceased after the passage of only 1 coulomb in 18 hours. Thus, it was thought that the evolution of gas at the anode was related to small amounts of impurities in the sample, although the anode gas flow did not cease entirely after the apparent depletion of the impurity.

In view of the time-consuming nature of this study, it was decided to examine the electrolysis of an imidazole melt. When electrolysed at low current densities using Pt electrodes, molten imidazole evolved hydrogen at the cathode and formed a brown-black product around the anode. At higher current densities, the rate of evolution of hydrogen increased, and a colourless gas was evolved in copious quantities at the anode together with further dark solid. The gas was not identified, but infrared spectra of the (blackened) electrolysed and the (clear) unelectrolysed melts were the same, indicating that the dark solid is an amorphous carbonaceous residue.

3 : 2 : 5 Micro - Potentiometric Titration

Several attempts were made to detect, by titration, a concentration gradient of base (imidazole is basic in aqueous solution) across an electrolysed block of imidazole pellets. Although the percentage error in the determination of base content of unelectrolysed imidazole pellets was less than 0.4%, similar determinations of the base content of electrolysed pellets showed a scatter as large as 1.2% per pellet. Table 3 : 2.1 shows the results of a run in which a block

of 10 pellets was electrolysed for 5 days at about 7×10^{-6} A, during which time 4 coulombs of charge was passed through the sample. The pellets were separated under anhydrous conditions, each pellet was divided into quarters, and their content of base determined.

TABLE 3 : 2. 1. Percentage Purity of Electrolysed Imidazole

Sample	B	A_1	A_2	A_3	A_{10}
Percentage Purity	100. 4 $\pm$ 0. 2	101. 0 $\pm$ 0. 2	100. 0 $\pm$ 0. 0	102. 6 $\pm$ 1. 1	99. 7 $\pm$ 1. 2

Where B = blank, unelectrolyzed imidazole pellet

A_1 = anode pellet

A_2 = second pellet from the anode

.
.
.

A_{10} = tenth pellet from the anode (i. e., the cathode pellet)

According to the amount of charge transferred, it should have been possible to detect a change in the content of base, even if the depletion of protons was uniformly graded across the sample, but the percentage error in the determation was too large to do so.

Since the percentage error in the base determation of unelectrolysed imidazole was much smaller, the large scatter in the results for the electrolysed material might be indicative of preferred paths for the current passing through the pellets.

3 : 2 : 6 Dielectric Measurements

The complex dielectric constant changes with frequency according to the semi-empirical equation (Cole and Cole 1961):

$$\varepsilon^* = \varepsilon'_\infty + \frac{\varepsilon'_s - \varepsilon'_\infty}{1 + (j\omega\tau_c)^{1-h}} \quad \ldots\ldots\ldots \quad (3:2.1)$$

where τ_c is a constant known as the mean relaxation time around which the dispersion centres, and subscripts s,∞ denote the static dielectric constant, and the dielectric constant at infinite frequency, respectively; h is an empirical parameter chosen to fit the data, its value lying between 0 and 1. When h = 0, the distribution of relaxation times reduces to a single value, τ, and equation (3 : 2 . 1) reduces to the Debye equation

$$\varepsilon^* - \varepsilon'_\infty = \frac{\varepsilon'_s - \varepsilon'_\infty}{1 + j\omega\tau} \quad \ldots\ldots\ldots\ldots \quad (3:2.2)$$

A plot on the complex plane of the dielectric dispersion parameters, ε' vs ε'' is known as a Cole-Cole plot (after Cole and Cole 1941), and yields a semicircle if the dielectric medium has a single relaxation time, or the arc of a circle with depressed centre if there is a distribution of relaxation times. The relaxation time τ (or τ_c) is defined as equal to $1/\omega_{max}$, where ω_{max} is the frequency in radians evaluated at the dielectric loss peak. The frequency ω_{max} generally varies with temperature according to the relationship:

$$\omega_{max} = \omega_{o_{max}} e^{-H/RT} \quad \ldots\ldots\ldots\ldots \quad (3:2.3)$$

where H is the energy of activation and $\omega_{o_{max}}$ is a constant. In terms of relaxation time,

$$\tau = \tau_o e^{H/RT} \quad \ldots\ldots\ldots\ldots\ldots\ldots \quad (3:2.4)$$

where τ_o is a constant.

The Cole-Cole plots of the dielectric dispersion of imidazole powders at 65 and 75°C (fig. 3 : 2. 6) exhibit the characteristic profile associated with protonic semiconductors (see section 1 : 10 : 3), namely a low-frequency "tail" which increases rapidly with temperature, and a broad high-frequency dispersion which is almost temperature-independent in position and breadth. The extent of the distribution of relaxation times about τ_c is given by the Cole-Cole parameter, h. (Table 3 : 2. 2) shows the variation of the dielectric dispersion parameters of the imidazole powders.

TABLE: 3 : 2. 2 Temperature-dependence of the dielectric dispersion parameters of imidazole powder.

dielectric dispersion parameters	ε'_o	ε'_∞	τ/s	h
65°C	14	2. 6	2×10^{-5}	0. 47
75°C	14	2. 4	5×10^{-6}	0. 43

At a fixed temperature the static dielectric constant, and the dielectric constant at infinite frequency, were read by extrapolating the arc to the abscissa. The constant, h, was calculated from the relationship

$$\theta\frac{\pi}{180} = h\,\frac{\pi}{2}$$

where the angle θ (in degrees) is indicated on the graph. From this data, an energy of activation was estimated at 26 kcal mol^{-1}.

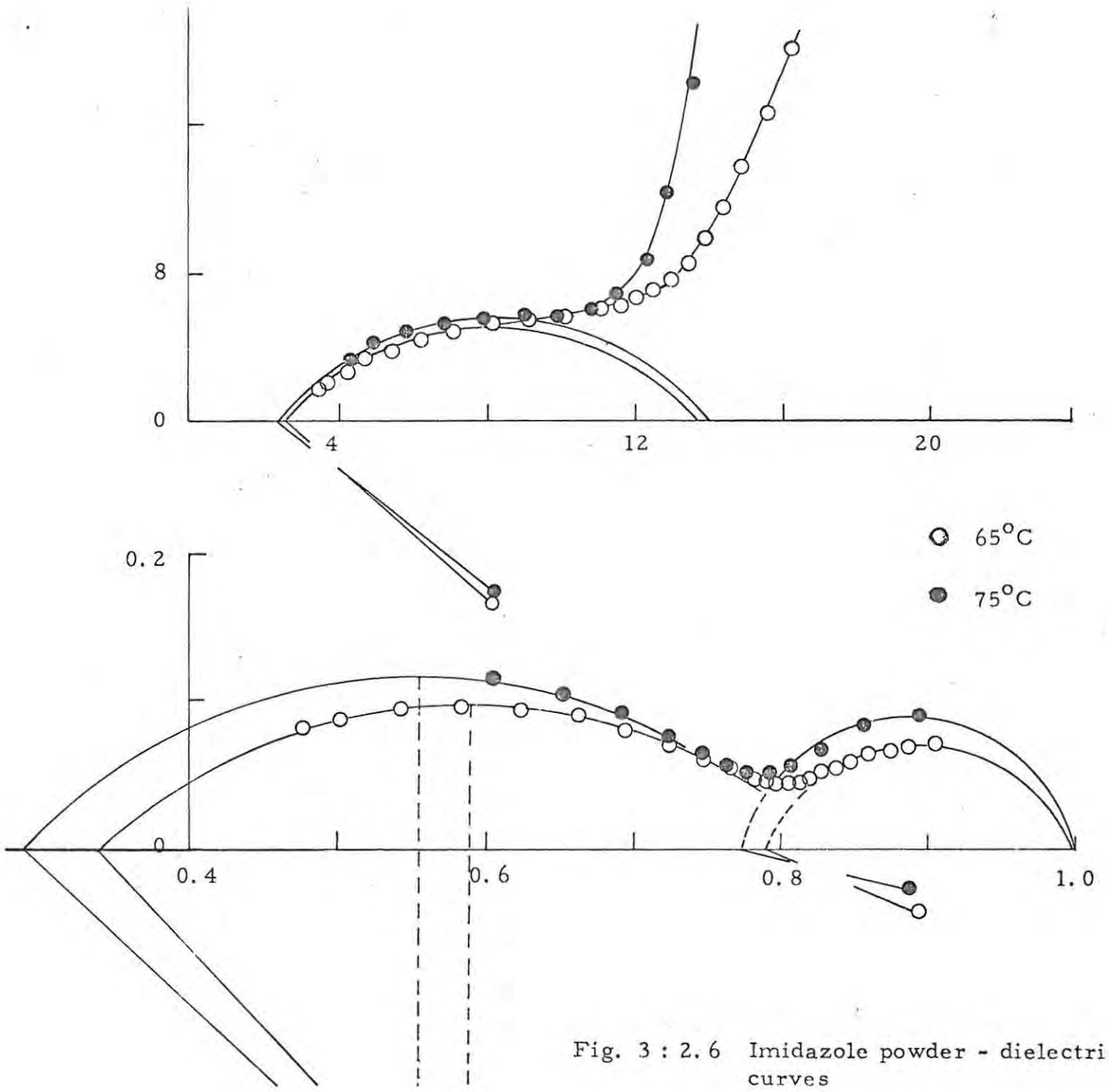

Fig. 3 : 2.6 Imidazole powder - dielectric dispersion curves

SECTION 3 : 3 UREA POWDERS

3 : 3 : 1 Dielectric Measurements

Dielectric measurements from 70°C to 90°C were performed on powder pellets of urea. A freshly-prepared pellet showed a remarkably large dielectric dispersion (fig. 3 : 3. 1), which reduced to a steady condition after desiccating in vacuum over P_2O_5 for several days. Thus it would seem that the low frequency dispersion of the freshly-prepared pellet is due to occluded mother liquor, freed on grinding and/or pressing the pellet (Dryden and Meakins 1953). The dielectric dispersion curves of the desiccated sample (fig. 3 : 3. 2) are similar to those of imidazole, displaying a low-frequency "tail" at high temperature (90°C) and a broad high-frequency dispersion. The parameters of the dispersion (table 3 : 3. 1) are, however, very different from those for imidazole. The static dielectric constant, and the dielectric constant at infinite frequency, are approximately temperature independent.

The dispersion for urea is almost four times that for imidazole, and the relaxation time is 10^3 times longer ($\tau_c = 3\times10^{-3}$ s at 70°C for urea) but the activation energy (fig. 3 : 3. 3) is about the same at 23 kcal mol^{-1}.

3 : 3 : 2 D. C. Conductivity

The electrical properties of urea, recrystallised twice from methanol and vacuum desiccated for a period of 2 to 5 days, were found

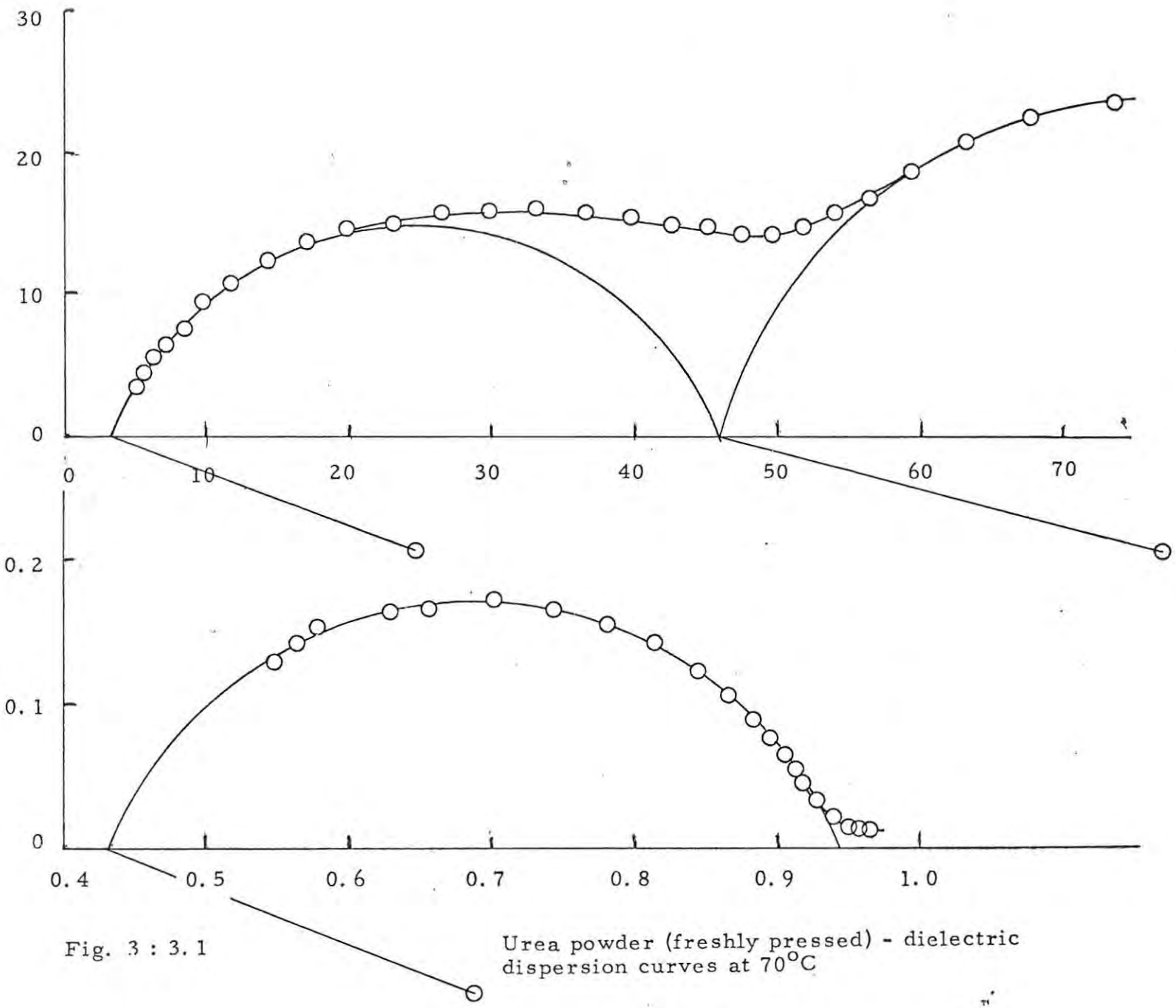

Fig. 3 : 3.1

Urea powder (freshly pressed) - dielectric dispersion curves at 70°C

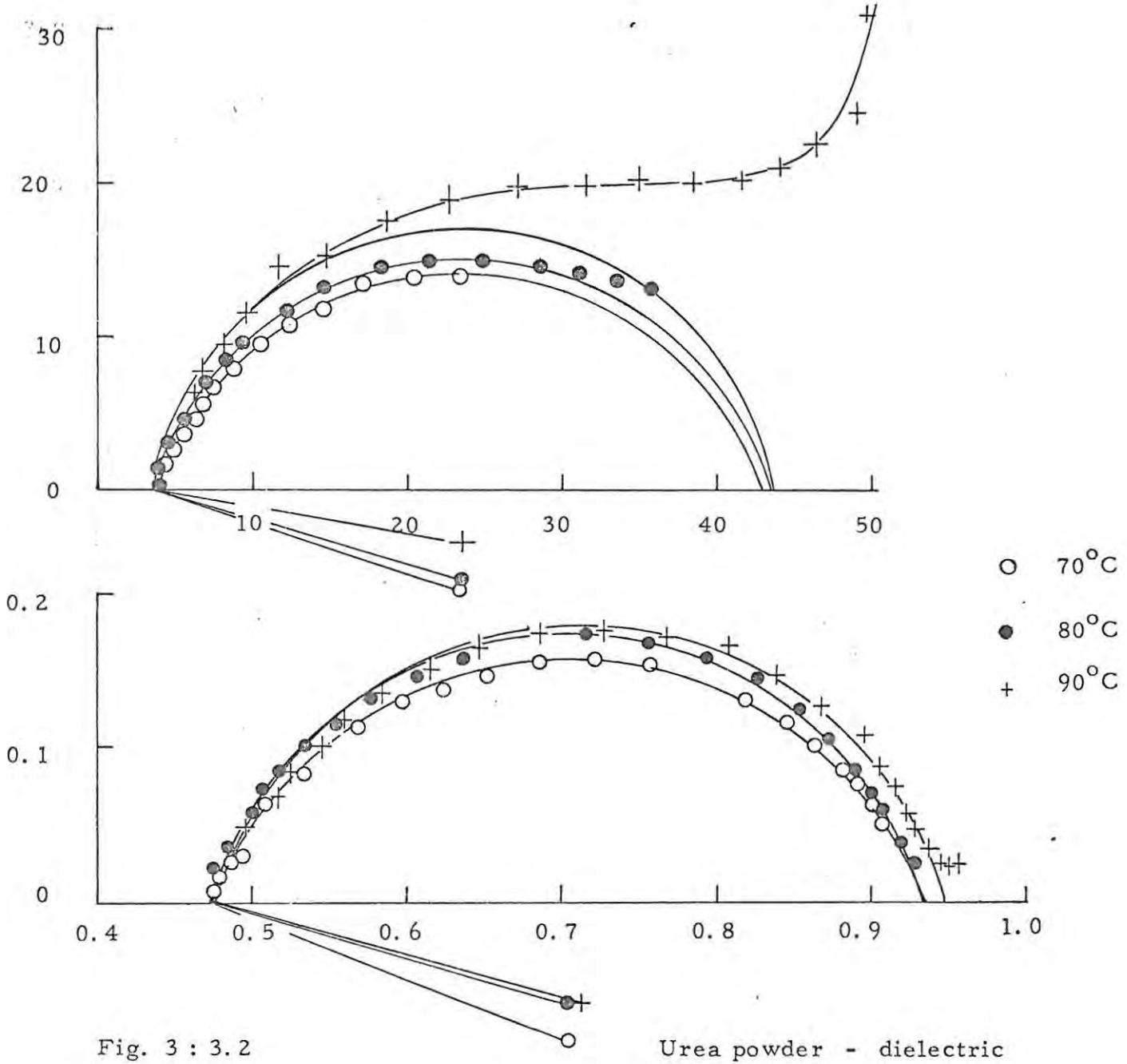

Fig. 3 : 3.2

Urea powder - dielectric dispersion curves

TABLE 3 : 3.1 Temperature-dependence of the dielectric dispersion parameters of urea powder (the same sample was used for all these measurements)

Dielectric dispersion parameters	ε'_o	ε'_∞	τ /s	h	Condition
70°C *	46	3.2	3×10^{-5}	0.23	freshly pressed
70°C **	108	46	3×10^{-3}	0.17	freshly pressed
70°C	43	4.0	3×10^{-3}	0.21	Desiccated for 6 days
80°C	43	4.0	8×10^{-4}	0.19	Desiccated for 5 days
90°C	43	4.0	3×10^{-4}	0.12	Desiccated for 7 days

* high frequency
** low frequency

to be similar, using either P_2O_5 or silica gel as desiccant; the conductivity at 60° in the form of powder pellets, is about 4.4×10^{-11} ohm^{-1} cm^{-1} using blocking electrodes. However, if the pellets are subjected to a hard vacuum for 15 minutes before pressing in the die, the conductivity increases by a factor of 10 to about 8.3×10^{-10} ohm^{-1} cm^{-1}, but the current density versus field strength (J-V) characteristics are unaffected, being initially ohmic and showing signs of polarization at higher field strengths (3-6 $kVcm^{-1}$).

An activation energy of 35 kcal mol^{-1} (fig. 3 : 3.4 and table 3 : 3.2) was obtained from a pellet of urea which had been electrolysed in the conductivity cell for 4 hours, until polarization had substantially ceased, before the conductivity measurements were made at various temperatures.

TABLE 3 : 3.2 Variation of conductivity with temperature of a polarized pellet of urea

$t/^oC$	60	50	40	30
$\sigma / 10^{-12} ohm^{-1} cm^{-1}$	26.5	5.10	0.760	0.135

Application of a Pd/H_2 protode had little effect on the conductivity, which was essentially the same as with blocking electrodes, but the current displayed a slight super-linear rise with applied potential at about 5 $kVcm^{-1}$, and breakdown potential was reached at 10 kV cm^{-1}. On the other hand, using imidazole as a protode, there were definite signs of proton injection. A comparison of the (J-V) characteristics of urea using Pt electrodes, an imidazole anode and a Pd/H_2 anode (fig. 3 : 3.5) shows that imidazole is an effective protode for urea

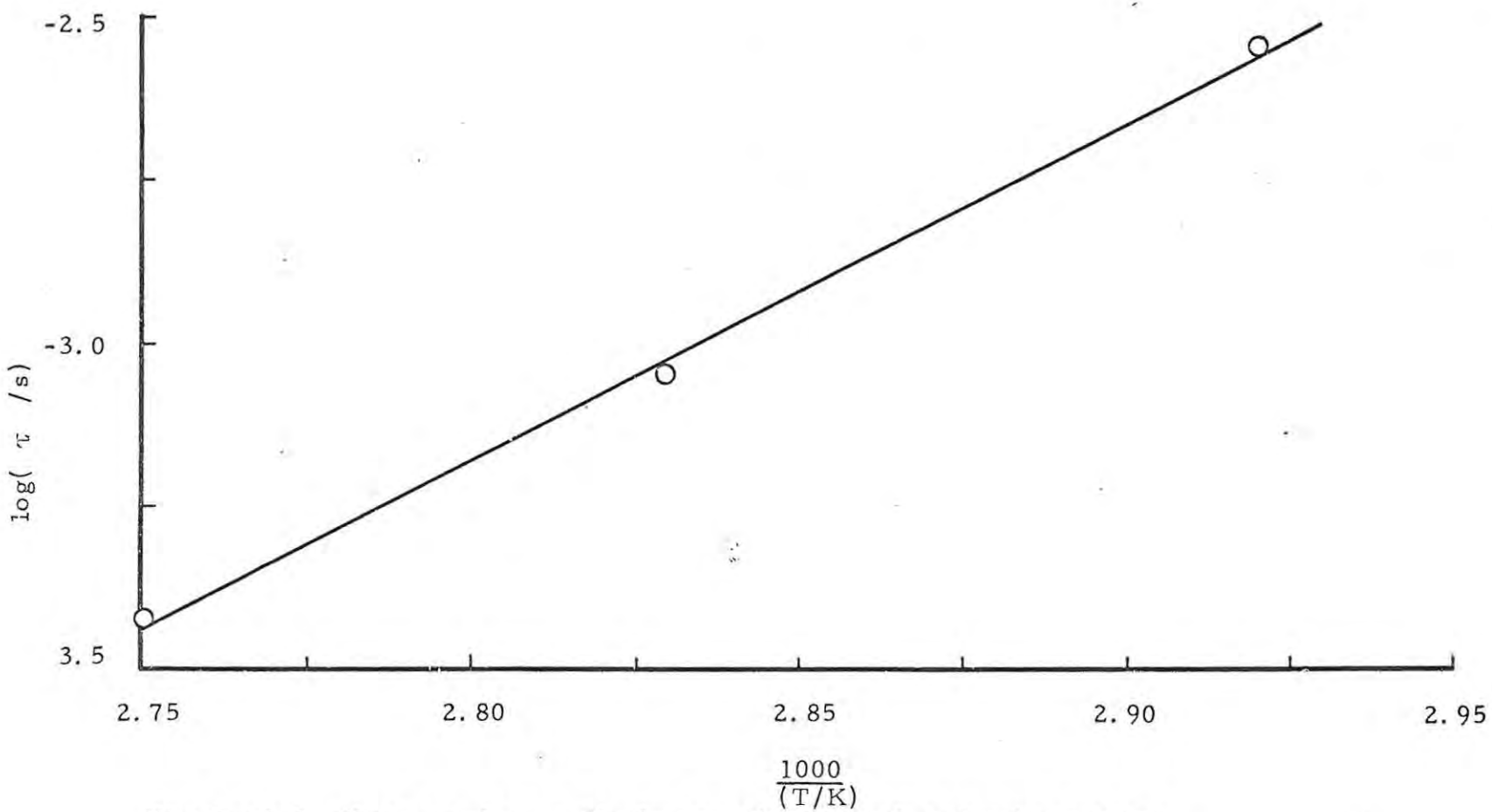

Fig: 3 : 3.3 Urea powder - dipole re-orientational activation energy

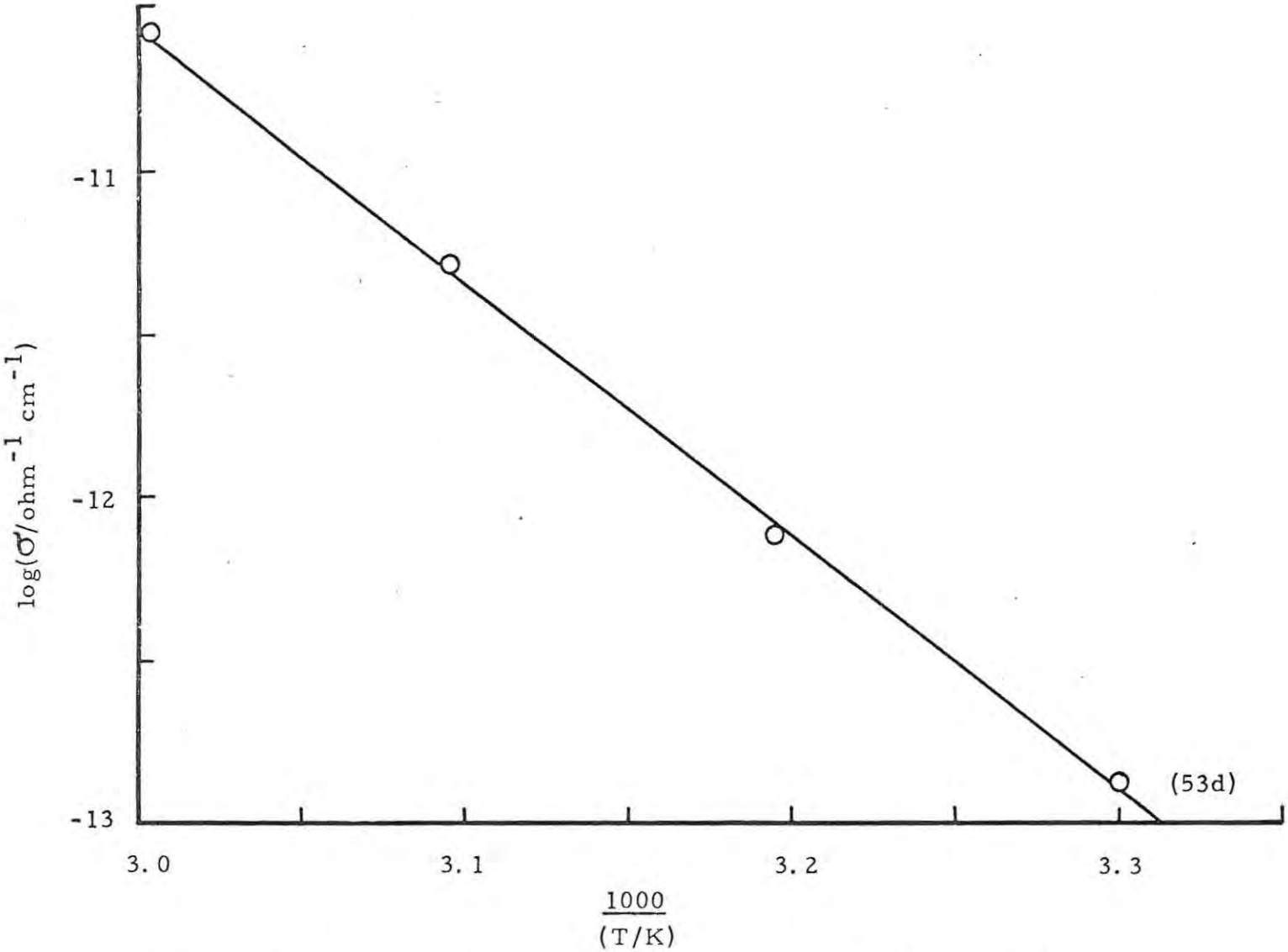

Fig. 3 : 3.4 Urea powder - activation energy - blocking electrodes

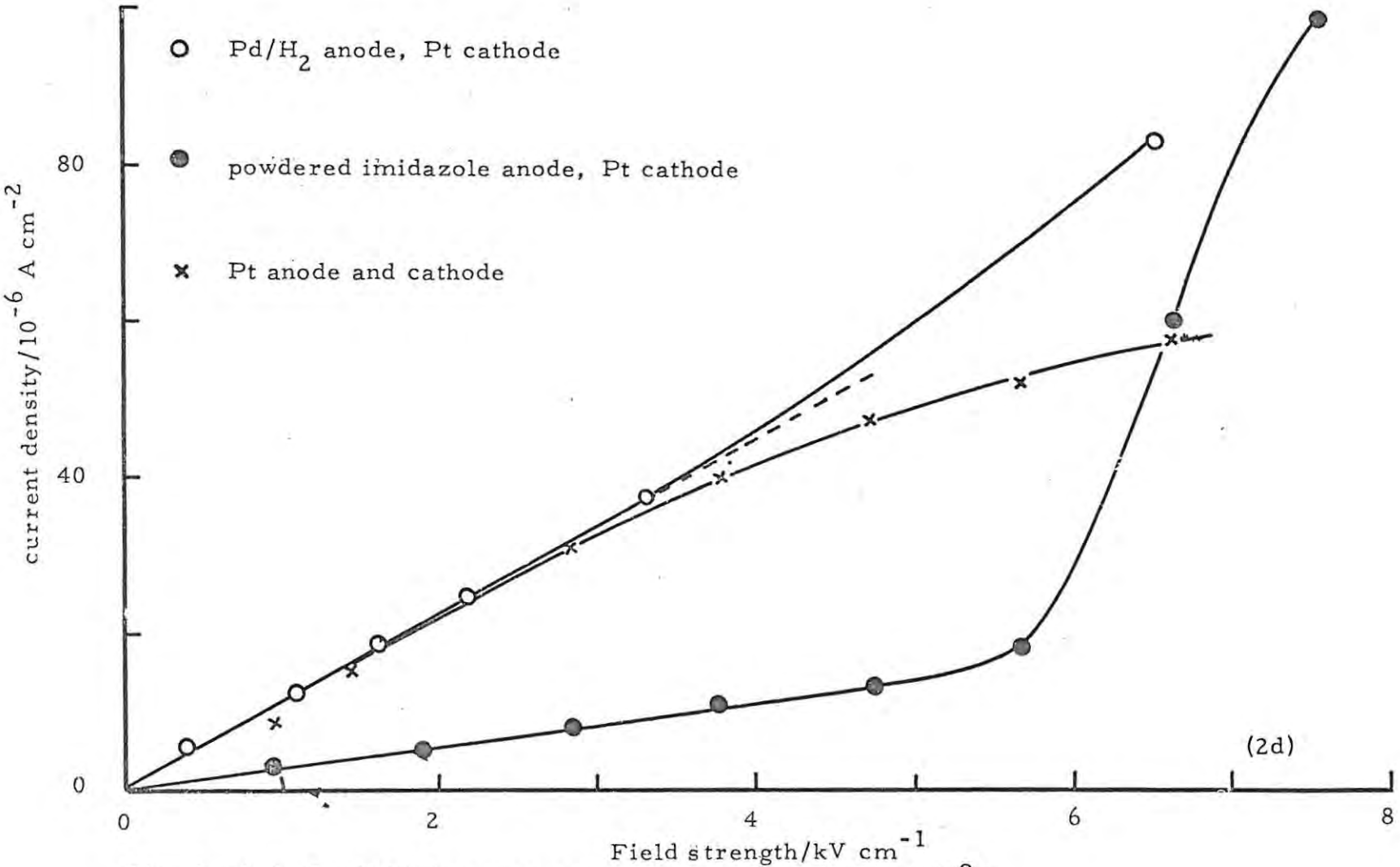

Fig. 3 : 3.5 Conductivity measurements on urea powder at 60°C

(the effects of this protode are further discussed in the following section).

3 : 3 : 3 Electrolysis

Electrolysis of a urea pellet at 60°C yielded some gas at the anode (fig. 3 : 3. 6) at a proton efficiency of 59%, but since the rate of evolution rapidly decreased after the passage of 0. 08 coulombs of charge, it is believed that urea is not an intrinsic proton conductor. The rapid decrease of gas evolution at the anode was ascribed to the depletion of minute quantities of impurities (possibly traces of adsorbed methanol). After the passage of 0. 13 coulombs of charge, the sample conductivity was examined in the range 0-40 $kVcm^{-1}$ and found to be highly ohmic (fig. 3 : 3. 7) with a conductivity of 7.9×10^{-12} $ohm^{-1}\ cm^{-1}$. Since the conductivity of imidazole at 60°C is high, only about 10^{-8} $ohm^{-1}\ cm^{-1}$ (Aftergut and Brown 1962), imidazole was tried as a proton-injecting electrode (protode) on the electrolysed urea pellet. When the imidazole pellet was initially biased negative, the current was, as expected, controlled by the sum of the pellet resistances in series, but when the direction of the applied voltage was reversed, the current increased slowly at first, and then rapidly, to reach values corresponding to a conductivity of the pair - sample of about 10^{-8} $ohm^{-1}\ cm^{-1}$, the proton efficiency being 91%. Reversing the bias resulted in decreasing conductivity, until the sample broke down under the high voltage applied.

A compound pellet consisting of urea with an imidazole pellet as anode, pressed together in a die, gave a proton efficiency of 87%. A slight lag in gas evolution at the anode was noted (fig. 3 : 3. 8).

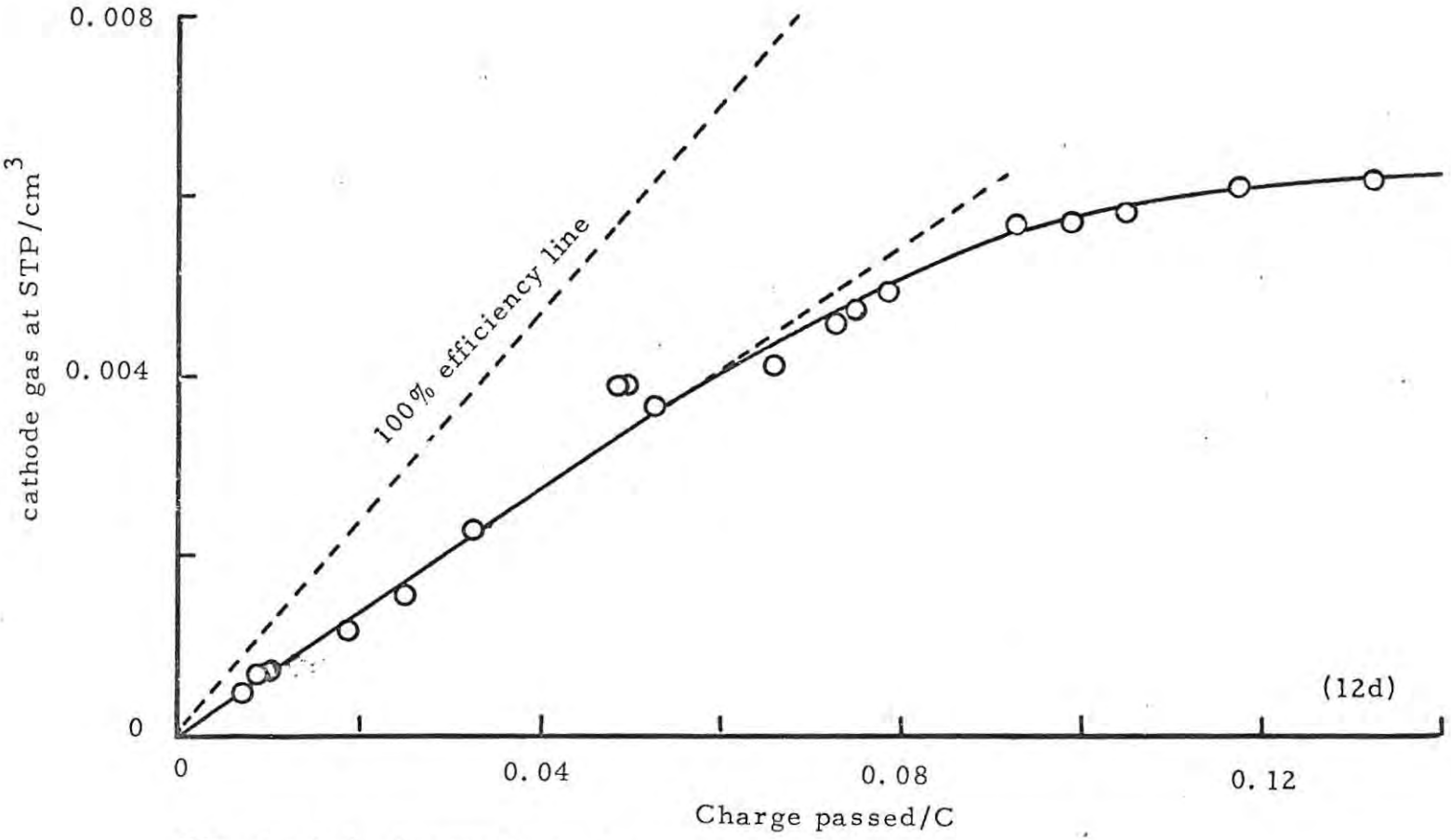

Fig. 3 : 3.6 Electrolysis of urea powder compact

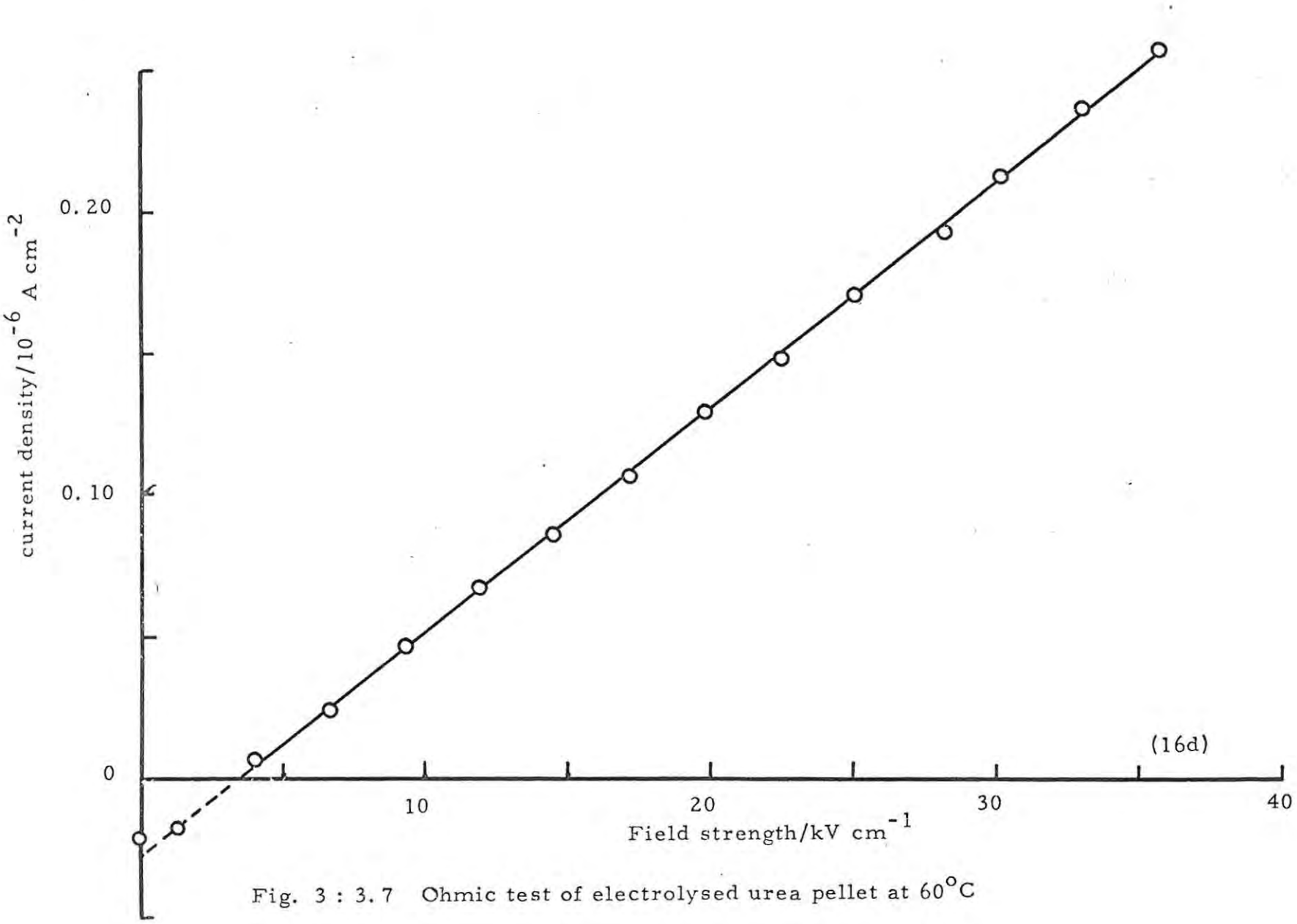

Fig. 3 : 3.7 Ohmic test of electrolysed urea pellet at 60°C

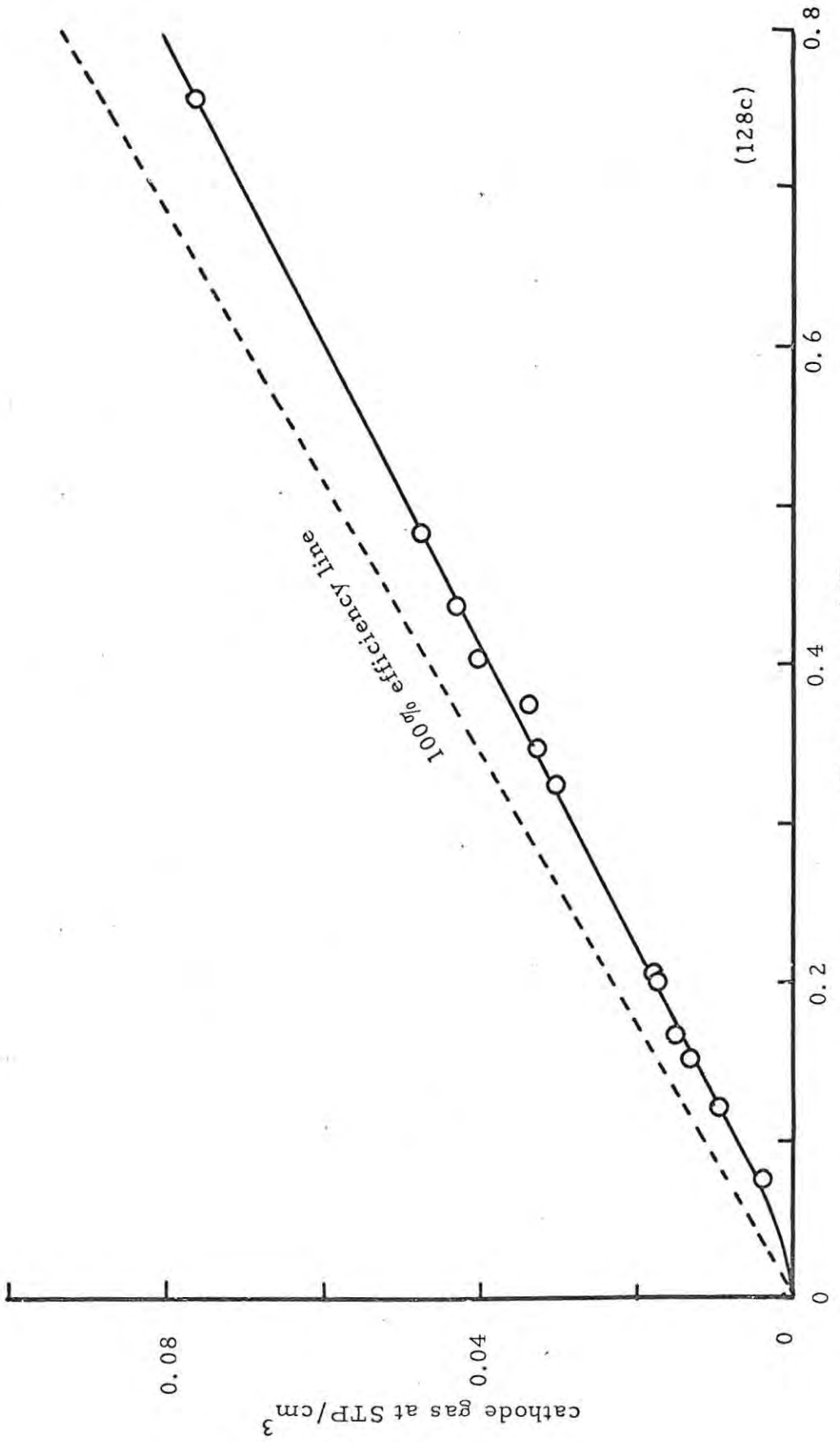

Fig. 3 : 3.8 Electrolysis of urea powder compact with imidazole-coated anode

Molten urea, on electrolysis, deposited no solid products, but gases were produced at the anode and cathode. Simple chemical tests indicated that the anode gas probably contained CO_2 and the cathode gas probably contained some NH_3/H_2.

SECTION 3 : 4 : SINGLE CRYSTALS OF UREA

3 : 4 : 1 D. C. Conductivity

The conductivity of urea single crystals requires to be measured only in the unique c direction and normal to it to establish the conductivity ellipsoid fully, because the crystal belongs to the tetragonal system. The activation energies in table 3: 4.1 were obtained from $\log\sigma$ vs $1/T$ plots (fig. 3 : 4.1) in the usual way. Conductivity measurements were also made on a single crystal grown from a saturated solution of 90 g urea in 300 ml methanol containing 2.5 g ammonium bromide to control the crystal habit. Although this crystal was not analysed for ammonium bromide content, according to Andrew and Hyndman (1955), urea crystals grown from such a solution did not give a positive reaction to a test for ammonia using Nessler's reagent. Nevertheless the electrical properties differ from those of a crystal grown from undoped solution. It is perhaps interesting to note that Fuller and Patten (1970) used urea to control the crystal habit of NH_4Cl single crystal growth; the presence of urea in these crystals could not be detected by NMR and infrared absorption techniques, and such crystals were used in their electrical measurements.

Unlike urea powders, when imidazole pellets were applied to urea single crystals, there were no delayed effects; the apparent conductivity was immediately increased, so that the current in the a direction increased by a factor of 4 above that with the same voltage for the urea crystal alone, and approximately 100 times for the c direction of the crystal, along which the hydrogen bond chains lie. The pair-samples showed ohmic behaviour, in general.

TABLE 3 : 4.1 TEMPERATURE-DEPENDENCE OF THE CONDUCTIVITY OF UREA SINGLE CRYSTALS

Conductivity σ / ($ohm^{-1} cm^{-1}$)	Temperature (t/ °C)				Activation Energy (E/kcal mol^{-1})
	30	40	50	60	
a axis	–	4.4×10^{-14}	69×10^{-14}	73×10^{-14}	54
c axis	4.5×10^{-12}	23×10^{-12}	114×10^{-12}	290×10^{-12}	31
c axis *	1.3×10^{-10}	3.5×10^{-10}	9.0×10^{-10}	27×10^{-10}	19

* Single crystal grown from a saturated solution containing some ammonium bromide to inhibit crystal growth in the c direction

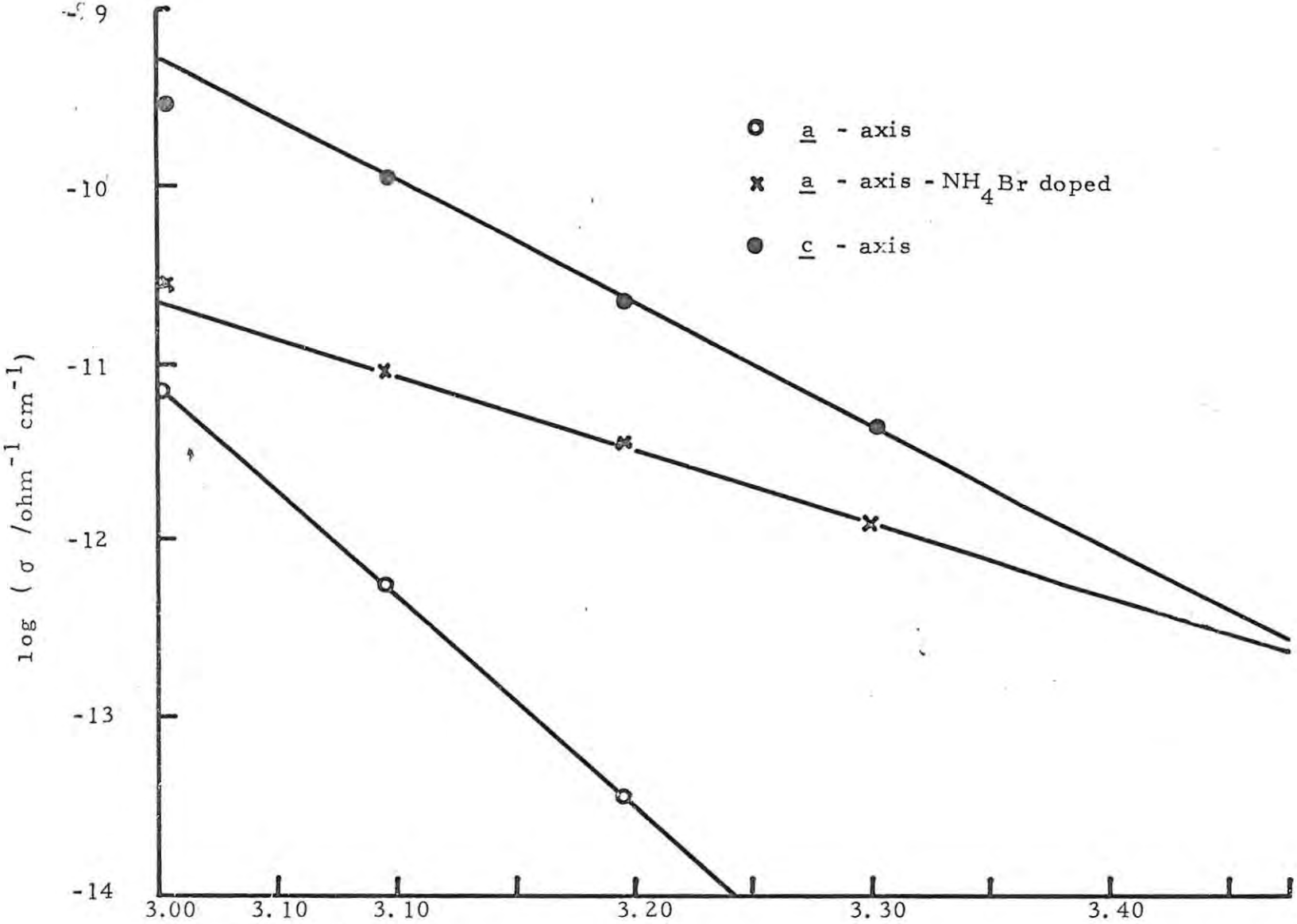

Fig. 3:4.1 Activation energy for conduction in urea single crystal

3 : 4 : 2 Electrolysis

The protolysis of urea, using an imidazole protode, was studied along the c axis (parallel to the hydrogen bond chain). In the initial stages of protolysis hydrogen gas evolution at the cathode was minimal (fig. 3 : 4.2), but after the passage of 0.1 coulomb of charge, the proton efficiency rose, and remained constant at 73%.

Gas evolution at the cathode in crystals mounted for protolysis in the a direction was either absent or too small to detect.

3 : 4 : 3 Evidence for the Existence of a Grothuss Mechanism of Proton Conduction in Urea

In some further work done in this laboratory by F. M. Saba, an imidazole protode, deuterated in the 1 position, was applied to a urea pellet. The electrolysis gas was analysed using mass spectrometric techniques and was found to contain 47% hydrogen and 1% deuterium. The remainder of the gas sample consisted of air due to contamination in the process of collection, and some mercury vapour. Thus the ratio of hydrogen to deuterium in the electrolysis gas is about 50 to 1. This result may be taken as evidence for a Grothuss mechanism of proton conduction in urea, since an interstitial mode of proton conduction would have yielded a cathode gas containing predominantly deuterium. The small amount of deuterium in the cathode gas could be ascribed to a small contribution to the charge transport by an interstitial mechanism, but the following is perhaps a more likely explanation:

Extrinsic proton conduction in urea is approximately 90% efficient, while the intrinsic proton conduction efficiency of imidazole is about 98%. This implies that the extrinsic conduction of urea has an electronic

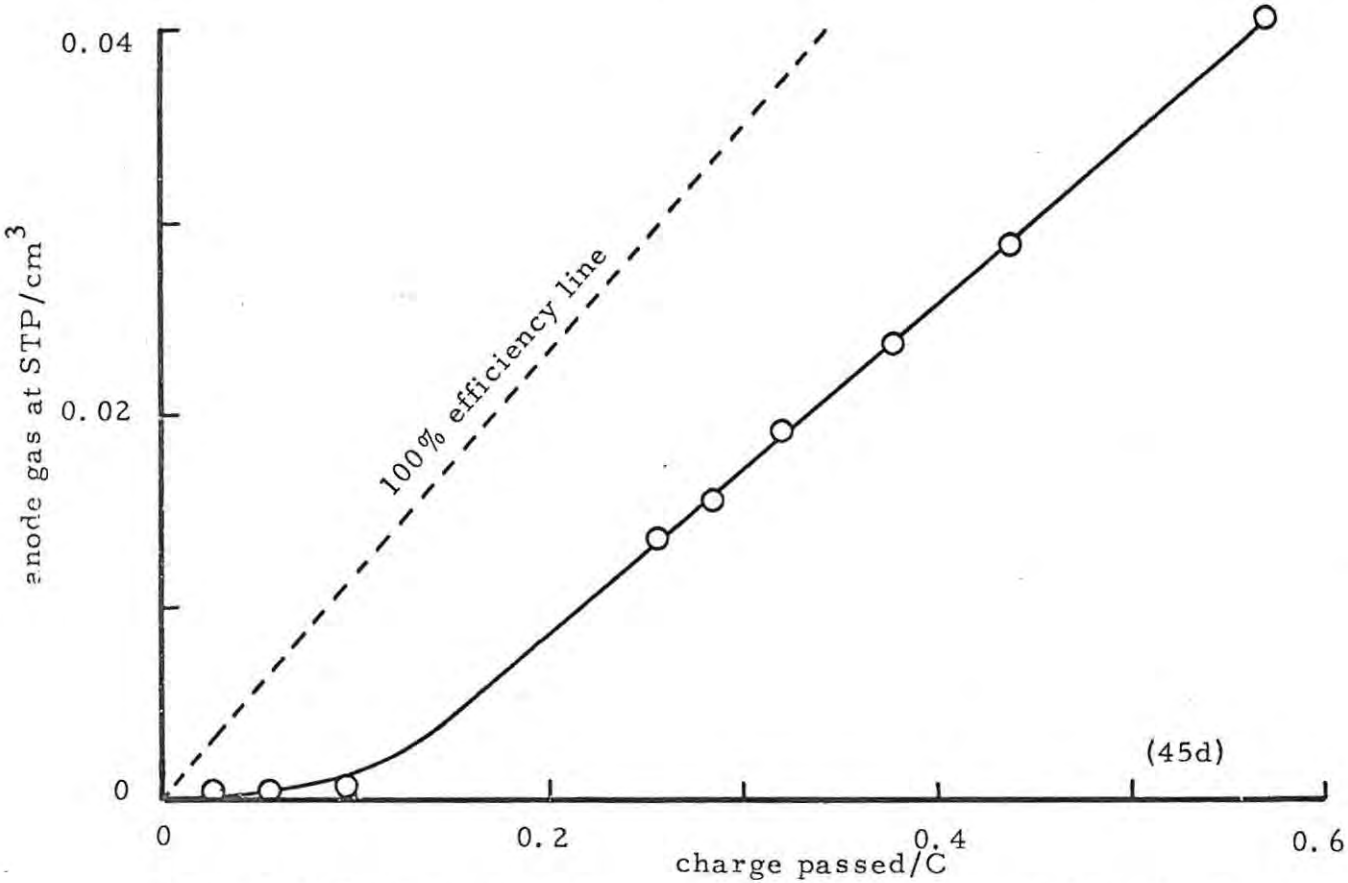

Fig. 3 : 4.2 Urea crystal - c axis - protolysis with imidazole anode and Pt cathode

conduction component of approximately 10%, while that in imidazole is perhaps 2%. The difference in the electron conduction components (8%) can be accounted for by assuming that at the imidazole/urea interface, the 8% of electronic charge is consumed by reducing deuterons to produce D_2 gas, some of which then diffused through the powdered urea into the electrolysis cell.

CHAPTER 4

DISCUSSION

SECTION 4 : 1 DIELECTRIC MEASUREMENTS

The comparatively large activation energies for dipole re-orientation, and their long relaxation times, for both imidazole and urea (see tables 3 : 3.1 - 2) do not support the proposition of movement of protons across hydrogen bonds as the mechanism of dipole absorption. There is, however, the possibility that dipole re-orientation occurs via a "tour" mechanism whereby there is a sequence of proton migrations round a molecule, from carbon to carbon. This effect has been discussed for the case of carbanions, whose stability depends on extensive charge delocalisation, and which are planar (Cram 1967), as are both urea and imidazole. Imidazole lends itself to such a process, since the intermolecular -H...N- separation (Will 1969) is much less than the bond length in hydrogen (0.74A^{o}); the strong hydrogen bond might be expected to suppress rotation of the imidazole molecules. On the other hand, the dipole re-orientation process in urea probably involves molecular rotation since the relaxation time is about 10^3 times longer than in imidazole. Although the urea molecule undergoes a particularly large libration about the c axis (Bodger and White 1967) this motion cannot contribute to dipole re-orientation absorption, as there is no net movement of the dipole in this motion. In order for molecular rotation to contribute to dipole reorientation, the molecule would have to undergo end-over-end

rotation about the H-bonds, thus reversing its orientation in the chain of molecules in the c axial direction.

The dipole moments for urea and for imidazole, estimated from dielectric data in dilute solution are 4.6 D and 4.0 D, respectively (Kumler and Fohlen 1944 for urea, and Simonov et al. 1961 for imidazole). On substituting these values for the dielectric dispersion parameters of imidazole and urea together with the appropriate experimentally evaluated quantities into the Kirkwood-Fröhlich equation (see Hill et al. 1969), it was found that the concentrations of such re-orienting dipoles in imidazole and in urea both correspond to about 2×10^{21} cm^{-3}. Thus, the dielectric dispersions of urea and imidazole correspond to the rotational motion of perhaps 20% of dipoles having the moments of the free molecules. Alternatively, this is equivalent to the effective dipole moment in the solid being about half that in solution, assuming that every molecule in the solid contributes to the dipole re-orientation process. Similarly, about 20% of "equivalent" water molecules were found to participate in localised motions in HF-doped ice, in borax and in $Li_2SO_4 . H_2O$ (Van Beek 1963).

According to the reaction rate theory of dielectrics (Kauzmann 1942), long values of the relaxation time are indicative of an ordering process, whereas short values of relaxation time indicate a disordering process. Since the relaxation time of urea is a thousand times longer than that of imidazole, the activation step of the relaxation process in urea must be more "ordered" than in imidazole; this could be thought to indicate that the range of the co-operation in urea is longer. Although longer co-operation corresponds to a larger

effective dipole moment of the relaxing system, the dispersion in imidazole is much larger; the concentration of co-operative processes in urea must therefore be less, although each one has a longer range.

SECTION 4 : 2 : BLOCKING ELECTRODES

A rough estimate of the density of the thermally produced carriers in imidazole has been made by applying equation 1 : 4. 5. Using an average value of 14 for the static dielectric constant and a cross-over voltage of 120 V, a density of 2×10^{13} cm^{-3} is obtained which, on substitution into the conductivity formula, yields a mobility of 2×10^{-5} $cm^2 V^{-1} s^{-1}$. This value of the mobility is of the expected order, being nearly equal to that in copper sulphate pentahydrate, 1×10^{-5} $cm^2 V^{-1} s^{-1}$ (Williams et al. 1967), but smaller than the mobility for the imidazole melt (Kawada et al. 1970) by a factor of a hundred, and much less than that for isocytosine, 2 $cm^2 V^{-1} s^{-1}$ (Thomas et al. 1969). Taking a total concentration of protons of about 10^{22} cm^{-3}, the proportion participating in conduction at any one time is only about 1 in 10^{10}, in contrast to the large proportion of "equivalent" dipoles which our prior calculation would show to be participating in the dielectric absorption process; dipole re-orientation must therefore be a co-operative effect especially in view of the fact that X-ray and other data show the urea molecule to be in a firmly-established orientation in the solid.

Although the proton in its hydrogen bond is highly mobile (Joop and Zimmermann 1962, 1964), the charge carrier mobility in imidazole is not very large. This may be due to the fact that the thermal concentration of defects in imidazole is very low, perhaps owing to the high energy of formation of D defects. The mechanism of re-orientation therefore depends on L defect injection at the cathode (Kawada et al. 1970). Although L defect initiation requires energy (probably of the order of 20 kcal mol^{-1}), this energy term does not appear in the activation energy for conduction, since the energy is

supplied by the field, and is therefore temperature-independent. Since conduction in urea under non-injecting conditions is electronic, the number of thermally produced carriers is not of interest, and will not be discussed.

SECTION 4 : 3 : NON-BLOCKING ELECTRODES

The Pd/H_2 protode has proved to be unreliable, and perhaps even ineffective, as a protode; this may be due to poor electrical contact of the metal electrode with the sample. In marked contrast, imidazole has been demonstrated to be a very successful protode for urea, with which many-fold increases in current through the urea have been achieved. However, the use of imidazole as a protode has introduced further complications; the conductivity of urea cannot be determined, since the conductivity of imidazole, with urea acting as a proton acceptor, is unknown. Consequently, evaluation of activation energies and of the number of thermally produced carriers, as well as of mobilities of such pair-samples is not practical.

SECTION 4 : 4 : CONDUCTION MECHANISM

Imidazole:

The mechanism for proton conduction in imidazole proposed by Kawada et al. (1970) is modelled on that of ice, and appears to be sound. However, there is doubt about the validity of their assumption that the observed energy of activation for conduction (40 kcal mol^{-1}) can be ascribed to rotation alone (see Section 1 : 6 : 3). Using the activation energy for re-orientation of dipoles, $E_{reorient}$ (26 kcal mol^{-1}) obtained from our dielectric results, and assuming Kawada et al's activation energy for conduction, E, we have

$$E = \tfrac{1}{2}E_d + E_m + E_{reorient}$$

or $$40 = \tfrac{1}{2}E_d + E_m + 26$$

where E_d is the dissociation energy, and E_m is the activation energy for mobility. Thus

$$\frac{E_d}{2} + E_m = 19 \text{ kcal mol}^{-1}$$

E_m is expected to be very small, since the hydrogen bond is very short and the probability of tunnelling is high. Therefore E_d is approximately 38 kcal mol^{-1}. There is a possibility that the mechanism for re-orientation of the chains involves an intramolecular proton migration, i. e. a tour round the molecule (see Section 4 : 1), instead of the usually postulated molecular rotation step. This hypothesis could be tested by methylating the imidazole ring in the 2- or the (4, 5) - position; if the re-orientation involves an intramolecular proton migration, then proton conduction should not be observed.

Urea:

Urea is an extrinsic proton conductor, since proton conduction can only be induced in the solid by injection of protons. This implies that there is either no thermal or induced ionization of the molecules, or that any ions present in the solid are not mobile. The explanation as to why urea is an extrinsic but not an intrinsic proton conductor must be sought from the crystal structure. The urea molecules are extensively hydrogen-bonded in three dimensions (Caron and Donahue 1964). The strongest of these hydrogen bonds lie in the c crystallographic direction, the direction along which extrinsic proton conduction takes place. Despite the large libration of the urea molecule about the c axis, extrinsic proton conduction normal to this direction is absent, probably because the protons in the hydrogen bonds are not suitably disposed for co-operative motion of the protons. On the other hand, the dielectric results seem to indicate that there is some co-operative end-over-end tumbling of the urea molecules, possibly using the hydrogen bonds in the a b plane as axes, and with an activation energy of 23 kcal mol^{-1}.

It is therefore postulated that the injected protons are transmitted along the c direction by a series of transferences, the injected proton being conveyed on the oxygen atoms of urea, and transferred from molecule to molecule whenever two oxygen atoms on adjacent molecules meet as a result of a molecular rotation. In the absence of proton injection, no proton is available for the oxygen atom to carry, unless thermal ionisation could occur, i.e., motion of the proton across the structurally established hydrogen bond -N-H ... O-. This thermal ionisation must be unlikely because intrinsic proton conduction is either small or absent. Since transfer of a proton between the oxygen atoms should occur rapidly, with little activation energy, molecular rotation is expected to be the rate-

determining step. If the "activation energy" under injecting conditions were meaningful, then the observed activation energy for conduction would be approximately that of molecular rotation.

BIBLIOGRAPHY

Andrew E. R. (1950) J. Chem. Phys. 18, 607

Andrew E. R. and Hyndman D. (1955) Disc. Far. Soc. 19, 195.

Auty R. P. and Cole R. H. (1952) J. Chem. Phys. 20, 1309.

Baker W. O. and Yager W. A. (1942) J. Amer. Chem. Soc. 64, 2171.

Barr M. R., Durrell B. A. and Grant R. F. (1963) Can. J. Chem. 41, 1188.

Beckett A. H. and Tinley E. H. (third edition) in "Titrations in Non-Aqueous Solvents", The British Drug Houses Ltd. (B. D. H. Laboratory Chemicals Division), Poole, Dorset.

Beilstein's Handbuch der Organischen Chemie (1954) 2nd supplement, 23, 34. (The value quoted here seems to refer to liquid).

Beilstein's Handbuch der Organischen Chemie (1921, reprinted 1943), 4th edition, 3, 45.

Bernal J. D. and Fowler R. H. (1933) J. Chem. Phys. 1, 515.

Bjerrum N. (1951) Kgl. Dansk. Selskab. Mat. Fys. Medd. 27, 56.

Bjerrum N. (1952) Science. 115, 385.

Bodger E. O. and White W. J. (1967) Chem. Comm. 74.

Bradley R. S. (1957) Trans. Far. Soc. 53, 687.

Bragg W. H. (1921) Proc. Phys. Soc. Lond. 34, 98.

Brown G. P. and Aftergut S. (1962) in "Organic Semiconductors" ed. J. J. Brophy and J. W. Buttery, MacMillan, New York, 89.

Brown G. P. and Aftergut S. (1963) J. Chem. Phys. 38, 1356.

Bullemer B., Engelhardt H. and Riehl N. (1969) in "Physics of Ice" ed. N. Riehl, B. Bullemer and H. Engelhardt, Plenum Press, New York, 424.
See also Bullemer B., Eisele I., Engelhardt M., Riehl N. and Seige P. (1968) Solid State Comm. 6, 663.

Cardew H. H. and Eley D. D. (1959) Disc. Far. Soc. 27, 115.

Campbell N. and Cairns-Smith N. G. (1961) J. Chem. Soc. 1191.

Chan-Henry R. and Glasser L. (1970a) National Symposium on Electrochemistry, Pretoria, April.

Chan-Henry R. and Glasser L. (1970b) "Proton Conduction in Solid Amino Compounds" (Second International Symposium on Organic Solid-State Chemistry) Rehovoth, Israel.

Clifford J. (1962) Nature 195, 568.

Clifford J. (1967) Chem. Comm. 880.

Cohan N. V., Cotti M. Iribarne J. V. and Weissman M. (1962) Trans. Far. Soc. 58, 490.

Cole K. S. and Cole R. H. (1941) J. Chem. Phys, 9, 341.

Cram D. J. (1967) S. A. Chem. Inst. Convention 10th-14th June.

Cuthbert J. D. and Petch H. E. (1963) Can. J. Phys. 41, 1629.

Czech J. (1957) "The Cathode Ray Oscilloscope" Philips, Eindhoven.

Daycock J. T., Jones G. P., Evans J. R. N. and Thomas J. M. (1968) Nature, 218, 672.

Deprez G. and Fontaine H. (1965) Bull. Soc. Franc. Miner. Crist. 88 (4), 697.

Dryden J. S. and Meakins R. J. (1953) Nature, 171, 307.

Dunitz J. D. (1963) Nature, 197, 860.

Eley D. D. (1967) J. Polymer Sci. Pt. C. 17, 73.

Eley D. D. (1968) in "Organic Semiconducting Polymers" ed. by J. E. Katon, Marcel Dekker Inc., New York.

Eley D. D. and Spivey D. I. (1961) Trans. Far. Soc. 57, 2280.

Eigen M. and De Maeyer L. (1958) Proc. Roy. Soc. (London) A 247, 505.

Eigen M. De Maeyer L. and Spatz H. Ch. (1964) Ber. Bunsenges. 68, 19.

Engelhardt H., Bullemer B. and Riehl N. (1969) in "Physics of Ice" ed. N. Riehl, B. Bullemer and H. Engelhardt, Plenum Press, New York, 430.

Engelhard H. and Riehl N. (1965) Phys. Lett. 14, 20.

Engelhard H. and Riehl N. (1966) Physik Kondens. Materie. 5, 73.

Eisenberg D. and Coulson C. A. (1963) Nature, 199, 368.

Eisenberg D. and Kauzmann W. (1969) "The Structure and Properties of Water", Oxford, U.P., 116.

Faraday M. (1850) Proc. Roy. Inst. Great Britain.

Fieser L.F. and Fieser M. (1967) in "Reagents for Organic Synthesis", Wiley, 835.

Fripiat J.J., van der Meersche C., Touilliaux R. and Jelli A. (1970) J. Phys. Chem. 74, 382.

Garrett C.G.B. (1959) in "Semiconductors" ed. N.B. Hannay, Reinhold Publ. Corp. New York, 634.

Giesekke E.W. (1965a) Ph.D. Thesis, Witwatersrand.

Giesekke E.W. (1965b) Ph.D. Thesis, Witwatersrand, 23.

Giesekke E.W. (1965c) Ph.D. Thesis, Witwatersrand, 38.

Giesekke E.W. and Glasser L. (1967) J. Phys Chem. 71, 2573.

Glasser L. (1960a) Ph.D. Thesis, London.

Glasser L. (1960b) Ph.D. Thesis, London, 261.

Glasser L. (1960c) Ph.D. Thesis, London, 281.

Glen J.W. (1969) Sc. Progr. Oxford, 57, 1.

Gränicher H. (1958) Z. Krist. 110, 432.

Gränicher H. (1963) Phys. Kondens. Materie 1, 1.

Gränicher H., Jaccard C., Scherrer P. and Steinemann A. (1957) Disc. Far. Soc. 23, 50.

Gravatt C.C. and Gross P.M. (1967) J. Chem. Phys. 46, 413.

Gurevich V.M. and Zheludev I.S. (1960) Soviet Physics Cryst. (English trans.) 5, 767.

Gurney R.W. (1931) Proc. Roy. Soc. (London) A134, 137.

Gutowsky H.S. and Pake G.E. (1950) J. Chem. Phys. 18, 162.

Guttmann F. and Lyons L.E. (1967a) "Organic Semiconductors", Wiley, New York, pp. 428-435.

Guttman F. and Lyons L.E. (1967b) "Organic Semiconductors" John Wiley and Sons, Inc. New York.

Haas C. (1962) Phys. Lett. 3, 126.

Hill N., Vaughan W.E., Price A.H. and Davies M. (1969) in "Dielectric Properties and Molecular Behaviour", von Nostrand, New York.

Holden A. N. and Singer P. (1961) "Crystals and Crystal Growing", Heinemann, London.
See also Petrov. T. G.,Treivus E. B. and Kasatkin A. P. (1969) in "Growing Crystals from Solution", ed. A. Tybulewicz, Consultants Bureau, New York.

Inikuchi H. and Akamatu H. (1961) Solid State Physics, 12, 93.

Itoh J., Kusaka R., Kiviyama R. and Yabumoto S. (1953) J. Chem. Phys. 21, 1895.

Jaccard C. (1959) Helv. Phys. Acta. 32, 89.

Jaccard C. (1965) Ann. N. Y. Acad. Sci. 125, 390.

Joop N. and Zimmermann H. (1962) Ber. Bunsenges. Physik. Chem. 66, 440.

Kakiuchi Y., Komatsu H. and Kyoya S. (1951) J. Phys. Soc. Jap. 6, 321.

Kawada A., McGhie A. R. and Labes M. M. (1970) J. Chem. Phys. 52, 3121.

Kauzmann W. (1942) Rev. Mod. Phys. 14, 12 described by C. P. Smyth in "Dielectric Behaviour and Structure", McGraw-Hill, New York, 1955.

Kemeny G. and Rosenberg B. (1970) J. Chem. Phys 52, 4151. See also Kemeny G. and Rosenberg B. (1970) J. Chem. Phys. 53, 3549.

King G. and Medley J. A. (1949) J. Colloid Sci. 4, 9.

Koch E. and Wagner C. (1937) Z. phys. Chem. B38, 295.

Kröger F. A. (1964) "The Chemistry of Imperfect Crystals" Wiley, New York.

Lampert M. A. (1956) Phys. Rev. 103, 1648.

Lampert M. A. (1964) Rept. Prog. Phys. 27, 329.

Linder E. C. (1931) Phys. Rev. 38, 679.

Löwdin P. O. (1963) Rev. Mod. Phys. 35, 724.

MacDonald J. R. (1953) Phys. Rev. 92, 4.

Many A., Harnik E. and Gerlich D. (1955) J. Chem. Phys. 23, 1733.

Mata Arjona A. and Fripiat J. J. (1967) Trans. Far. Soc. 63, 2936.

Maricic S. and Pifat G. (1966) Abhand Deut. Akad. Wiss. Berlin, kl. Math. Phys. Tech. 4, 63.

Maricic S., Pravdic V. and Veksli Z. (1961) Croat. Chem. Acta 33, 187.

Maricic S., Pravdic V. and Veksli Z. (1962) J. Phys. Chem. Solids 23, 1651.

Maricic S. and Pintar G. (1966) Abhand. Deut. Akad. Wiss., Berlin, kl. Math. Phys. Tech. 4, 63.

Maricic S., Veksli Z., and Pintar M. (1962) J. Phys. Chem. Solids 23, 743.

Martinez-Carrera S. (1966) Acta Cryst. 20, 783.

Meyer W. and Neidel H. (1937) Z. Tech. Physik 18, 588.

Mooser E. and Pearson W. B. (1960) in "Progress in Semiconductors" ed. A. F. Gibson, Heywood and Co. Ltd., London, 5, 129.

Murphy E. J. (1950) Phys. Rev. 79, 396.

Murphy E. J. (1960) J. Phys. Chem. Solids 15, 66; 16, 115.

Murphy E. J. (1963) Can. J. Phys. 41, 1022.

Murphy E. J. (1964) J. App. Phys. 35, 2609.

Mott N. F. and Gurney R. W. (1940) in "Electronic Processes in Ionic Crystals" (2nd ed.), Oxford U. P., 43.

Northrop D. C. and Simpson O. (1956) Proc. Roy. Soc. (London) A234, 124.

Okamato Y. and Brenner W. (1964) "Organic Semiconductors" Reinhold Publ. Corp., New York.

O'Keefe M. and Perrino C. T. (1967) J. Phys. Chem. Solids 28, 211.

Onsager L. (1969) Science 166 (3911), 1359.

Onsager L. and Dupuis M. (1962) in "Electrolytes" ed. B. Pesce, Pergamon Press, London.

Onsager L. and Runnels L. K. (1969) J. Chem. Phys. 50, 1089.

Pauling L. (1935) J. Amer. Chem. Soc. 57, 2680.

Pauling L. (1960) "The Nature of the Chemical Bond" (3rd ed.) Cornell University Press, Ithaca, New York.

Pollock J. M. and Sharan M. (1967) J. Chem. Phys. 47, 4064.

Pollock J. M. and Sharan M. (1969) J. Chem. Phys. 51, 3604.

Pollock J. M. and Ubbelohde A. R. (1956) Trans. Far. Soc. 52, 1112.

Pullman B. and Pullman A. (1962) Nature, 196, 1137.

Ralph III E. K. and Grunwald E. (1968) J. Amer. Chem. Soc. 90, 517.

Richards R. E. and Smith J. A. S. (1951) Trans. Far. Soc. 47, 1261.

Riehl N. (1940) Naturwiss. 28, 601.

Riehl N. (1957) Kolloid - Z. 151, 66.

Riehl N. (1965) Trans. N. Y. Acad. Sci. Ser II, 27, 772.

Robertson J. M. (1959) Z. Krist. 112, 68.

Rogers E. and Ubbelohde A. R. (1950) Trans. Far. Soc. 46, 1051.

Rose A. (1955) Phys. Rev. 97, 1538.

Rosenberg B. (1962) J. Chem. Phys. 36, 816.

Rosenberg B. (1962) Nature, 193, 364.

Rosenberg B., Bhowmik B. B., Harder H. C. and Postow E. (1968) J. Chem. Phys. 49, 4108.
See also Rosenberg B. and Postow E. (1969) Ann. N. Y. Acad. Sci. 158, 161.

Rosenherg B. and Bhowmik B. B. (1969) Chem. Phys. Lipids 3(2), 109.

Schmidt V. H. (1965) J. Sci. Instrum. 42, 889.

Shedlovsky T. (1952) Cold Spring Harbor Symp. Quant. Biol. 17, 97.

Shockley W. and Prim R. C. (1953) Phys. Rev. 90, 753.

Slater J. C. (1941) J. Chem. Phys. 9, 16.

Smith G. W. (1969) J. Chem. Phys 50, 3595.

Smith F. R. and Heintze H. U. (1969) Can. J. Chem. 48, 203.

Steinemann A. and Gränicher H. (1957) Helv. Phys. Acta 30, 553.

Sutter P. H. and Norwick A. S. (1963) J. Appl. Phys. 34, 734.

Szent-Györgyi A. (1941) Nature, 148, 157; (1941) Science, 93, 609.

Szent-Györgyi A. (1946) Nature, 157, 875.

Szent-Györgyi A. (1959) Disc. Far. Soc. 27, 111.

Terenin A. N. (1961) Proc. Chem. Soc. 321.

Terenin A., Putzeiko E. and Akimov I. (1959) Disc. Far. Soc. 27, 83.

Thomas J. M. and Clarke T. A. (1969) Trans. Far. Soc. 65, 2718.

Thomas J. M., Evans J. R. N., Lewis T. J. and Secker P. (1969) Nature 222, 375.

Thomas J. M. and Williams J. O. (1968) Chem. Comm. 209

Thomas J. M., Williams, J. O. and Turton L. M. (1968) Trans. Far. Soc. 64, 2505.

van Beek L. K. H. (1963a) Physica 29, 215.

van Beek L. K. H. (1963b) Physica 29, 1323.

Vanderkooy J, Cuthbert J. D. and Petch H. E. (1964) Can. J. Phys. 42, 1871.

Wallwork S. C. (1962) Acta Cryst. 15, 758.

Watson J. D. and Crick F. H. C. (1953) Nature, 171, 737.

Wannier G. H. (1935) Ann. Physik, 24, 545.

Weisz S. Z., Cobas A., Richardson P. E., Szmant H. H. and Trester S. (1966) J. Chem. Phys. 44, 1364.

Will G. (1969) Z. Krist. 129, 211.

Williams D. F., Sykes B. and Schneider W. G. (1967) Can. J. Chem. 45, 1109.

Wise H. (1967) J. Phys. Chem. 71, 2843.

APPENDIX 1

Tables of results : essential data

Each set of results is preceded by the note book reference (page number, and book a - d) in brackets.

The symbols used in the dielectric results are the standard symbols defined in the General Radio Type 716-C capacitance bridge manual.

Abbreviations for d. c. results

A	=	cross-sectional area of sample, cm^2, which is 1.327 cm^2 if not specified
L	=	thickness of sample, mm
T	=	temperature of sample in ^{o}C, room temperature (20-25^{o}C) if not specified
E	=	applied potential, volts
I	=	current, amps
V	=	volume of gas collected corrected to STP, cm^3
q	=	charge, coulombs
H	=	time of electrolysis, hours
P	=	sample vacuum-desiccated over P_2O_5
S	=	sample " " " silica gel
Im	=	imidazole
U	=	urea
Hg Pt Pd	=	electrode of the corresponding material
Pd/H_2	=	hydrogen-saturated palladium electrode. If only one electrode material is specified, then two similar electrodes were used. The anode specified first.

RESORCINOL RUN NO. 3

MEAN TEMP. 74.0 DEG.C. C' 585.67 D' -0.029 C 567.00

MEAN	WGT	DENSITY
7.008	G	G/CC
4.880	4.9573	1.1648

NO.	FREQ. C/S	C. PF	D. %
1	23.7	499.80	42.000
2	31.6	512.79	26.540
3	42.2	522.23	16.400
4	56.2	529.20	10.220
5	75.0	534.34	6.330
6	100.0	538.15	3.890
7	133.0	538.90	3.480
8	178.0	543.11	1.440
9	237.0	544.63	0.879
10	316.0	547.12	5.400
11	422.0	548.19	3.290
12	562.0	548.99	1.980
13	750.0	549.61	1.210
14	1000.0	550.11	0.734
15	1330.0	550.49	0.440
16	1780.0	550.81	0.259
17	3160.0	551.60	1.020
18	5620.0	551.91	0.361
19	10000.0	552.10	0.121
20	17800.0	552.30	0.031
21	31600.0	552.30	0.139
22	56200.0	552.30	0.048
23	100000.0	552.50	- 0.005
24	178000.0	552.50	- 0.005
25	316000.0	552.90	- 0.003

RESORCINOL RUN NO. 4

MEAN TEMP. 73.0 DEG.C. C' 585.75 D' -0.028 C 567.20

MEAN	WGT	DENSITY
7.061	G	G/CC
4.879	4.9359	1.1307

NO.	FREQ. C/S	C. PF	D. %
1	23.7	542.30	10.903
2	31.6	545.41	7.420
3	42.2	547.12	4.480
4	56.2	548.50	2.720
5	75.0	549.54	1.660
6	100.0	550.40	1.010
7	133.0	551.00	0.610
8	178.0	551.50	0.363
9	237.0	551.83	0.214
10	316.0	552.68	1.440
11	422.0	552.95	0.868
12	562.0	553.18	0.518
13	750.0	553.32	0.309
14	1000.0	553.44	0.178
15	1330.0	553.55	0.102
16	1780.0	553.60	0.056
17	2370.0	553.61	0.028
18	3160.0	553.83	0.248
19	5620.0	553.91	0.079
20	10000.0	554.00	0.019
21	17800.0	554.03	- 0.008
22	23700.0	554.08	- 0.018
23	31600.0	554.00	0.039
24	56200.0	554.00	0.001
25	100000.0	554.04	- 0.017
26	178000.0	554.20	- 0.021
27	237000.0	554.31	- 0.020
28	316000.0	554.40	- 0.020
29	562000.0	553.90	0.019

RESORCINOL RUN NO. 5

MEAN TEMP. 30.0 DEG.C. C' 585.80 D' -0.030 C 567.30

MEAN	WGT	DENSITY
7.060	G	G/CC
4.879	4.9359	1.1311

NO.	FREQ. C/S	C. PF	D. %
1	23.7	524.40	11.000
2	31.6	538.00	10.320
3	42.2	540.79	6.760
4	56.2	543.12	4.120
5	75.0	544.84	2.540
6	100.0	546.19	1.550
7	133.0	547.15	0.952
8	178.0	547.95	0.572
9	237.0	548.51	0.350
10	316.0	549.70	2.290
11	422.0	550.12	1.370
12	562.0	550.50	0.838
13	750.0	550.79	0.509
14	1000.0	551.00	0.309
15	1330.0	551.19	0.181
16	1780.0	551.30	0.109
17	3160.0	551.73	0.470
18	5620.0	551.90	0.169
19	10000.0	552.00	0.059
20	17800.0	552.18	0.010
21	31600.0	552.10	0.119
22	56200.0	552.20	0.039
23	100000.0	552.27	0.002
24	178000.0	552.41	- 0.015
25	316000.0	552.71	- 0.015
26	562000.0	552.30	0.021

IMIDAZOLE RUN NO. 1

MEAN TEMP. 50.0 DEG.C. C' 586.00 D' -0.038 C 559.00

MEAN	WGT	DENSITY
6.390	G	G/CC
4.872	3.2604	1.0736

NO.	FREQ. C/S	C. PF	D. %
1	31.6	497.00	8.390
2	56.2	504.62	4.150
3	100.0	509.12	2.090
4	178.0	513.02	1.050
5	316.0	517.69	5.570
6	562.0	521.22	2.790
7	1000.0	524.31	1.410
8	1780.0	527.02	0.702
9	3160.0	530.03	3.690
10	5620.0	532.36	1.830
11	10000.0	534.39	0.909
12	17800.0	536.20	0.445
13	31600.0	537.90	2.300
14	56200.0	539.38	1.100
15	100000.0	540.63	0.531
16	178000.0	541.80	0.242
17	316000.0	542.91	0.110
18	562000.0	542.90	0.078

IMIDAZOLE RUN NO. 2

MEAN TEMP. 74.9 DEG.C. C' 586.00 D' -0.038 C 559.00

MEAN	WGT	DENSITY
6.390	G	G/CC
4.872	3.2604	1.0736

NO.	FREQ. C/S	C. PF	D. %
1	562.0	383.25	47.270
2	1000.0	415.50	16.020
3	1780.0	430.90	5.830
4	3160.0	443.80	23.000
5	5620.0	452.00	10.150
6	10000.0	459.70	5.000
7	17800.0	467.60	2.670
8	31600.0	478.10	14.890
9	56200.0	488.30	8.220
10	100000.0	498.80	4.420
11	178000.0	508.65	2.230
12	316000.0	516.95	1.070
13	562000.0	522.10	0.500

IMIDAZOLE RUN NO. 3

MEAN TEMP. 65.0 DEG.C. C' 585.80 D' 0.001 C 559.00

MEAN	WGT	DENSITY
6.340	G	G/CC
4.931	3.2604	1.1566

NO.	FREQ. C/S	C. PF	D. %
1	56.2	338.40	51.100
2	75.0	367.28	29.390
3	100.0	386.20	17.620
4	133.0	399.32	10.722
5	178.0	409.05	6.580
6	237.0	416.20	4.200
7	316.0	426.65	25.980
8	422.0	432.20	17.010
9	562.0	437.32	11.450
10	750.0	442.18	7.910
11	1000.0	446.80	5.560
12	1330.0	451.30	4.000
13	1780.0	455.80	2.870
14	3160.0	466.88	15.020
15	5620.0	476.50	8.110
16	10000.0	486.10	4.410
17	17800.0	495.48	2.320
18	31600.0	505.70	11.900
19	56200.0	513.80	5.736
20	100000.0	520.35	2.730
21	178000.0	525.72	1.240
22	316000.0	530.00	0.555
23	562000.0	531.80	0.271

UREA RUN NO. 3

4.850 PF IS ZERO CAPACITANCE

/ 970.70 (MEAN) 69.9

/ 0.000 953.90

WGT G 9.8407

DENSITY G/CC 12.8140

MEAN 0.817 0.433

NO	FREQ C/S	C PF%	D PF
1	56.2	600.40	20.400
2	75.0	627.80	14.500
3	100.0	651.00	10.020
4	133.0	670.10	6.800
5	178.0	684.10	4.620
6	237.0	695.50	3.220
7	316.0	711.90	22.030
8	422.0	721.70	16.120
9	562.0	731.80	12.090
10	750.0	742.00	9.300
11	1000.0	753.10	7.190
12	1330.0	765.00	5.570
13	1780.0	778.00	4.320
14	2370.0	792.20	3.300
15	3160.0	812.90	24.220
16	4220.0	828.70	17.780
17	5620.0	843.80	12.990
18	7500.0	858.50	9.330
19	10000.0	872.40	6.550
20	13300.0	885.50	4.500
21	17800.0	896.80	3.000
22	23700.0	906.30	1.970
23	31600.0	918.10	11.920
24	42200.0	924.10	7.420
25	56200.0	928.40	4.550
26	75000.0	931.80	2.800
27	100000.0	934.20	1.630
28	133000.0	935.60	1.100
29	178000.0	937.70	0.620
30	237000.0	938.20	0.414
31	316000.0	938.40	0.271

UREA RUN NO. 4

4.850 PF IS ZERO CAPACITANCE

69.9	(MEAN)	/ 970.90	/ -0.002	954.20

MEAN	WGT	DENSITY
8.183	G	G/CC
4.334	9.8407	1.2781

NO	FREQ C/S	C PF%	D PF
1	56.2	844.00	12.000
2	75.0	857.70	9.000
3	100.5	872.30	6.400
4	133.0	883.70	4.400
5	178.0	894.70	2.950
6	237.0	903.90	1.950
7	316.0	915.00	12.120
8	422.0	923.00	7.560
9	562.0	925.50	4.730
10	750.0	928.80	2.940
11	1004.0	931.40	1.780
12	1330.0	933.20	1.110
13	1780.0	934.70	0.697
14	2370.0	935.80	0.437
15	3160.0	937.60	2.560
16	5620.0	939.00	0.950
17	10000.0	940.00	0.367
18	17800.0	940.60	0.149
19	31600.0	940.90	0.489
20	56200.0	941.40	0.170
21	100000.0	941.60	0.039
22	178000.0	942.20	0.035
23	237000.0	942.00	0.080

UREA RUN NO. 5

4.850 PF IS ZERO CAPACITANCE

/ 0.002 953.90

/ 970.80

80.1 (MEAN)

	WGT G	DENSITY G/CC
MEAN	9.8407	1.2844
8.194		
4.364		

NO	FREQ C/S	C PF%	D PF
1	56.2	788.20	11.240
2	75.0	797.20	8.800
3	100.5	807.60	6.790
4	133.0	818.40	5.330
5	178.0	831.90	4.120
6	237.0	846.80	3.130
7	316.0	867.70	21.980
8	422.0	883.20	15.220
9	562.0	896.80	10.098
10	750.0	907.70	6.550
11	1000.0	915.90	4.160
12	1330.0	921.90	2.560
13	1780.0	926.10	1.570
14	2370.0	929.20	0.965
15	3160.0	933.20	0.693
16	4220.0	935.10	3.410
17	5620.0	936.30	2.110
18	7500.0	937.40	1.280
19	10000.0	938.20	0.778
20	13300.0	938.90	0.480
21	17800.0	939.40	0.292
22	23700.0	939.80	0.179
23	31600.0	940.20	1.020
24	56200.0	940.80	0.338
25	100000.0	941.40	0.112
26	178000.0	942.20	0.077
27	316000.0	941.60	0.088

UREA RUN NO. 6

4.850 PF IS ZERO CAPACITANCE

/ 0.004 952.60

/ 969.30

89.9 (MEAN)

MEAN	WGT G	DENSITY G/CC
0.818	9.8407	12.7996
0.433		

NO	FREQ C/S	C PF%	D PF
1	42.2	700.00	36.700
2	56.2	713.00	21.300
3	75.0	727.00	14.700
4	100.0	739.90	10.300
5	133.0	751.10	7.450
6	178.0	763.30	5.560
7	237.0	776.60	4.240
8	316.0	800.10	30.960
9	422.0	819.30	22.890
10	562.0	839.90	16.480
11	750.0	859.50	11.580
12	1000.0	877.10	7.810
13	1330.0	892.10	5.490
14	1780.0	903.60	3.210
15	2370.0	912.00	1.980
16	3160.0	921.40	11.880
17	4220.0	925.80	7.110
18	5620.0	929.00	4.310
19	7500.0	931.30	2.610
20	10000.0	933.10	1.530
21	13300.0	934.40	0.955
22	17800.0	935.50	0.575
23	23700.0	936.30	0.354
24	31600.0	937.20	2.090
25	42200.0	937.90	1.240
26	56200.0	938.20	0.742
27	100000.0	939.00	0.280
28	237000.0	940.20	0.108
29	422000.0	939.80	0.095

PRATLEY PASTE

(81b) A = 0.385, L = 4.0 S Hg

$Ex10^{-2}$	2	4	6	8
$Ix10^{10}$	5	9	13	18

GUARD RING EFFECTS

(104b) Im T = 50, A = 0.503, L = 1.19, Hg

$Ex10^{-1}$	1	2	3	4	5	6	7	8	9	10	11	12	
$Ix10^{6}$	19	40	58	78	93	105	115	125	130	138	140	145	with guard ring
$Ix10^{6}$	17	36	55	74	90	103	113	127	140	148	158	166	without guard ring

IMIDAZOLE

(70c) Triply sublimed			T = 28, L = 1.2, P											
$Ex10^{-1}$	2	4	6	8	10	12	16	20	24	28				
$1x10^{9}$	4	9	14	19	24	32	38	50	61	110	Pt			
$Ix10^{9}$	14	28	44	57	67	83	112	150	180	205	Pd/H_2, Pd			
(70c) Doubly sublimed			T = 28, L = 0.9, P											
$Ex10^{-1}$	2	4	6	8	10	12	16	20	24					
$Ix10^{8}$	2.5	5.3	9.4	15	23	27	38	51	57	Pt				
$Ix10^{8}$	12	24	39	56	72	89	130	170	200	Pd/H_2, Pd				
(85c) Triply sublimed			T = 25, L = 1.196											
$Ex10^{-2}$	2	4	6	8	10	12	14	16	18	20	22	24	26	
$Ix10^{8}$	17	32	45	56	68	82	94	105	114	125	135	Pd, Pd/H_2		
$Ix10^{8}$	21	42	63	85	104	125	146	172	195	225	255	290	320	Pd/H_2, Pd
(90c) Triply sublimed			T = 25, L = 1.62, P											
$Ex10^{-2}$	4	6	8	10	12	14	16	20	24					
$Ix10^{5}$	29	41	53	66	81	100	118	150	190	Pd, Pd/H_2				
$Ix10^{5}$	40	64	83	108	120	150	190	235	290	Pd/H_2, Pd				

(91c) Triply sublimed T = 25, L = 1.54, P

$Ex10^{-2}$	4	6	8	10	12	14	16	20	
$Ix10^{6}$	6	11	20	25	31	38	48	67	Pt
$Ix10^{6}$	21	31	43	49	50	62	74		Pd/H_2, Pd

(92c) Triply sublimed T = 25, L = 1.32, P

$Ex10^{-2}$	4	6	8	10	12	14	16	
$Ix10^{7}$	32	48	71	100	116	142	170	Pt
$Ix10^{7}$	64	92	120	130	150	170	180	Pd/H_2, Pd

ELECTROLYSIS OF Im POWDERS

(47c) Ten Im pellets pressed into a block T = 50, L = 9.9, S, Hg

$qx10^{2}$	6	12	16	20	30	40	49	62	74	84	93	105	116
$Vx10^{3}$	6	11	16	20	30	41	50	63	76	86	95	108	120
		125	135	144	153	160	168	178	188				
		129	140	150	159	166	176	180	198				

This electrolysed block of pellets was analysed by a micro-potentiometric titration (see 152b)

(55c) Reverse electrolysis single pellet T = 50 L = 0.76, S, Hg

q	0	3	6	8	9	11	12	13	14	15	17
$Vx10^{3}$	31	1	8	16	24	55	74	92	114	119	122

UREA POWDER RECRYSTALLISED TWICE FROM METHANOL

(1d) T = 60, L = 0.915, S

$Ex10^{-1}$	2	4	10	15	20	30	60	100	150	
$Ix10^{8}$	3.7	7.4	17	26	33	50	110	200	inf.	Pd/H_2, Pt

(2d) T = 60, L = 2.113, S

$Ex10^{2}$	2	3	4	6	8	10	12	14	16	
$Ix10^{8}$		21		42	55	62	69	78	Pt	
$Ix10^{6}$	4		8	11	15	19	24	79	inf.	Powdered Im, Pt

(3d) T = 60, L = 1.313

$Ex10^{-2}$	2	4	6	8	10	12	14	16	18	20	22	
$Ix10^{6}$	18	30	41	50	55	57	Pt					
$Ix10^{6}$	4	8	12	15	18	21	22	26	36	45		Im, Pt

(3d) T = 60, L = 1.313

$Ex10^{-2}$	2	4	6	8	10	12	14	16	18	20	22	
$Ix10^{6}$	18	30	41	50	55	57	Pt					
$Ix10^{6}$	4	8	12	15	18	21	22	26	36	45		Im, Pt

(4d) T = 60, L = 1.367

$Ex10^{-2}$	2	4	6	8	10	12	14	
$Ix10^{6}$	4	8	12	14	15	16	14	Pt

(5d) T = 60, L = 1.461, P

$Ex10^{-2}$	2	4	6	8	10	12									
$Ix10^{8}$	7	14	21	26	31	36	Pt								
$Ix10^{7}$	8	15	21	27	31	35	40	45	50	57	62	77	100	120	
												Powdered Im, Pt			

(16d) Conductivity of an electrolysed pellet (see 128c under electrolysis) after 0.13 coulombs passed T = 60, A = 1.03 L = 1.513, P

$Ex10^{-2}$	58	54	50	46	42	38	34	30	26	22	18	14	10	6	2	0
$Ix10^{8}$	29	27	25	22	20	18	16	14	11	9	7	5	3	0.6	-1	-2 Hg

(53d) Die containing urea powder evacuated for 15 minutes before pressing pellet. Sample electrolysed for 4 hours until polarization ceased, L = 1.260, P, Pt

$Ex10^{-2}$	2	4	6	8	10	12	14	
$Ix10^{11}$	29	64	100	150	210	T = 30		
$Ix10^{10}$	16	41	63	90	120	T = 40		
$Ix10^{9}$	11	22	35	48	62	T = 50		
$Ix10^{9}$	55	120	170	224	283	336	390	T = 60

UREA SINGLE CRYSTALS

(30d) Single Crystal (S_1) grown from saturated solution of 90 g urea in 300 Methanol containing 2.5 g NH_4Br, I in a direction. A = 0.3025, L = 1.315 P, Pt

$Ex10^{-2}$	2	4	6	8	10	12	
$Ix10^{10}$	6	12	18	24	28	36	T = 30
$Ix10^{10}$	17	33	50	63	77		T = 40
$Ix10^{10}$	44	84	126	167	205		T = 50
$Ix10^{9}$	11	21	31	41	53		T = 60

(31d) Im used as a protode for crystal (S_1) T =60, A = 1.77

L = 1.421, P

$E \times 10^{-1}$	2	4	6	8	10	
$I \times 10^{5}$	6	12	20	29	34	Pt

(33d) Crystal (S_1) using Im protode; Measurements commenced after current passed for 2 hours at 800V T = 60, A = 0.3025, L = 1.315, P

$Ex10^{-2}$	2	4	6	8	10	12	14	16	18	
$Ix10^{9}$	11	20	33	45	59	71	83	95	115	Im, Pt

(35d) Single crystal (S_2), I in c direction A = 0.1744, L = 1.549, P, Pt

$Ex10^{-2}$	2	4	6	8	10	12	
$Ix10^{10}$	10	21	31	42	54	66	T = 30
$Ix10^{10}$	52	104	162	220	274	335	T = 40
$Ix10^{9}$	28	55	80	107	135	162	T = 50
$Ix10^{8}$	6.6	13	20	26	33	37	T = 60

(38d) Im protode for crystal (S_2) T = 60, A = 1.77, L = 1.142, P

$Ex10^{-1}$	2	4	6	8	10	
$Ix10^{6}$	11	22	33	44	56	Pt

(41d) Crystal (S_2) using Im protode ; measurements commenced after 5 hours at 1000 V T = 60, A = 0.1744, L 1.549, P

$Ex10^{-2}$	2	4	6	8	10	12	14	16	
$Ix10^{6}$	6	10	14	17	21	27	30	33	Im, Pt

(43d) Single crystal (S_3) I in c direction A = 0.2250, L = 1.559, P, Pt

$Ex10^{-2}$	2	4	6	8	10	12	
$Ix10^{10}$	9	18	27	36	rising rapidly		T = 30
$Ix10^{9}$	4	8	14	19	26		T = 40
$Ix10^{9}$	23	47	71	96	160	unstable	T = 50
$Ix10^{9}$	80	168	240	330		unstable	T = 60

(44d) Im protode for crystal (S_3) T = 60, A = 1.77, L = 0.763, P

$Ex10^{-1}$	2	4	6	8	10	
$Ix10^{6}$	33	55	80	100	120	Pt

(47d) Crystal (S_3) using Im protode; measurement commenced after 46 hours electolysis (see single crystal electrolysis S_3) A = 0.2250, L = 1.559, P, Im, Pt

$Ex10^{-2}$	14	12	10	8	6	4	2	
$Ix10^{7}$	56	45	36	27	18	11	5	T = 60
$Ix10^{8}$	66	52	40	27	17	10		T = 50
$Ix10^{8}$	18	14	11	8	6	3		T = 40

(49d) Single crystal (S_4) I in a direction A = 0.5012 L = 1.569, P, Pt

$Ex10^{-2}$	2	4	6	8	10	12	13	14	
$Ix10^{9}$	6	12	18	24	28	T = 60			
$Ix10^{10}$	4	9	15	21	28	38	42	T = 50	
$Ix10^{11}$	2	9	17	26	39	51	-	69	T = 40
$Ix10^{11}$	0.9	4	8	12	17	23	-	31	T = 30

(51d) Im protode for crystal (S4) T = 60, A = 1.77 L = 1.007, P

$Ex10^{-1}$	2	4	6	8	
$Ix10^{6}$	5	10	14	16	Pt

(51d) Crystal (S4) Using Im protode; measurement commenced after 3.6 hours at 1000 volts A = 0.5012 L = 1.569 P, Im, Pt

$Ex10^{-2}$	10	8	6	4	2	
$Ix10^{9}$	213	145	85	41	1	T = 60
$Ix10^{9}$	99	70	43	21	6	T = 50
$Ix10^{9}$	48	36	25	14	5	T = 40
$Ix10^{10}$	114	85	58	34	12	T = 30

ELECTROLYSIS OF UREA POWDER

(128c) U/Im "sandwich" pellet pressed in 13 mm die. T = 60, L = 1.865, P, Im, Hg

H	0	0.4	0.8	1.6	2.4	3.2	3.6	9.2	17.2	22.0
$Ex10^{-2}$	1	50	46	34	32	30	30	31	28	28
$qx10^{2}$	0	8	12	15	17	20	21	33	35	38
$Vx10^{3}$	0	4	10	13	15	17	18	30	33	34
	34.8	41.2	46.4	58.8	64.4	66.4	72.8	81.6		
	28	31	34	34	31	28	28	28		
	41	44	48	76	89	91	97	99		
	40	43	48	76	88	93	98	103		

(12d) T = 60, L = 1.513, P Hg

H	0	0.5	1.3	2.0	8.9	14.0	20.4	33.6	34.2
$Ex10^{-2}$	2	40	42	44	44	48	50	54	56
$qx10^{3}$	0	8	9	10	19	25	33	49	50
$Vx10^{4}$	0	5	7	7	12	16	23	39	39

36.4	47.0	off	0	2.8	15.4	21.4	26.0	38.4	52.0
58	58	?	57	57	57	57	57	57	57
53	66	73	75	79	93	99	104	118	133
37	42	46	48	50	57	57	58	62	62

at this stage, the sample was tested for ohmic behaviour (see 16d under conductivity). An Im protode was then applied to the U sample and the electrolysis continued:-

T = 60, L = 1.513, P, Im, Hg

H	0	0.4	0.8	1.2	1.6	2.0	2.4	8.8	12.0
$Ex10^{-2}$	2	16	20	14	14	12	10	60	60
$qx10^{2}$	0	2	7	16	25	33	41	120	174
$Vx10^{3}$	0	2	8	17	25	34	41	126	186

ELECTROLYSIS OF UREA SINGLE CRYSTAL

(45d) Single crystal (S_3), I along c axis (see 44d under single crystal conductivity) T = 60, A = 2.25, L = 1.559, P, Im, Hg

H	0	1.2	3.6	6.2	22.2	23.6	25.9	29.6	33.7	42.3
$Ex10^{-2}$	14	14	14	14	14	14	14	14	14	14
$qx10^{2}$	0	24	57	96	257	282	320	379	436	570
$Vx10^{3}$	0	0.5	0.5	0.6	14	16	19	24	29	41